DEHYDROGENATION OF CYCLOHEXANE

by

S. Viswanathan

A thesis submitted in partial fulfillment of the requirements

for the degree of

MASTER OF SCIENCE

in the

DEPARTMENT OF CHEMICAL ENGINEERING

UNIVERSITY OF OTTAWA

Ottawa, Canada December, 1965.

Approved by

M.Sc. Candidate.

ACKNOWLEDGMENT

The author wishes to acknowledge his sincere gratitude to Dr. B.C.Y. Lu for providing the facilities for this research work, to Dr. R.S. Mann, who directed its course, for his advice and encouragement, to Messrs. F. Giacobbi and G. Gasperetti, for their technical assistance and to Miss J. Craven for typing the manuscript.

The author is much indebted to the members of the teaching staff of the Chemical Engineering Department for stimulating discussions and suggestions.

Finally, the author wishes to express his sincere thanks to the National Research Council, Ottawa for providing the financial assistance.

To

dear departed parents.

TABLE OF CONTENTS

LIST OF FIGURES

LIST OF TABLES

ABSTRACT

The kinetics and mechanism of the dehydrogenation of cyclohexane to benzene over several supported and unsupported catalysts in the form of pellets and powders was studied in the temperature range of about 200 to 600°C in a flow system.

Catalysts used in the study included several commercial catalysts - platinum on alumina, palladium on alumina, cobalt oxide on alumina, nickel oxide, chromium oxide, nickel oxide on alumina, and nickel oxide on kieselguhr (supplied by Girdler Co.) and nickel oxide powder and nickel oxide supported on pumice.

The activation energies (in k cals/mole) and frequency factors were found to be: nickel oxide powder - 13.7, 327.9; nickel oxide on pumice - 8.3, 14.6; nickel oxide on kieselguhr - 5.7, 3.5; nickel oxide on alumina - 9.0, 50.9; nickel oxide, chromium oxide - 10.2, 17.4; platinum on alumina - 6.9, 35.8; and cobalt oxide on alumina - 21.7, 9623.

The data obtained seemed to suggest that surface reaction was the rate-controlling step. Following the procedure of Hougen and Watson, rate equations for the various catalysts were obtained. Rate constants and adsorption equilibriums for hydrogen, cyclohexane and benzene were also

determined. It has been found that the rate data can be satisfactorily correlated by the equation:

$$r = \frac{k\left(P_{C_6H_{12}} - \frac{P_{C_6H_6}\,(P_{H_2})^3}{K}\right)}{\left(1 + P_{C_6H_{12}}K_{C_6H_{12}} + P_{C_6H_6}K_{C_6H_6} + P_{H_2}K_{H_2}\right)^2} \qquad (1)$$

CHAPTER I.

INTRODUCTION

I. INTRODUCTION

Since the successful hydrogenation of ethylene on nickel oxide in 1897 by Sabatier and Sendersen, there have been a large number of studies on the catalytic hydrogenation of light olefines and benzene to cyclohexane.

In the past, several persons have studied the hydrogenation of benzene over various metal catalysts not only to find the extent of relationship between catalytic activity and position of the metal in the periodic table and formulation of a general theory of catalysis, but also the more fundamental problem of interaction between solid surfaces and surrounding phases.

Recently, Ross and Walsh have studied the dehydrogenation of cyclohexane to benzene to study the mechanism of hydrogenation of benzene, whereby they found that there is a reversal in the mechanism at about 170°C.

Most of the studies in the past on the catalytic dehydrogenation of cyclohexane suffered from the fact that either the process control was not very good or too many side products like cyclohexene, methyl pentane etc. were formed making the analysis of the products and a satisfactory correlation of the data very difficult.

The present investigation of the kinetics and mechanism of the catalytic dehydrogenation of cyclohexane to benzene was undertaken to reconcile the apparent differences in the behaviour of different catalyst preparations and to extend the work of Ross and Walsh to several other catalysts to see how the kinetics of the reaction differs and to what extent the compensation effect exists for these.

CHAPTER II.

LITERATURE SURVEY

II. LITERATURE SURVEY

Dehydrogenation of cyclohexane is the reverse process of hydrogenation of benzene.

$$C_6H_{12} \rightleftharpoons C_6H_6 + 3H_2$$

Though the hydrogenation of benzene has been studied fairly extensively, yet the reverse process has not received as much attention. Ross and Valentine (1) point out that "very few kinetic results are available for cyclohexane dehydrogenation".

Bayer first synthesised cyclohexane in 1893 and Sabatiers obtained it in 1898 by the hydrogenation of benzene.

Cyclohexane is liquid at ordinary temperatures. It is easily vaporised, readily inflammable and is less toxic than benzene. It is also an excellent solvent. Cyclohexane has approximately the same vapour pressure as benzene and behaves ideally over a wide temperature range.

Cyclohexane has been dehydrogenated to produce a variety of products by passing it over metal catalysts at elevated temperatures and atmospheric pressures. The products obtained depend largely on the type of catalysts used and the temperatures at which the reactions are carried out. Sabatiers and Senderns passed cyclohexane over finely (21) divided nickel at 270-280°C to produce benzene, methane

and hydrogen. Nickel on alumina at 190-270°C gave only benzene and hydrogen while a similar catalyst at 350°C gave a mixture of benzene, toluene, methane and hydrogen.

Dehydrogenation of cyclohexane over palladium and platinum black at 300°C gave yields of 82.5% and 62.5% benzene respectively. Zelinsky and co-workers (21) have shown that over palladium black, the reaction was reversible. At 100-110°C, benzene was hydrogenated, at 170°C dehydrogenation began, at 200°C equilibrium was reached and at 300°C dehydrogenation attained a maximum rate.

Palladium, platinum, nickel and copper have been tried as catalysts. Palladium has been found to be the most effective and copper the least. Palladium dehydrogenates cyclohexane but does not dehydrogenate cyclopentane or cycloheptane. Copper requires high temperatures and many intermediates are produced.

Oxides and sulphides of molybdenum, chromium and zinc have been found to give intermediates.

Potapova (2) studied the dehydrogenation of cyclohexane in a flow system and measured the temperatures throughout the catalyst layer length. He found that the operating length of the catalyst was much lower than the temperature measured at the entry or the exit ends of the reactor tube.

The catalyst was mixed with granulated alumina as diluent which was found to be inert in the reaction. He used 40 to 50 volumes of diluent per one volume of catalyst. Under these conditions the reaction was assumed to be taking place isothermally. At 470°C the reaction proceeded at flow rates of over 0.009 to 0.01 m/sec.

W. Wright and Sol W. Waller (3) in an exploratory study have shown stable activity for cyclohexane dehydrogenation at elevated hydrogen pressures.

P. Tetenyi, J. Kislay and L. Babernics (4) studied, by a flow technique, the dehydrogenation of binary mixtures of cyclohexane with hydrogen and argon over a nickel catalyst and obtained the adsorption coefficient of hydrogen. From the data at 273-373°C the heat of adsorption was calculated as 24.1 k cals/mole. Static experiments with hydrogen in the same temperature range indicated that adsorption isotherms could be better correlated by Freundlich equation rather than Langmuir's. It was shown that the surface of the catalyst was grossly heterogeneous.

A. E. Agronomov and Yu S. Mardashev (5) determined the specific activity of supported nickel catalysts grouped in such a way as to reveal

(1) the effect of the nature of the supporting agent

(2) the method of preparation of nickel

and (3) the ratio of the weight of nickel to the weight of the supporting agent.

The activity was measured by the dehydrogenation of cyclohexane at 270-320°C so that the conversion to benzene amounted to 10-30%. As supporting agents, kieselguhr (I), alumina (II), silica gel, asbestos and carbon black were used. The highest activity per gram of catalyst was obtained with Ni(I) and Ni(II).

The remaining catalysts had a low and apparently the same activity. The effect of the physical heterogeneity of the surface on the activity was small (except for chemical heterogeneity). The apparent activation energy 'Q' for each catalyst varied from 4.5 to 12.0 kilocalories per mole and was dependent on the nature of the supporting agent.

C. B. Mcgough (6) has studied the dehydrogenation of cyclohexane using rare earth oxides as catalysts.

Kh. M. Minachev, M.A. Markov and O.K. Shukina (7) studied the dehydrogenation of cyclohexane to benzene at 90-515°C on La_2O_3, Nd_2O_3, Sm_2O_3, Gd_2O_3, Ho_2O_3, Er_2O_3, Tm_2O_3, Yb_2O_3, and Y_2O_3 as catalysts. Cyclohexane was passed through a quartz tube containing ten c.cs of the oxide catalyst and the products contained benzene and cyclohexane analysed by chromatography.

Magyar and Hodassy (8) investigated the dehydrogenation of cyclohexane using nitrogen as the carrier gas in the temperature range 220-400°C for 2.0 and 17.3% palladium concentration in the catalyst. The activity of the catalyst decreased strongly during a two hour run. The reaction was first order and was inhibited by the adsorption of hydrogen on the palladium catalyst. This effect makes palladium a less effective catalyst than platinum.

A unique study termed as the rising temperature method was carried out by Mcgough and Houghton (9).

A rising temperature flow reactor was used to determine the activation energies, frequency factors and kinetics for the heterogeneous dehydrogenation of cyclohexane over La_2O_3, CeO_2, Pr_2O_3, Nd_2O_3 and Sm_2O_3. The effect of crystal structure was evaluated by preparing the oxides in their different crystal forms (A, B or C structures) and the effect of a support was investigated by depositing the oxides on alumina. Within the error of experiment, no effect of the support, crystal structure, paramagnetism or valence state could be detected, indicating perhaps that the catalytic activity of the lanthanide oxides is associated with the outer electronic states.

Ross and Valentine (1) dehydrogenated cyclohexane by passing the vapours over nickel on silica catalysts in a flow system from 100-260°C at atmospheric pressure. The fraction

of cyclohexane converted to benzene (C) was extremely low (about 0.01) between 100 and 180°C while at 235°C the conversion increased to a maximum value around 0.25 and then rapidly decreased with further rise in temperature. In the range 150-220°C the apparent activation energy was 30 ± 2 kcal/mole and the reaction rate dependence was zero order with respect to benzene, first order with respect to cyclohexane and to the inverse of the hydrogen concentration.

It is suggested that the slowest step in the reaction involved the initial formation of adsorbed cyclohexene and hydrogen from adsorbed cyclohexane. The results are contrasted and compared with earlier findings on benzene hydrogenation (22).

P. Tetenyi and co-workers (10) carried out complex investigations in respect to the catalytic and adsorptive properties of nickel catalysts prepared in various ways. The catalytic activity was characterized, in three model reactions, one of which was the dehydrogenation of cyclohexane. It was found that the mode of preparation actually influences both the specific surface and the catalytic activity to an appreciable extent. In the case of the three reactions investigated, changes in reaction rates were rather parallel in the various samples.

The dehydrogenation of cyclohexane over palladium adsorbed on active charcoal in a fluidised bed was tried by

Magyar and Neweth (11, 12). The reaction was studied at 255-330°C with the catalyst containing 20% palladium. The order of reaction did not change with increase of temperature although the rate slowed below 340°C. The order was the same as was found with fixed bed catalysis although in this case, the reaction was slower.

By studying the reaction in a fluidised bed at the transition temperature range of 225-330°C, it was found that the reaction mechanism was the same as in a stationary bed. Owing to the increased active catalyst surface, the reaction velocity was higher in the fluidised bed.

The mechanism of the dehydrogenation of cyclohexane was studied by Magyar and Hodassy (13). The kinetics was studied on palladium and platinum catalysts respectively. The curve obtained at 340°C was linear. This showed that the reaction was of first order at that temperature. Only slight deviations from a straight line occurred at higher temperatures; this was attributed to higher conversion rates caused by the increased reaction velocities. At lower temperatures the retarding action of hydrogen becomes evident. Contrary to the theoretical expectations the reaction activity on a palladium catalyst was lower than on a platinum catalyst. This was attributed to the fact that the hydrogen atoms formed in the primary phase of the reaction are more firmly bound to

the palladium surface than to the platinum surface. Hence its retarding action is more evident.

The catalytic inertness of amorphous nickel in reactions of hydrogenation of benzene and dehydrogenation of cyclohexane was examined by Rubinshtein and co-workers (14). A catalyst, 30% nickel and 70% aluminium oxide, was prepared from the corresponding nitrates treated with 30% sodium hydroxide. The resulting precipitate was dried at 110-120°C and formed into cylindrical pellets for use after calcining at 300, 350 or 425°C either after drying or directly with reduction by hydrogen at 350°C in both cases. Preliminary calcining at 425°C did not affect the hydrogenating-dehydrogenating activity of the catalyst. Catalysts that were calcined for ten to twelve hours at 350° or 425°C after hydrogen reduction showed absolutely no activity whereas omission of such calcining gave active catalysts. The inactive forms were amorphous or at least did not have crystal units of dimensions expected of the substances involved. Apparently 350-425°C is the lowest temperature limit at which NiO and Al_2O_3 can react chemically with each other, since calcining at 300°C does not affect the catalyst activity. Apparently the reaction of the oxides yields $NiAl_2O_4$ during calcining. Subsequent reduction with hydrogen produces Ni and Al_2O_3 and the isolated nickel atoms cannot associate to form crystals.

Bridges, Rymer and Macives (15) undertook the study of the mechanism of the alkali promotion of chromia alumina dehydrogenation catalysts by investigating the reaction of cyclohexane over a variety of promoted and unpromoted chromia catalysts. At the same time the magnetic and adsorptive properties of these materials were determined and correlated with catalyst activity and selectivity. From the results obtained, it was shown that there are, in general, two types of active sites on chromia-alumina; a dehydrogenation type associated with the chromia portion of the surface and an acid type associated with the alumina surface. The acid sites catalyse the formation of methylcyclopentane which acts as a poison for the chromia dehydrogenation sites. The addition of potassium as a promoter neutralises these acid sites thereby preventing the formation of methylcyclopentane and hence increasing the dehydrogenation activity. Potassium, in excess of that required for this "neutralisation" is associated with the chromia-portion of the surface in such a way that it blocks some of the dehydrogenation sites and thus lowers the dehydrogenation activity. The interaction of the potassium with the chromia apparently results in the formation of a potassium-chromium complex with the chromium in a + 6 oxidation state, which, under reaction conditions reduces to a + 3 state.

The effect of intra-particle diffusion rates on the product distribution and reaction rates during catalytic conversion

by consecutive reaction steps in a porous catalyst particle was demonstrated by Weisz and Swegler (16). The reaction, cyclohexane → cyclohexene → benzene on chromia-alumina catalyst was studied in a differential reactor. Conversion rate of cyclohexene to benzene is shown to depend on the catalyst particle size. Derivation of the ratio of the two successive reaction velocity constants must include the effect of finite diffusive residence time. When this is done, consistent results are obtained for all particle sizes. Criteria for the detectability of reaction intermediates are also given.

As mentioned earlier, the dehydrogenation of cyclohexane has not been extensively studied. The scientific literature available is rather sketchy and mostly qualitative in nature. Attempts have been made to study the conversion and yields with quite a few catalysts, but a careful survey of the literature available did not reveal the rate-controlling step of the reaction or the rate equation for the catalytic dehydrogenation of cyclohexane in a flow system.

CHAPTER III.

THEORY

III. THEORY

A brief description of the merits and demerits of the system used is furnished in this capter.

Before the kinetics of any reaction can be determined, experimental data must be obtained. In a batch reactor, the variables which could be independently set are temperature, pressure, feed composition and contact time. The dependent variable is the degree of conversion. In a flow reactor, the contact time does not appear as a variable but flow rate appears in its place.

The difference between a batch reactor or the static system and a flow reactor or the dynamic system can best be expressed as follows.

The sequence of events which characterise the static system are represented in figure 1-A. The abscissa is time progressing towards the right. At t = o, the catalyst represented by a little square box is contacted with a certain concentration of reactant(s), $f(C_o)$. After elapse of an element of time this gas composition has changed a little to $f(C_1)$, which now again contacts the (same) catalyst mass, which here is indicated as being present throughout or travelling along with time. From element to element of time the gas composition is changed until a final composition

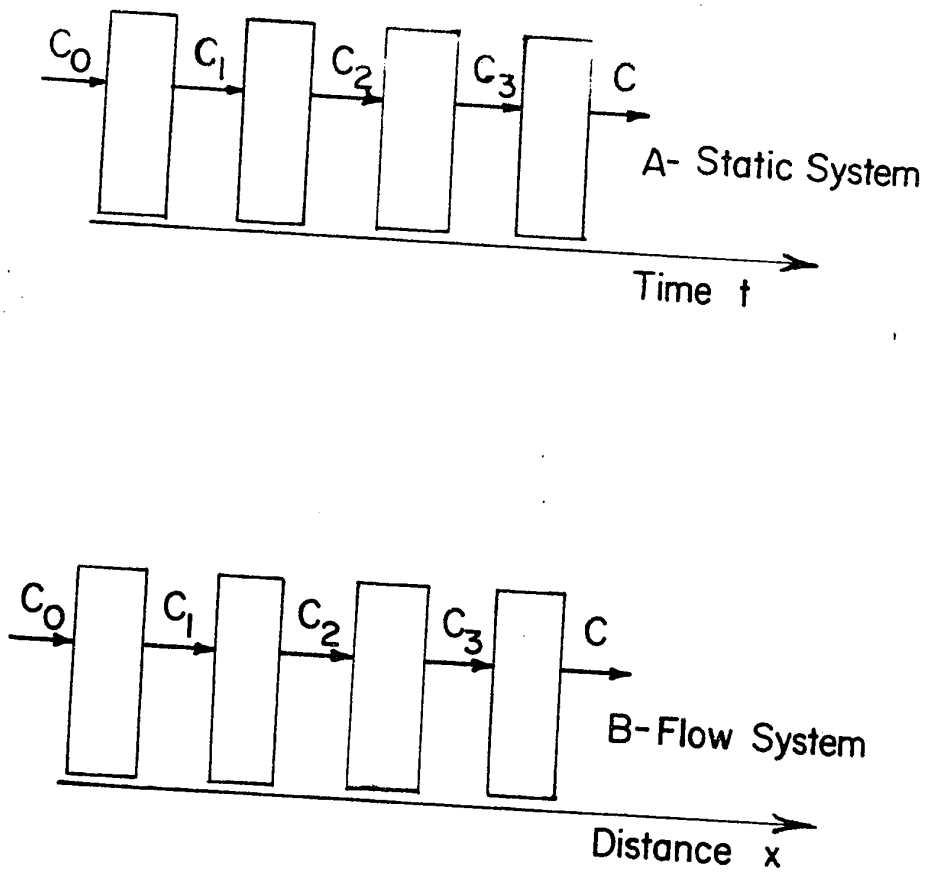

Figure 1 Time space conditions experienced by catalyst.

$f(C_f)$ is reached at time $t = t_f$.

The process of the flow-type reactor is shown in figure 1-B. Here the abscissa represents the progressive linear distance of traversal through the reactor, x. At first contact at $x = o$, the initial composition of $f(C_o)$ meets a certain amount of catalyst, is converted to $f(C_i)$, contacts another similar - although now not the identical - mass of catalyst and so forth until at $x = x_f$, the composition leaving the reactor is $f(C_f)$. A comparison of the physical pictures as represented in figures 1-A and 1-B leaves to the obvious conclusion that the formal description of the progress of the reaction in terms of reactant and product concentration will be similar and analogous in the two cases, with a space co-ordinate x in the case of the flow system replacing the former time co-ordinate t.

In view of this, the ability of the interpretation of data obtained from a flow-type system is generally subject to the same scope and limitations as those from a static system. The functional form of the reaction kinetics enters heavily into any interpretation of conversion. Analogous to the case of the static reactor, relative catalyst activities can be obtained from experiments adjusted so as to embrace the same total path of conversion in each experiment:

$$\frac{k_1}{k_2} = \frac{T_2}{T_1} \cdot \frac{S_2}{S_1} \qquad (2)$$

where T_2 and T_1 are the reactor residence times which lead to equal conversion in the two cases and S_1 and S_2 are the surface areas per unit reactor volume of the respective catalysts employed.

Again, as in the case of the static reactor, interpretation is possible only if k is constant throughout the experiment. Since in the flow system, the mass of catalyst in each space element dx is not exposed to identical gas phase conditions with respect to each other at any time, any changes of k which might occur on the basis of its previous exposure history, will, in the flow system, bring about a two-fold complication in the interpretation of data, since the catalyst histories will not only be functions of time but also of the space co-ordinate, x.

The relationship between flow rate and contact time is quite complicated and it is rather difficult to calculate contact time from flow rate accurately. However, kinetic data for catalysis are most easily obtained in a flow reactor and the ultimate use of the rate equation will also be for flow-reactor calculations. For this reason, the contact time is not used at all but a "time factor" is used. The time factor is the ratio of the catalyst mass to the feed rate, W/F. W is simply pounds of catalyst and F is pound

moles of feed per unit time. Once F is defined in a given problem, it must be consistent.

The basic equation for catalytic flow reactors is,

$$rdw = Fdx \tag{3}$$

where r = reaction rate,

w = mass of catalyst

and x = degree of conversion.

The above equation can also be written as

$$r\, d\left(\frac{W}{F}\right) = dx \tag{4}$$

$$r = \frac{dx}{d(W/F)} \tag{5}$$

This may also be expressed as Fdx/dW and has units of pound moles of feed converted per pound of catalyst per hour.

The weight of catalyst needed for a specified feed rate and conversion can then be calculated by rearranging the equation as follows:

$$\frac{W}{F} = \int_{o}^{x} \frac{dx}{r} \tag{6}$$

where W/F becomes the mass of catalyst needed per unit feed rate (usually expressed as moles of feed per unit time).

The ratio W/F is then the independent variable (for catalytic flow reactors) which is used in place of contact time. The term contact time is thus dispensed with for flow reactors.

FLOW REACTORS BEST FOR KINETIC DATA.

Kinetic data for catalytic systems are best obtained in flow reactors. Any change in catalyst activity can be detected and corrected for in a flow reactor. In a batch reactor, a decreasing activity of catalyst would not be taken into account. In a flow reactor, the time factor depends upon flow rate. If conversion drops off during a run while the flow rate is constant, it must be due to a decrease in the catalytic activity.

INTEGRAL AND DIFFERENTIAL REACTORS.

In determining kinetic data the reactor may be used as either an integral or a differential reactor. In the first case, the feed is generally unconverted reactant. The reacting mass remains in the reactor long enough for a finite amount of conversion to take place. Total conversion is determined by analysis of products. This total conversion is determined for several values of feed rates and is plotted against W/F.

Neither the integral nor the differential reactor is exclusively superior to the other. The chief advantage of the differential reactor is that it measures the reaction rate directly. Since most catalytic kinetic equations are in terms of rate, this term could be used directly to check

the equation. One disadvantage is that because of the small conversions involved, the analysis must be extremely accurate. In some reaction systems, the required accuracy would not be possible.

Another disadvantage is that although initial rates can be determined easily enough by using pure feed, rates corresponding to volume elements other than the initial one would require the use of feeds consisting of the same mixture of reactants and products that correspond to the desired value of conversion. This would be virtually impossible in a system that involved many side or secondary reactions.

INTEGRAL REACTOR MOST PRACTICAL.

The method most often used in experimental kinetic work is the integral reactor study. The advantage is that chemical analysis need not be so rigorous for a reasonable degree of accuracy because it is the total conversion that is measured. Also in each case, the feed may be pure reactants (except for recycle studies).

The main disadvantage of the integral reactor is that the rate is not measured directly. The rate is the slope of a tangent to the curve. Therefore it is the shape of the curve rather than the value of the ordinate that dtermines the rate equation. Any slight scattering of the

experimental points would have a great effect upon the values of these slopes.

Another disadvantage of the integral reactor is that the portion of the x vs. W/F curve which is most important in determining mechanisms is at low values of W/F. Yet, in this portion the accuracy of analysis becomes increasingly important since the conversion is low. Total conversion values become as difficult to obtain as differential reactor values when W/F approaches zero.

CHAPTER IV.

EXPERIMENTAL

IV. EXPERIMENTAL.

I. EQUIPMENT.

An experimental flow reactor generally consists of a reactor tube, a surrounding metal core, heating elements and suitable recording devices for temperature and pressure measurements. The reactor tube contains a support for the catalyst bed and a section for preheating the gases. The preheating section of the tube contains a spiral core so that the gas will pass rapidly through the preheat section and will come into intimate contact with the hot metal of the walls and core.

It is important that the reactants be brought up to the reaction temperature before entering the catalyst bed. The temperature within the bed must also be kept as nearly constant as possible. After passing through the reactor, the exit gases are condensed and analysed.

The equipment used for investigating the kinetics of catalytic dehydrogenation of cyclohexane is shown schematically in figures 2 and 3. A metered glass channel was provided up to a vertical preheater preceding the catalyst chamber. Cylinder nitrogen was passed through a de-oxo unit, a drying tower and then into a thermostatically controlled cyclohexane saturator. The tube carrying

Figure 2 Schematic diagram of the apparatus.

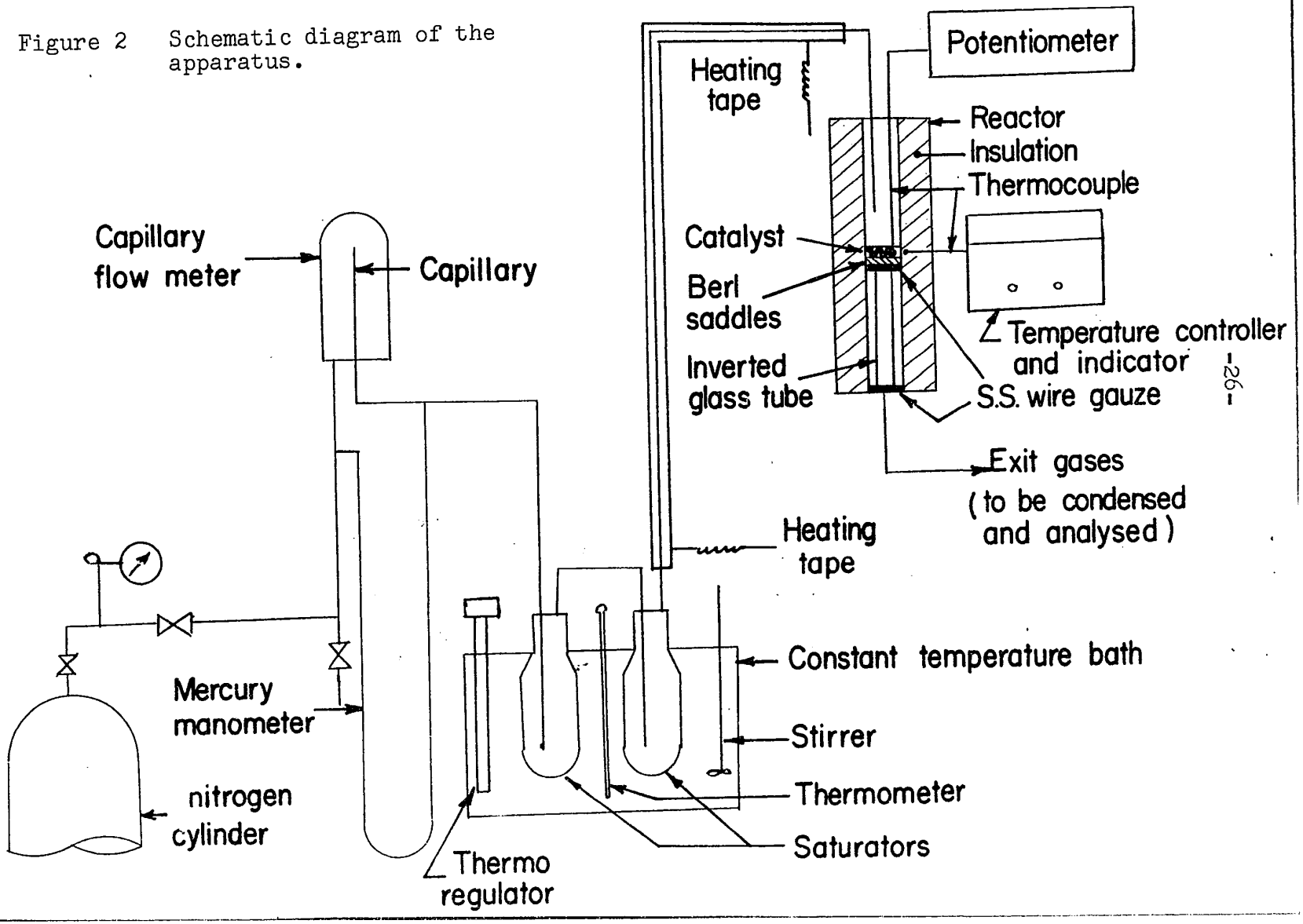

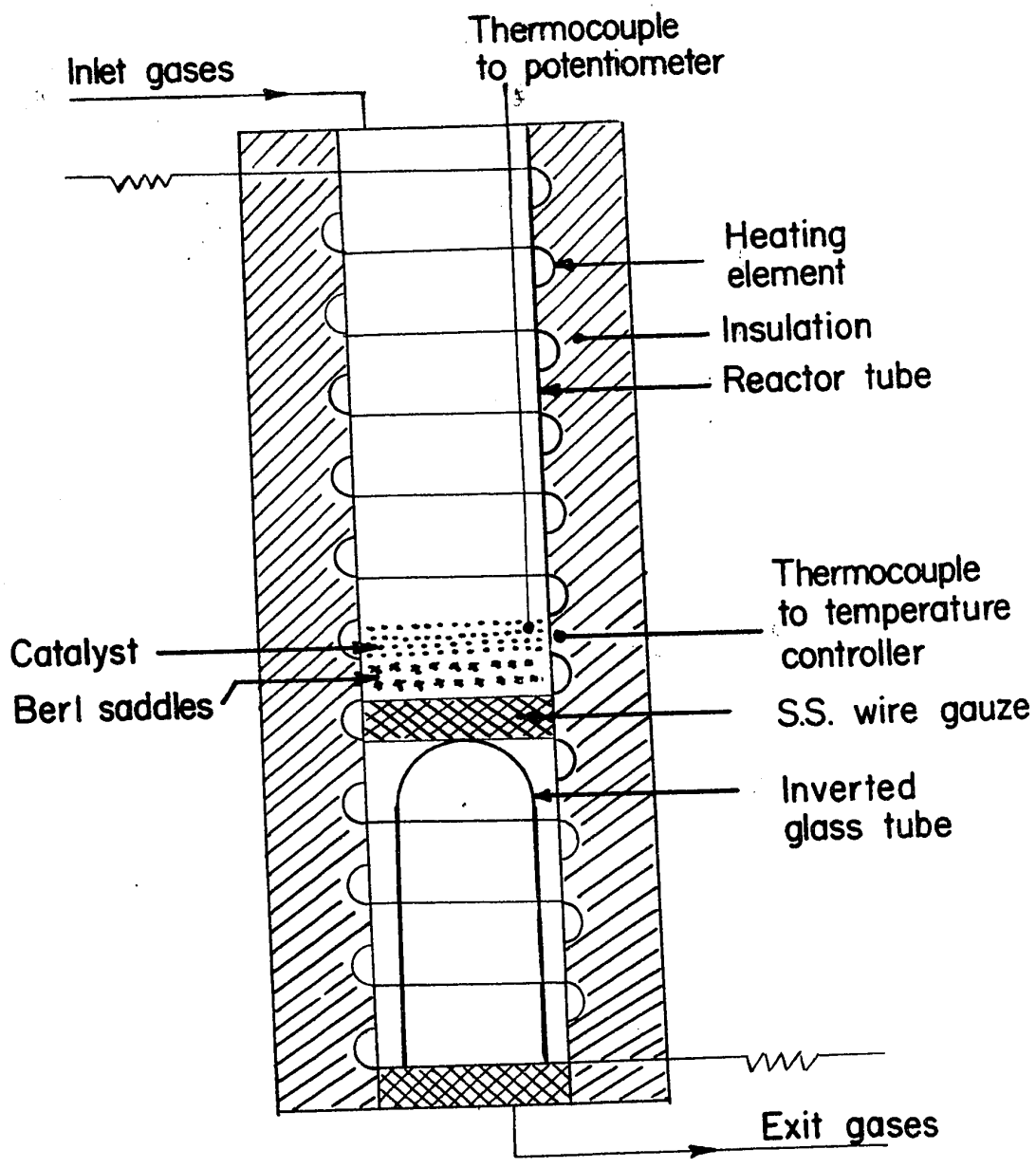

Figure 3 Reactor.

cyclohexane vapours into the reactor from the saturators was surrounded by a heating tape in order to prevent any condensation. All joints and stop-cocks were lubricated with Fisher's "Nonaq" stop-cock grease which was found to be very efficient in withstanding cyclohexane and benzene.

After passing through the preheating section of the reactor, the reactant came into contact with the catalyst bed which was supported as follows. An inverted pyrex glass tube was placed between two pieces of wire gauze made of stainless steel. Over the wire gauze at the top, berl saddles were placed and on top of this, catalyst pellets. This arrangement was found to provide a good support for the catalyst without increasing the resistance to gas flow appreciably.

The reactor tube made of quartz was equipped with heating coils and was well insulated on the outside with asbestos cement paste. A thermocouple just touching the outer wall of the reactor was connected to a Honeywell temperature controller to obtain the approximate temperature of the catalyst bed. Another thermocouple dipping into the catalyst bed was connected to a Honeywell potentiometer of the moving coil type to obtain the exact temperature of the catalyst bed.

A differential pressure capillary flow meter was used

in place of a rotameter to measure the rate of flow of the reactants. This consisted essentially of a glass chamber and a capillary tube. Nitrogen, prior to its bubbling, into the saturators containing cyclohexane and maintained at a constant temperature, passed into the glass chamber first and then through the capillary. The inlet and outlet of the glass chamber were connected to a mercury glass manometer. The difference in levels of the mercury was a measure of the rate of flow. The tip of the capillary tube was adjusted by trial and error to obtain the desired flow rate. The products issuing out of the reactor were condensed and analysed by chromatography.

II. REACTANTS.

1. Cyclohexane:

Analar grade cyclohexane with the following specifications was used.

Density at 20°C	0.779 gms/c.c.
Boiling range	80.6° to 80.8°C
Melting point	5°C
Residue on evaporation	0.00%

2. Nitrogen:

Nitrogen from cylinder was purified by passing through a " de-oxo" tube and a drying tower containing silica gel before bubbling into the saturators. Specifications of Union

Carbide on the dry nitrogen supply was as follows:

Minimum Purity	99.7%
Grains of water vapour	8.5 or less

1 grain = 3 ppm.

III. CATALYSTS

1. Nickel oxide on kieselguhr:

Girdler catalyst	T - 316
Nickel	50%
Pellet size	3/16" x 1/8"

2. Nickel oxide on alumina:

Girdler catalyst	T - 310
Nickel	10 - 12%
Pellet size	3/16" x 1/8"

3. Nickel oxide, chromium oxide:

Girdler catalyst	T - 314
Nickel	8 - 10% (plus chromium)
Pellet size	3/16" x 1/8"

4. Cobalt oxide on alumina:

Girdler catalyst	T-302
Cobalt	10 - 12%
Pellet size	3/16" x 1/8"

5. Platinum on alumina:

Girdler catalyst	T - 309
Platinum	0.10%
Pellet size	3/16" x 1/8"

6. Palladium on alumina:

Girdler catalyst	T - 308
Palladium	0.05%
Pellet size	1/8" x 1/8"

Catalysts 1 to 6 are experimental catalysts in the form of pellets supplied by Girdler catalysts, Chemical Products Division of Chemetron Corporation, P.O. Box 337, Louisville 1, Kentucky, U.S.A. In addition to these, two other catalysts were prepared as follows.

7. Nickel oxide on pumice:

Pumice stones were crushed to - 20, + 40 mesh size and boiled in concentrated hydrochloric acid for one hour, followed by evaporation to dryness. The dried pumice was washed with distilled water until successive washings gave no precipitate with silver nitrate (to ensure the complete removal of chloride ions) and the washed pumice dried. Nickel nitrate solution ($Ni(NO_3)_2 . 6H_2O$ - Fisher Scientific Co.) of desired concentration was prepared and mixed with required amount of pumice. The contents were well stirred, allowed to stand for a few hours and dried overnight. The dried

sample was calcined for six to eight hours at a temperature of 400 to 450°C.

8. Pure nickel oxide:

Excess of ammonium carbonate was added to a solution of nickel nitrate to precipitate nickel carbonate. The contents were well mixed and filtered. The precipitate was washed thoroughly with distilled water, dried overnight and calcined at about 350°C for six to eight hours.

IV. OPERATING PROCEDURE

1. Calibration:

To begin with, the capillary flow meter was calibrated to obtain the relationship between ΔP (difference in pressures as shown by manometer) and F_C and F_N (flow rates of cyclohexane and nitrogen respectively). This was achieved as follows.

The reactor was fitted in line with support for catalyst and at exact conditions of operation (except for filling catalyst). Nitrogen gas was admitted into the saturator and through the reactor to exit. Flow of nitrogen was adjusted to a steady value and the reading of the manometer was noted. Cyclohexane in the exit gases was condensed for a known period of time, and weighed, thereby obtaining cyclohexane flow rate. Flow rate of the uncondensed gas, nitrogen, was measured by the common soap bubble method.

Similarly, the procedure was repeated for various values of ΔP and flow rates of cyclohexane and nitrogen were plotted against ΔP to get the desired calibration curves, which are shown in fig. 4.

Periodically, during runs, the calibration was repeated to check for possible changes in flow rates.

2. Blank run:

Before starting runs with a catalyst, a series of blank runs (without catalyst) were performed and it was clearly established that no cyclohexane was converted to benzene in the temperature range of 200 to 600°C and in the absence of catalyst.

3. Experimental Details:

Figure 5 shows the general scheme of collecting data. For each of the catalysts tried two or more weights of catalyst was taken. For each weight of catalyst about ten temperatures were tried in order to obtain a fairly wide range of temperature, and for each temperature, four different flow rates were considered. As is to be expected, not all the runs showed conversion, probably either because the amount of catalyst used was less than the required minimum or the temperature of investigation happened to be lower than that at which the reaction would begin.

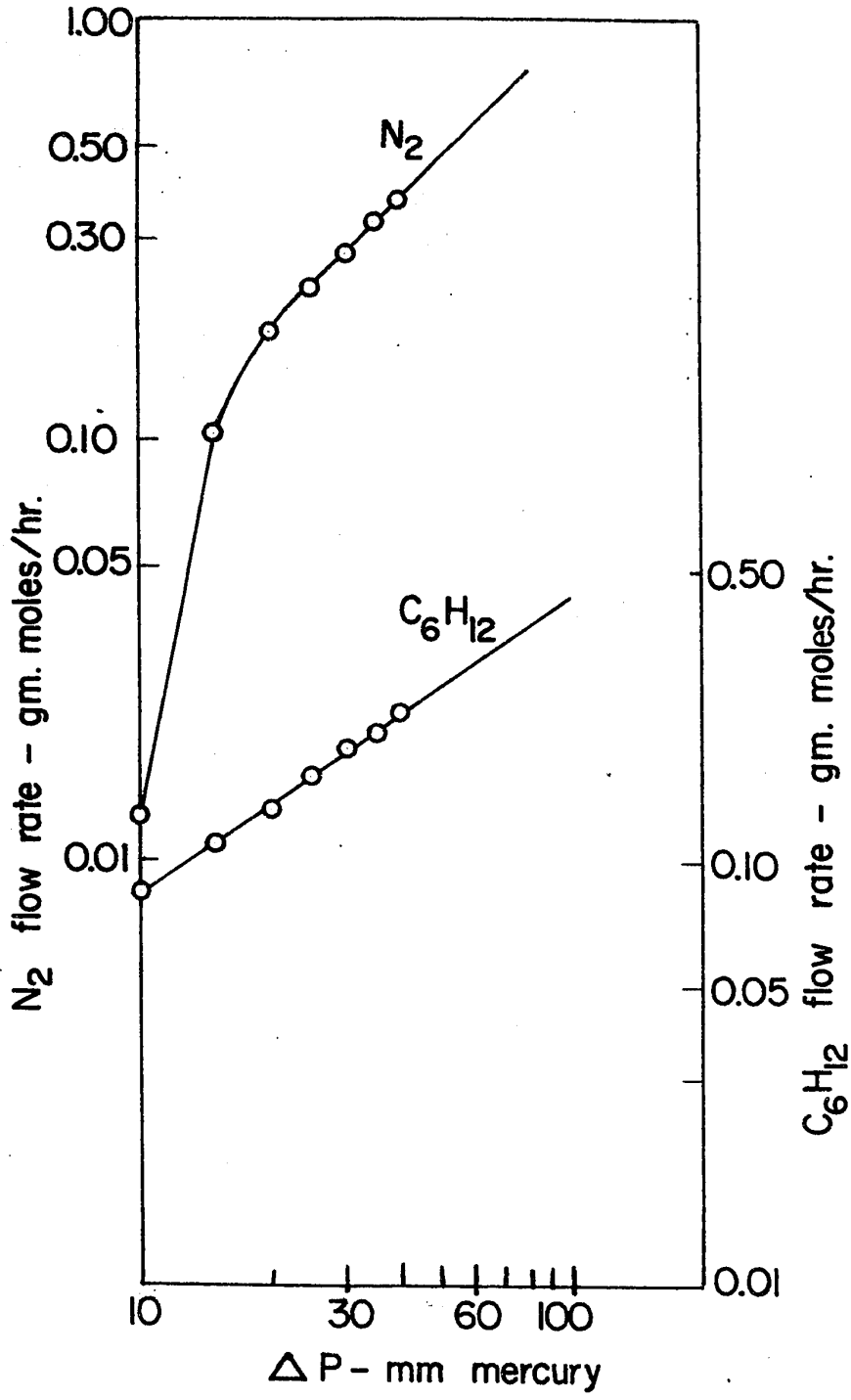

Figure 4 Calibration of saturator.

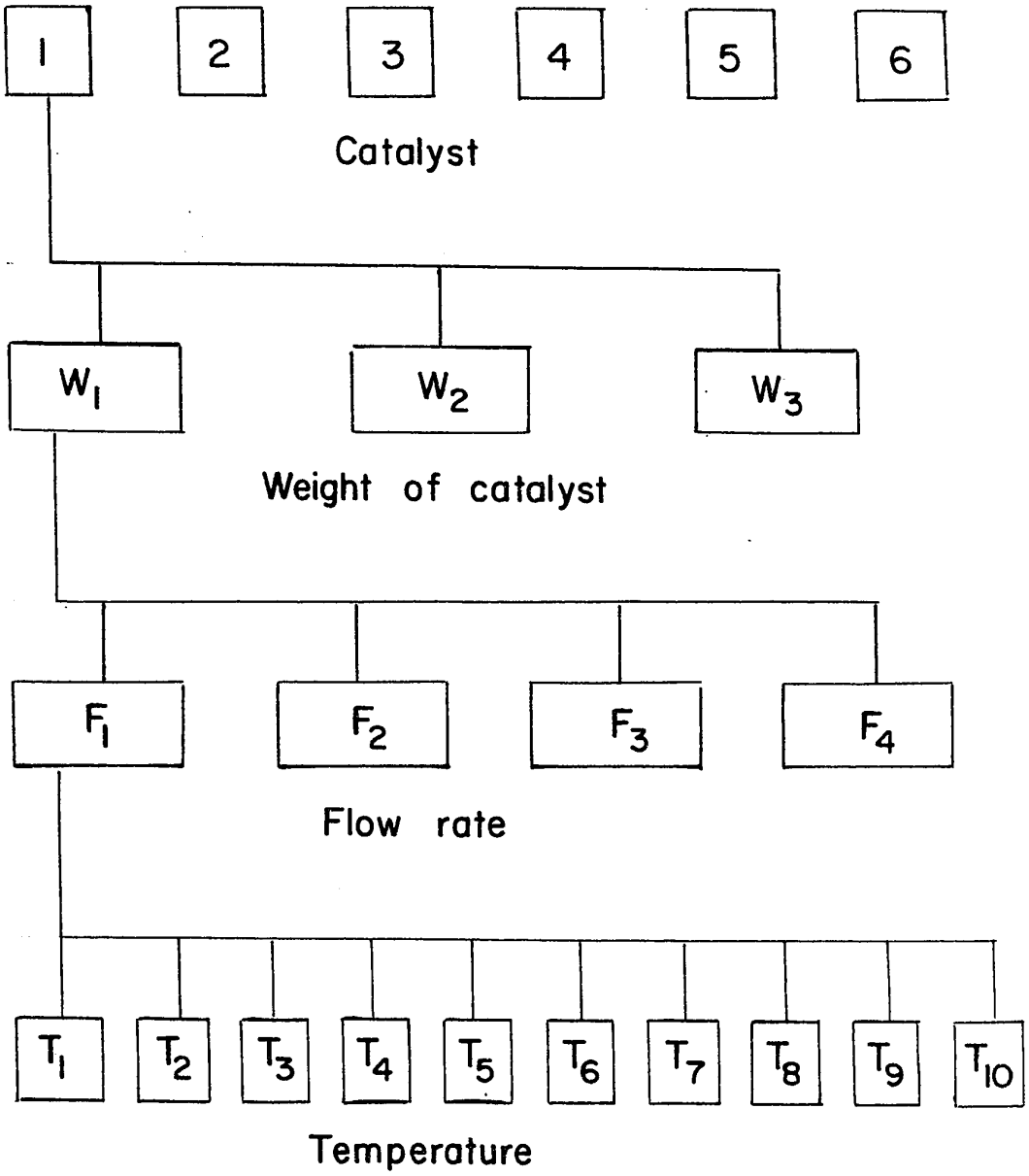

Figure 5 Collection of experimental data.

For the start of a run, nitrogen was slowly passed through the reactor while the catalyst was brought up to the required temperature. When the required temperature was attained, nitrogen flow was diverted into the saturators and the flow rate adjusted to the desired value. This was continued for about half an hour to reach steady state. Condensation of cyclohexane in the exit gases began and was continued for fifteen minutes at the end of which the run was stopped and the products analysed.

The procedure was repeated for other flow rates also. At regular intervals, during the run, the temperature of the catalyst bed was measured with the potentiometer and in cases of variation, the average value taken.

After finishing the runs at different flow rates for a certain temperature, the temperature was changed to another value and runs taken in an identical manner. This completed the series of runs for a certain weight of catalyst.

Next, the unit was switched off, gas flow was shut off and the reactor was removed, thoroughly cleaned and fitted back with a different amount of the same catalyst. The operation was repeated exactly as before.

Runs were made with a third amount of the same catalyst before switching over to another catalyst.

4. Product Analysis:

The products were analysed by a 154 D Perkin Elmer gas chromatograph containing two 4-meter colums of carbowax 1500 on teflon. By preliminary tests the following operating conditions were found to be the best.

Temperature coarse	150°C.
Temperature fine	150°C.
Power (for 50% on-off duty cycle)	80 watts
Carrier gas	Helium
Helium pressure	24 $^{lbs}/_{sq.in}$ gauge
Rotameter reading	4.0
Recorder chart reading	7.5
Recorder zero setting	3.91
Sensitivity	128

The recorder was coupled to a PT 1600 integrator, from which the values of the areas of the peaks were read off directly.

The chromatograph was calibrated with known mixtures of benzene and cyclohexane. Table 1 and figure 6 give details of the calibration.

Once the calibration plot was made, from the values of cyclohexane and/or benzene peaks obtained for any sample, the percentage conversion was directly read from the chart. Each

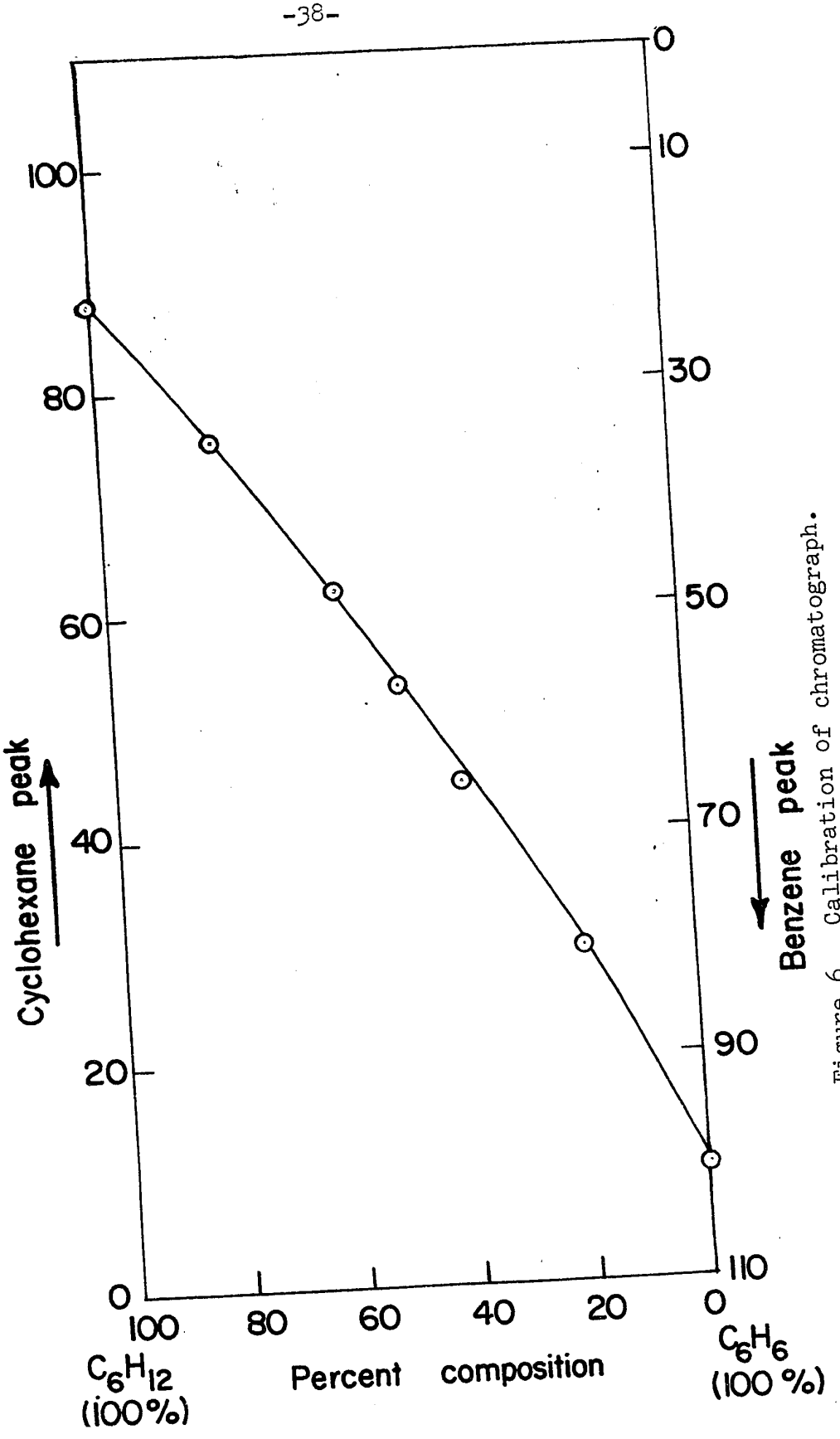

Figure 6 Calibration of chromatograph.

sample was analysed twice or more until concurrent values were obtained, though it is felt that this was unnecessary since the values were identical in most of the cases. Also, no trace of compounds other than benzene and cyclohexane were discovered, establishing that intermediate products, if any, were short-lived.

Figures 7 and 8 show the peaks obtained in a typical analysis of the products.

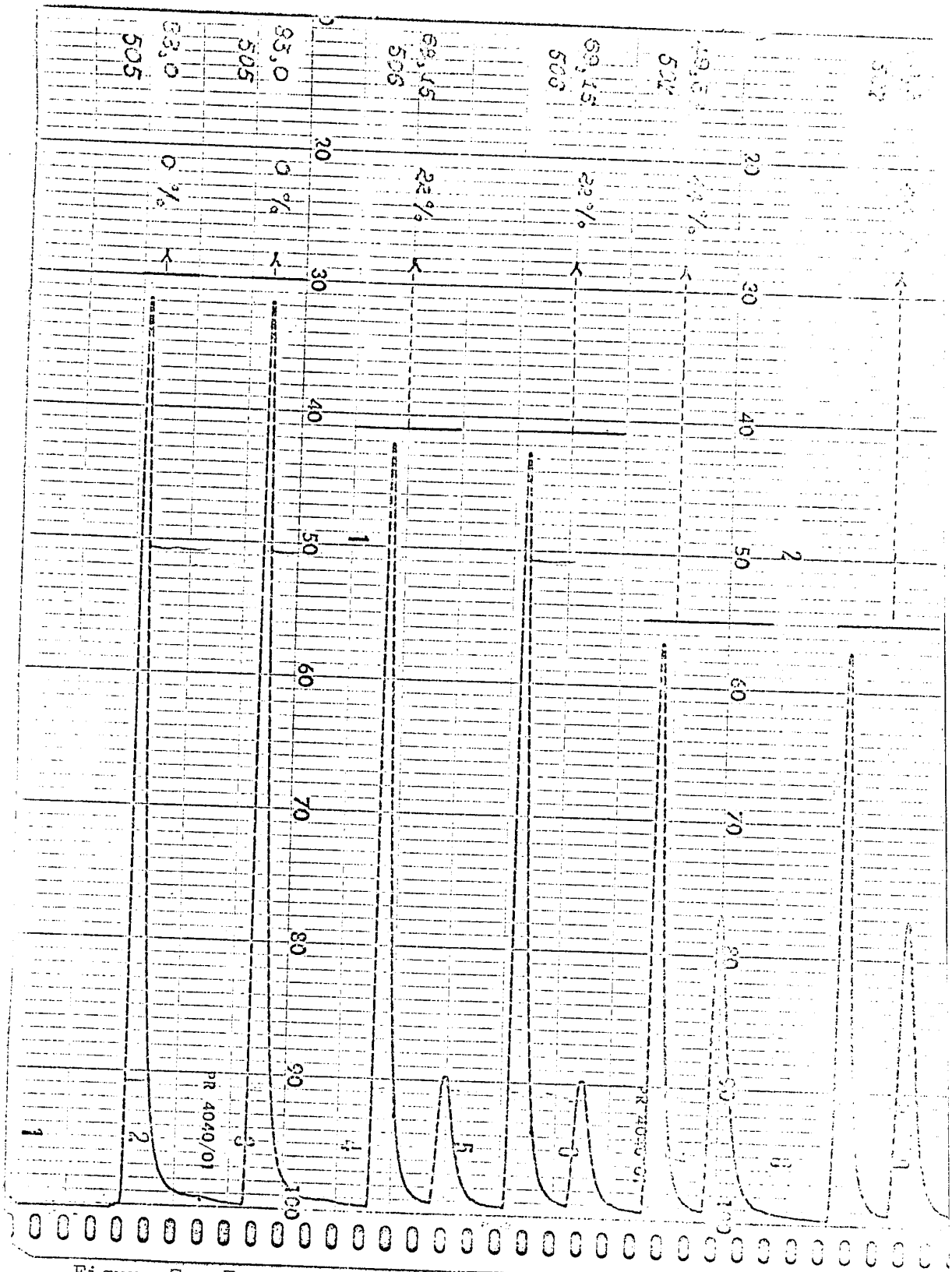

Figure 7 Typical analysis of products.

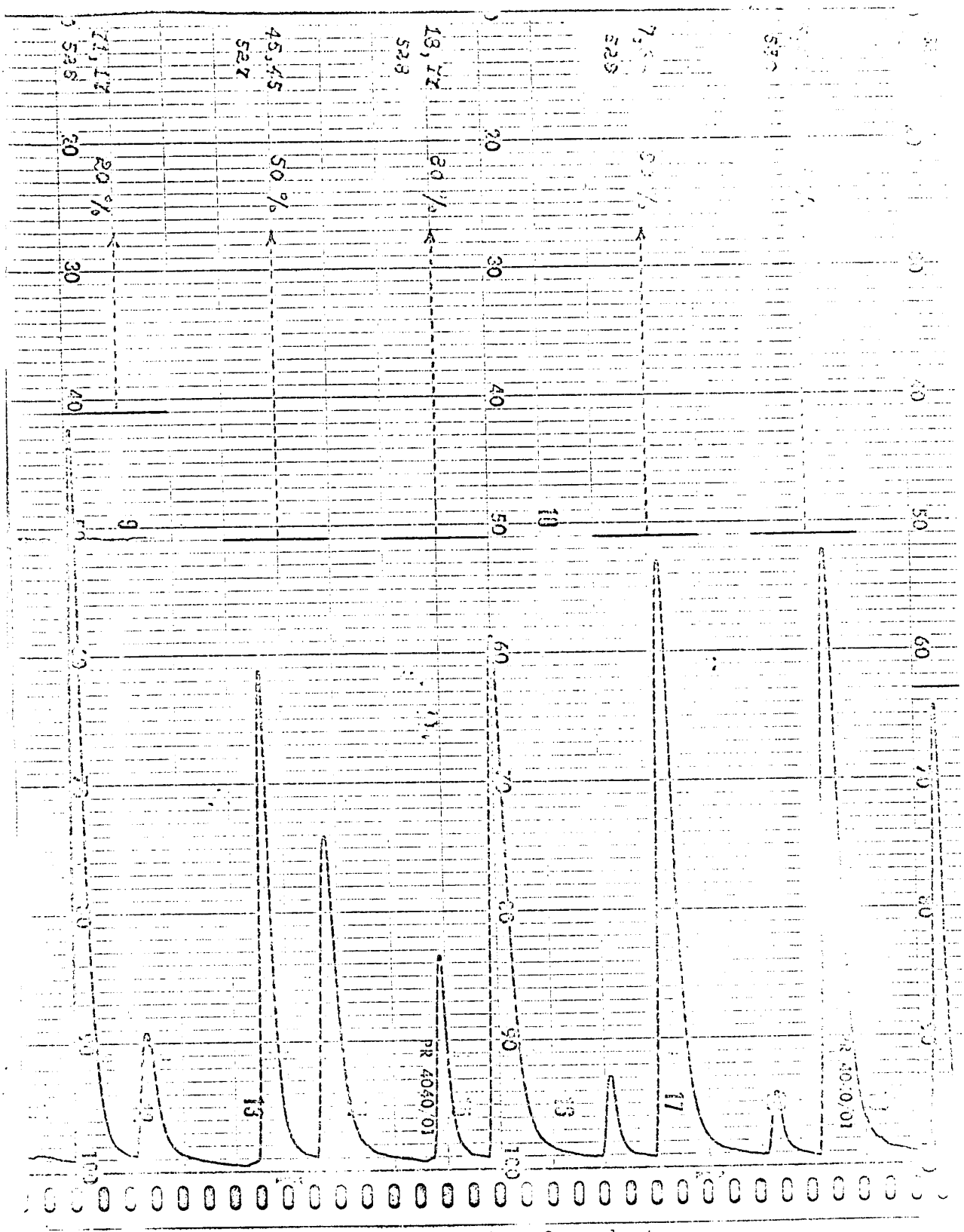

Figure 8 Typical analysis of products.

CHAPTER V.

KINETIC ANALYSIS OF DATA

V. KINETIC ANALYSIS OF DATA

Effect of temperature on conversion:

The effect of temperature on the conversion of cyclohexane to benzene was very similar to that observed by Ross and Valentine (1). The catalyst, platinum on alumina, behaved in a manner similar to that of nickel on silica catalyst studied by Ross and Valentine. They studied the behaviour as follows.

Using (a) hydrogen, (b) nitrogen and (c) hydrogen/nitrogen (2:3 $^{v}/_{v}$) as carrier gases, no appreciable reaction was observed below 150°C. In figure 9 the conversions are plotted against temperature. Each curve shows the same activity pattern which may be separated into three fairly well-defined regions. From 150° to 220°C there is a rapid rise in the conversion (activity of the catalyst). This starts to decline at the higher temperature and then almost remains steady for a further 20°. Finally from 240° to 280°C, the fraction converted falls rapidly from values in the region of 0.2 – the actual values depending on the carrier gas composition – to an indicated zero value.

In figure 10 is presented a comparison of the activity pattern on platinum on alumina catalyst and a striking similarity is noticeable. Up to 150°C no appreciable reaction

Carrier gas

Top curve : Nitrogen

Middle curve : Hydrogen/Nitrogen $(\frac{2}{3} \cdot \frac{V}{V})$

Bottom curve : Hydrogen

Inset : Arrhenius Ea plot

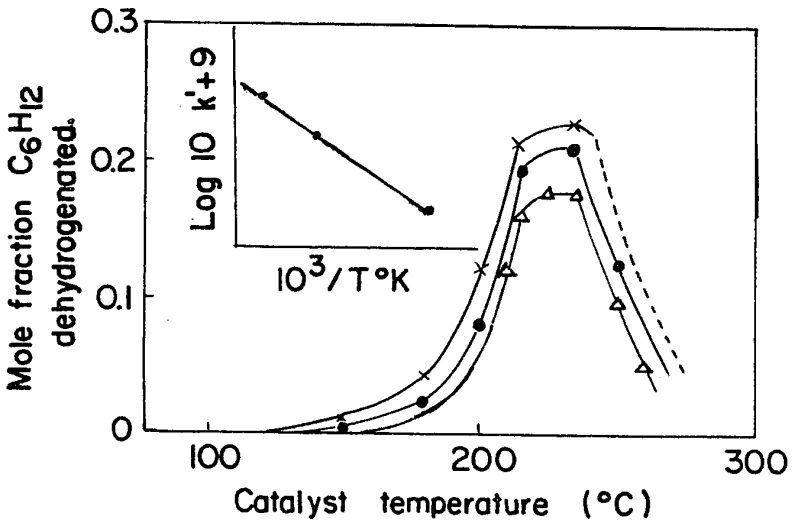

Figure 9 Effect of temperature on fraction dehydrogenated.

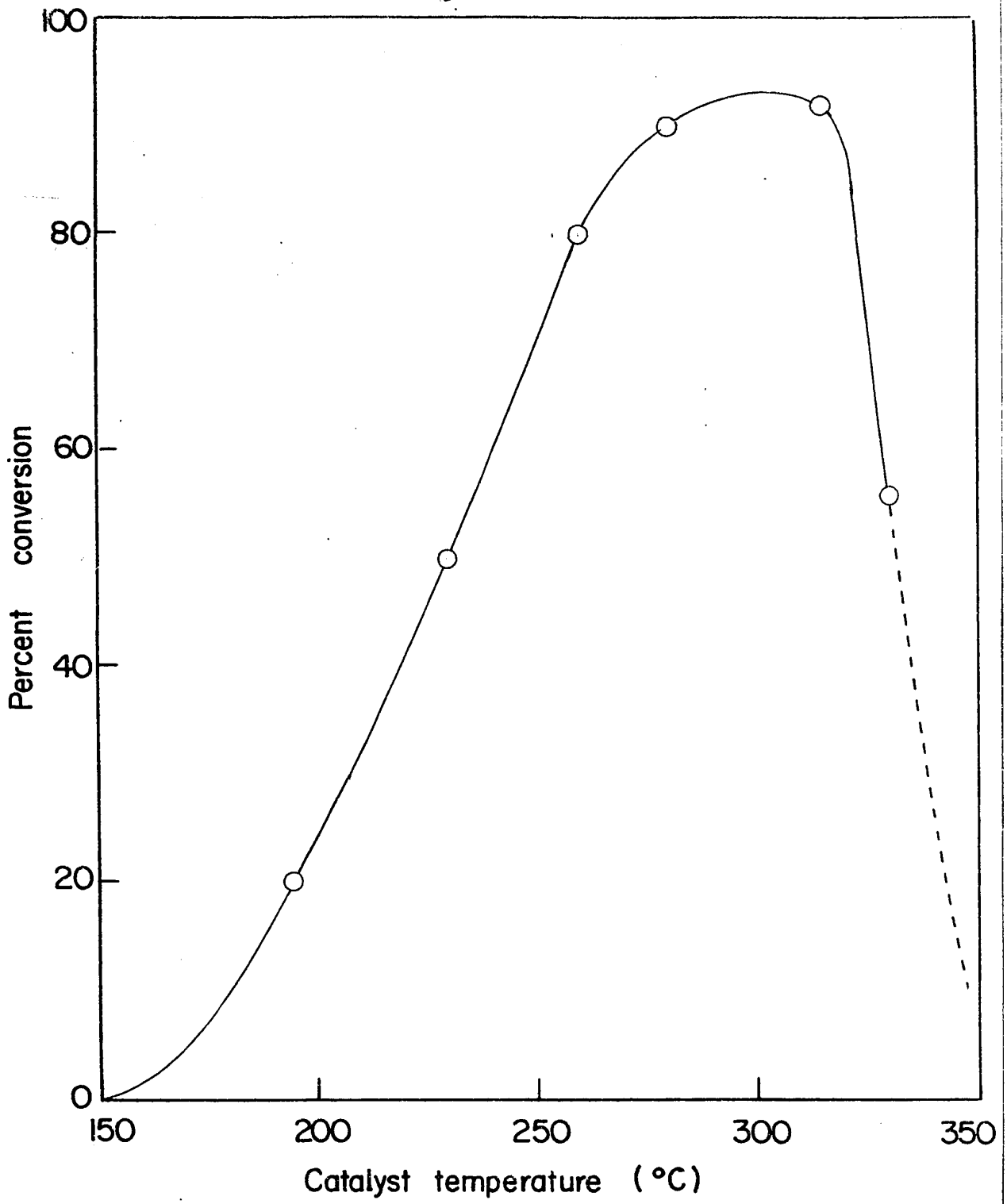

Figure 10 Effect of temperature on fraction dehydrogenated.

(conversion) was observed. From about 175 to 275°C the conversion rose rapidly. This was then followed by a steady value for about 25° and then rapidly declined.

As such, the activity pattern is found to be in excellent agreement with the earlier work; the only difference being that a very high value of conversion (around 92%) is observed over platinum on alumina while Ross and Valentine reported a peak conversion of around 25% over nickel on silica.

The activity pattern for catalysts other than platinum on alumina was not studied due to the conversion taking place only at high temperatures. All the investigations of kinetic parameters undertaken in this work were restricted to that portion of the curve in which conversion increased with temperature.

I. Experimental Data.

The experimental data thus obtained are presented in tables 2 to 8. On an average about sixty runs were made for each catalyst. After a steady state was attained, samples were collected for fifteen minutes interval for every run. A constant check on cyclohexane flow rate and catalyst temperature was maintained. The products thus collected were analysed by gas chromatography.

II. Effect of temperature on conversion:

As mentioned earlier, the studies on this work were restricted to that portion of the temperature-conversion curve where conversions increased with temperature. Plots of conversion against temperature with cyclohexane flow rate as parameter are shown in figures 11 and 12.

III. $^{W}/_{F}$ vs. X plots:

Integral reactor data are usually presented as X vs $(^{W}/_{F})$. From the experimental points collected and from the previously prepared calibration chart for flow rates, the value of $(^{W}/_{F})$ was calculated and plotted against conversion with temperature as parameter. Table 9 shows the values of $(^{W}/_{F})$ and X for the various temperatures of investigation. Different values for $(^{W}/_{F})$ were obtained by varying the flow rate for a fixed amount of catalyst and vice versa.

IV. Determination of initial rates:

The rate of reaction corresponding to any given value of $(^{W}/_{F})$ is the slope of the tangent to the curve at that point. The slope at $(^{W}/_{F}) = 0$, $X = 0$, is the initial rate, the rate when no products are present.

There are four possible methods for determining the initial rate from the $(^{W}/_{F})$ vs. X curve. They are,

Figure 11 Effect of temperature on conversion - cobalt oxide on alumina.

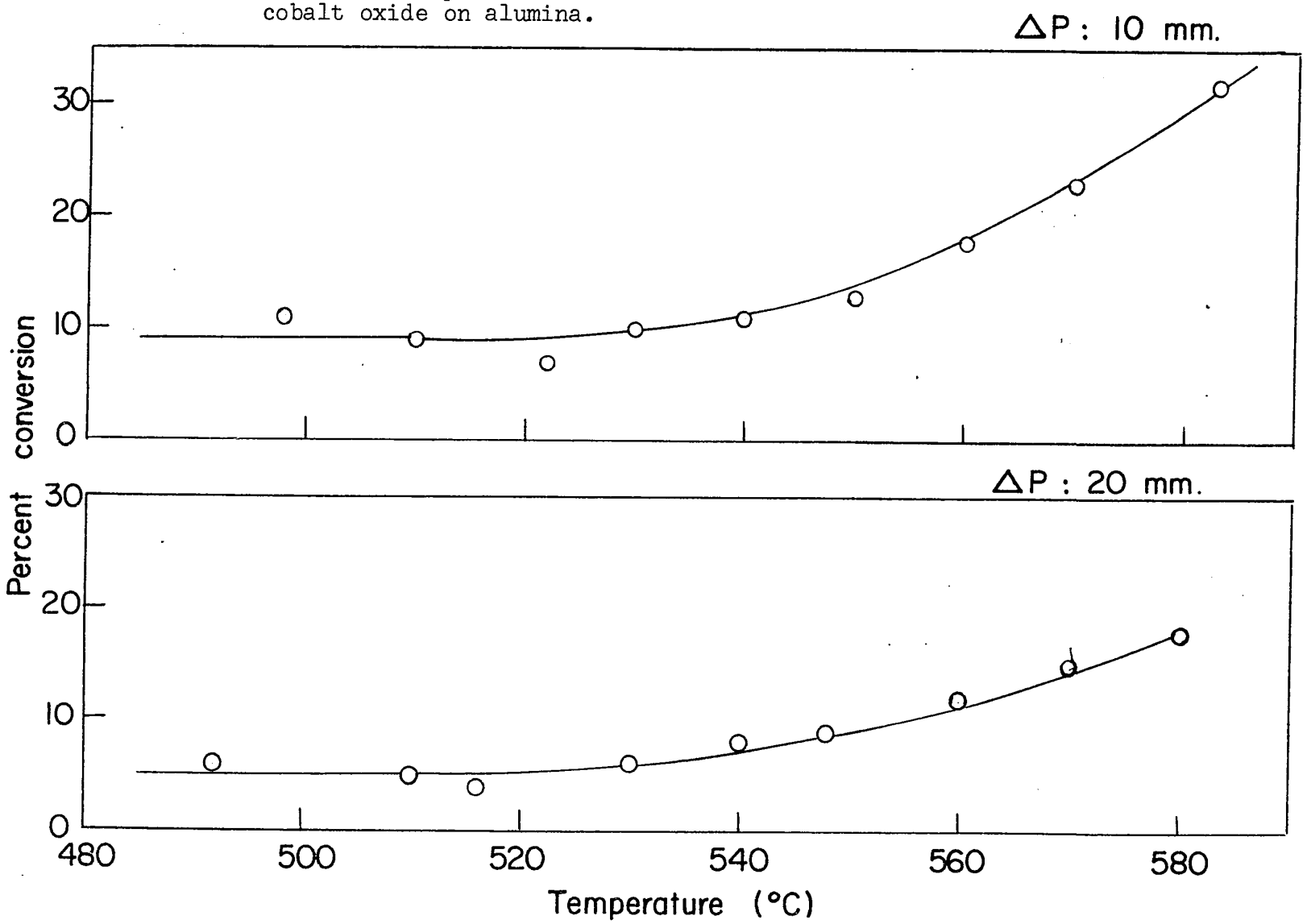

Figure 12 Effect of temperature on conversion - Cobalt oxide on alumina.

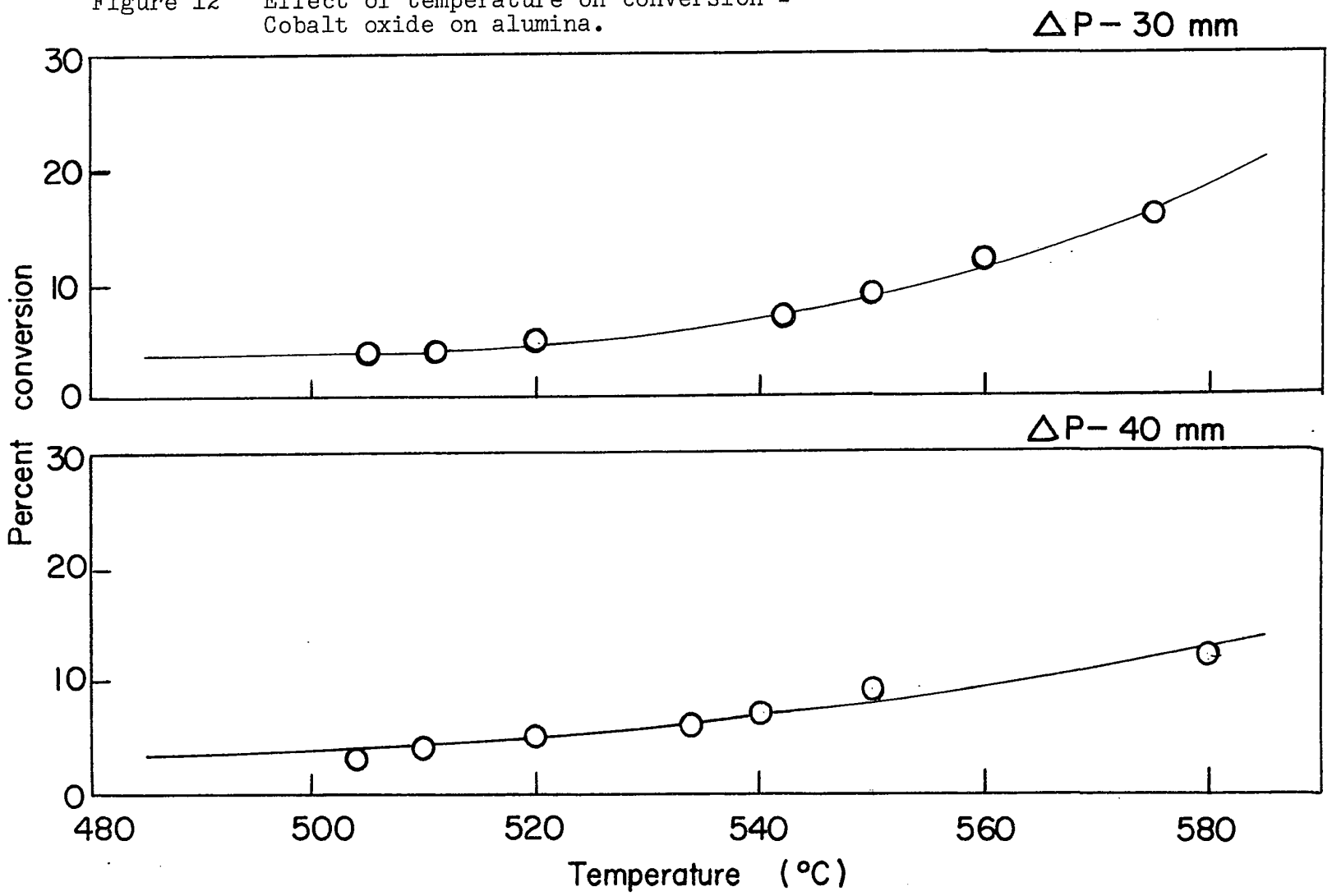

(1) Measure the slope of the tangent to the curve at the point $x = 0$, $(W/F) = 0$.

(2) Plot $\frac{x}{(W/F)}$ vs. (W/F) and extrapolate to $(W/F) = 0$

(3) Measure slopes of tangents at several values of (W/F), plot slopes vs. (W/F) and then extrapolate to $(W/F) = 0$.

(4) Fit an empirical equation to the x vs. (W/F) curve and differentiate the equation. An empirical equation which may sometimes be used is,

$$x = a \tanh (b (W/F))$$

All four methods have their disadvantages and no one is exclusively superior to the other three.

The first is the most direct method but the mechanics of obtaining an accurate tangent at the origin are difficult since the data are the least accurate here.

When the rates are determined by measuring the slopes of the tangents to the x vs. (W/F) curves, it is also essential that these tangents be drawn accurately. For a curve which is not circular, there is no exact geometric construction which gives a tangent. There is one device, the Simons Tangentiometer, which, by the use of mirrors, facilitates the construction of tangents to non-circular curves.

The second method of determining initial rates has the

advantage of avoiding the tangent construction; but the $\frac{x}{(W/F)}$ value may show a sharp increase even on log-paper as (W/F) approaches zero.

The third method uses data at finite (W/F) values where they are more accurate and also avoids the use of a tangent at the origin.

The fourth method is least cumbersome mechanically but it may not always be possible to find the correct equation. A series equation such as

$$x = a + b(W/F) + c(W/F)^2 + ...$$

should not be used since the initial rate would depend upon a single value of the constant b. A trigonometric, hyperbolic, Bessel or similar function is needed.

The method of obtaining initial rates is a matter of choice and in this work, mostly, the second method was followed.

From the values presented in table 9, curves of (W/F) vs. x were plotted and from the smoothed curves, table 10 was prepared showing (W/F), x and $\frac{x}{(W/F)}$. A plot of (W/F) vs. $\frac{x}{(W/F)}$ was made, extrapolated to $(W/F) = 0$, and the initial reaction rate was obtained. Figures 13 to 21 show the conversion curves for various temperatures.

In figures 22 and 23 (W/F) was plotted against $\frac{x}{(W/F)}$

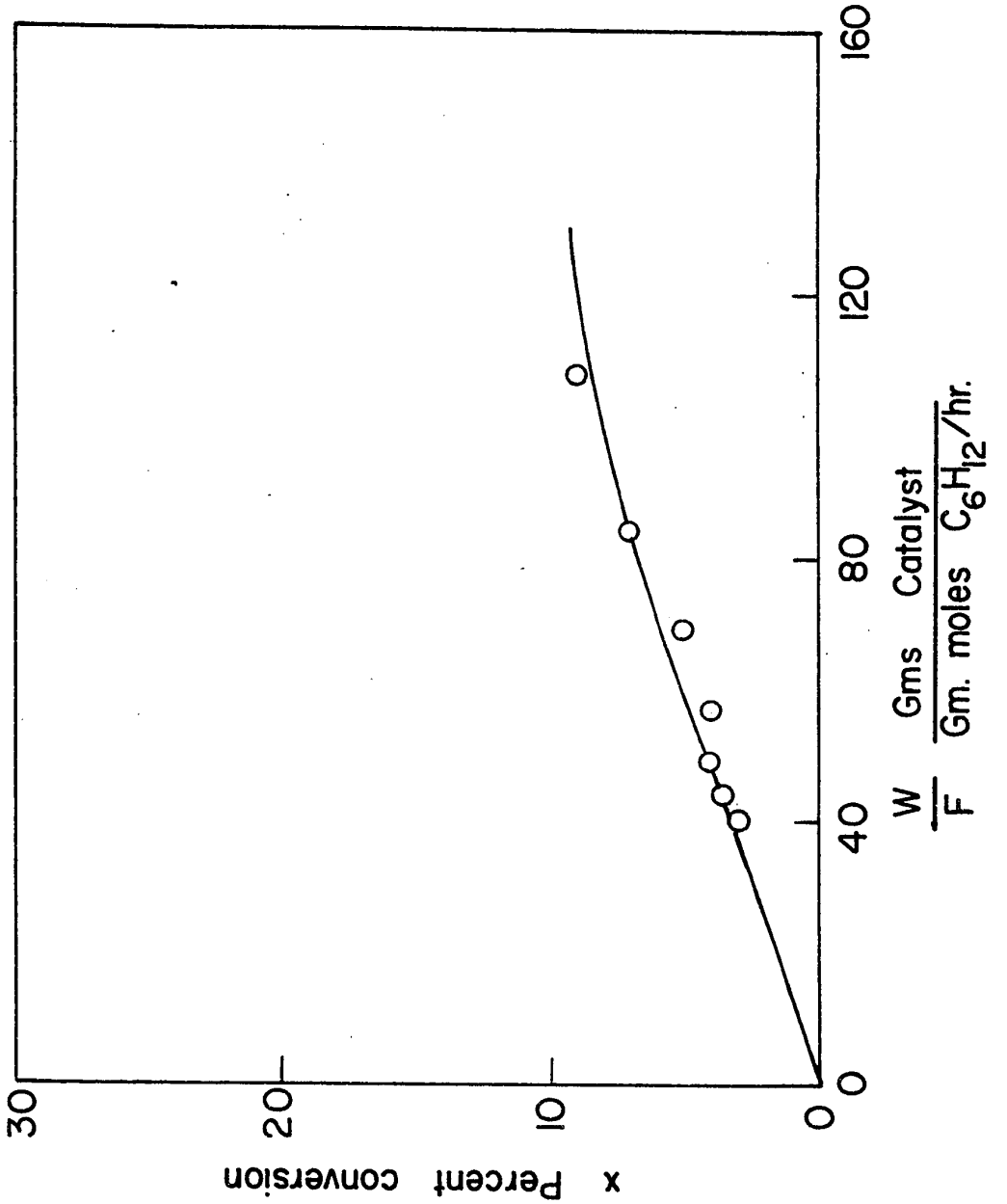

Figure 13 Conversion curve at 500°C.
Cobalt oxide on alumina.

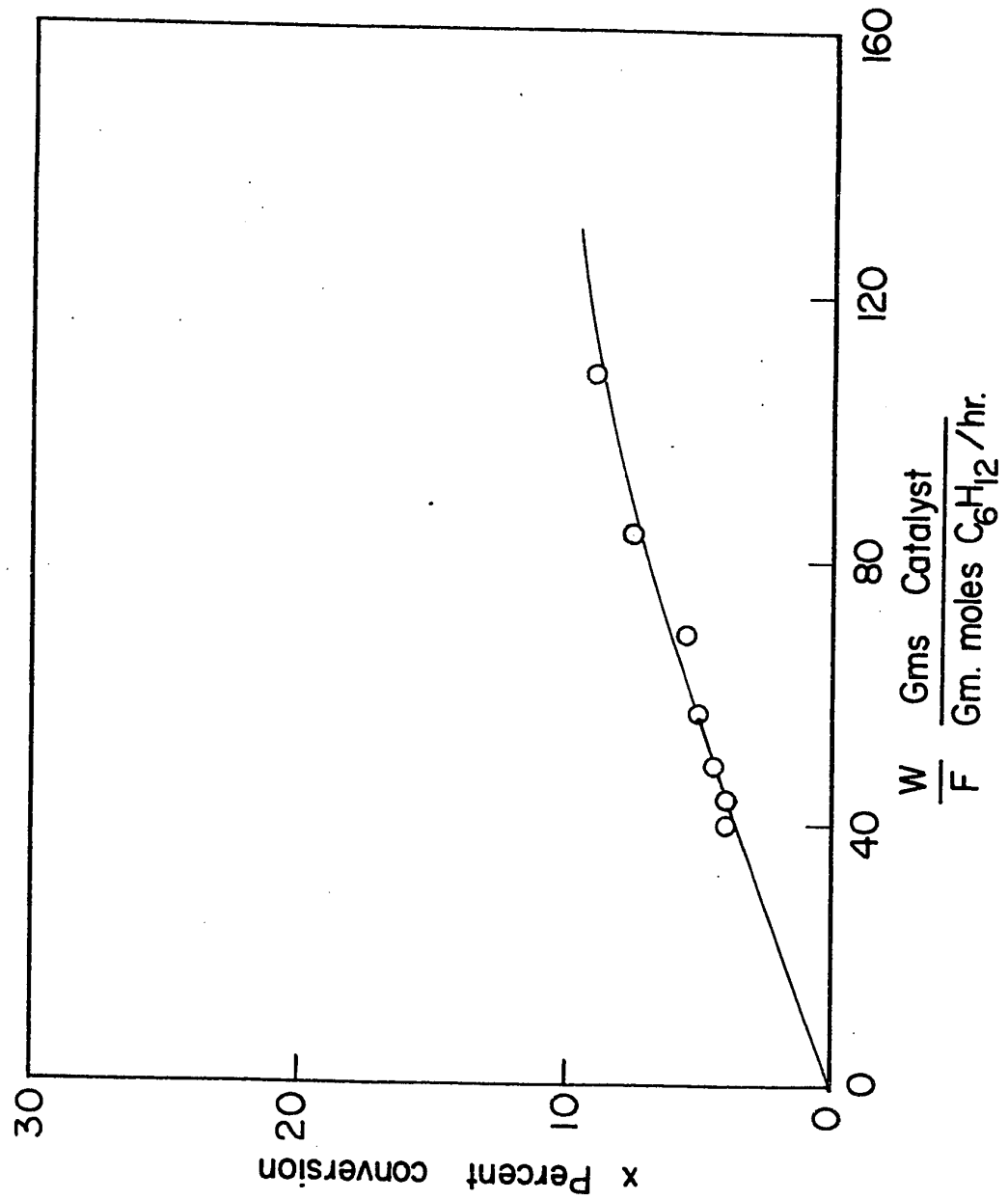

Figure 14 Conversion curve at 510°C.
Cobalt oxide on alumina.

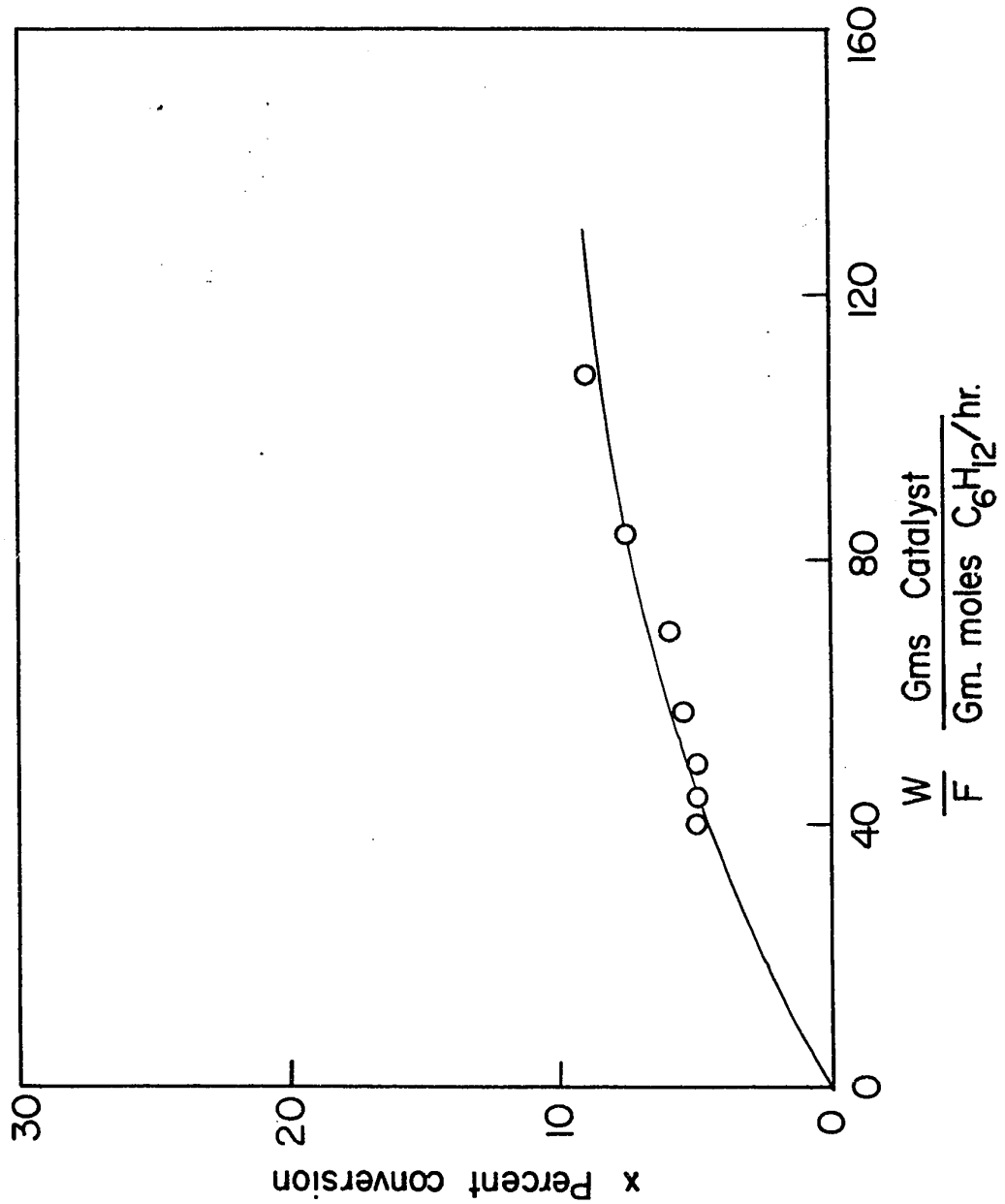

Figure 15 Conversion curve at 520°C.
Cobalt oxide on alumina.

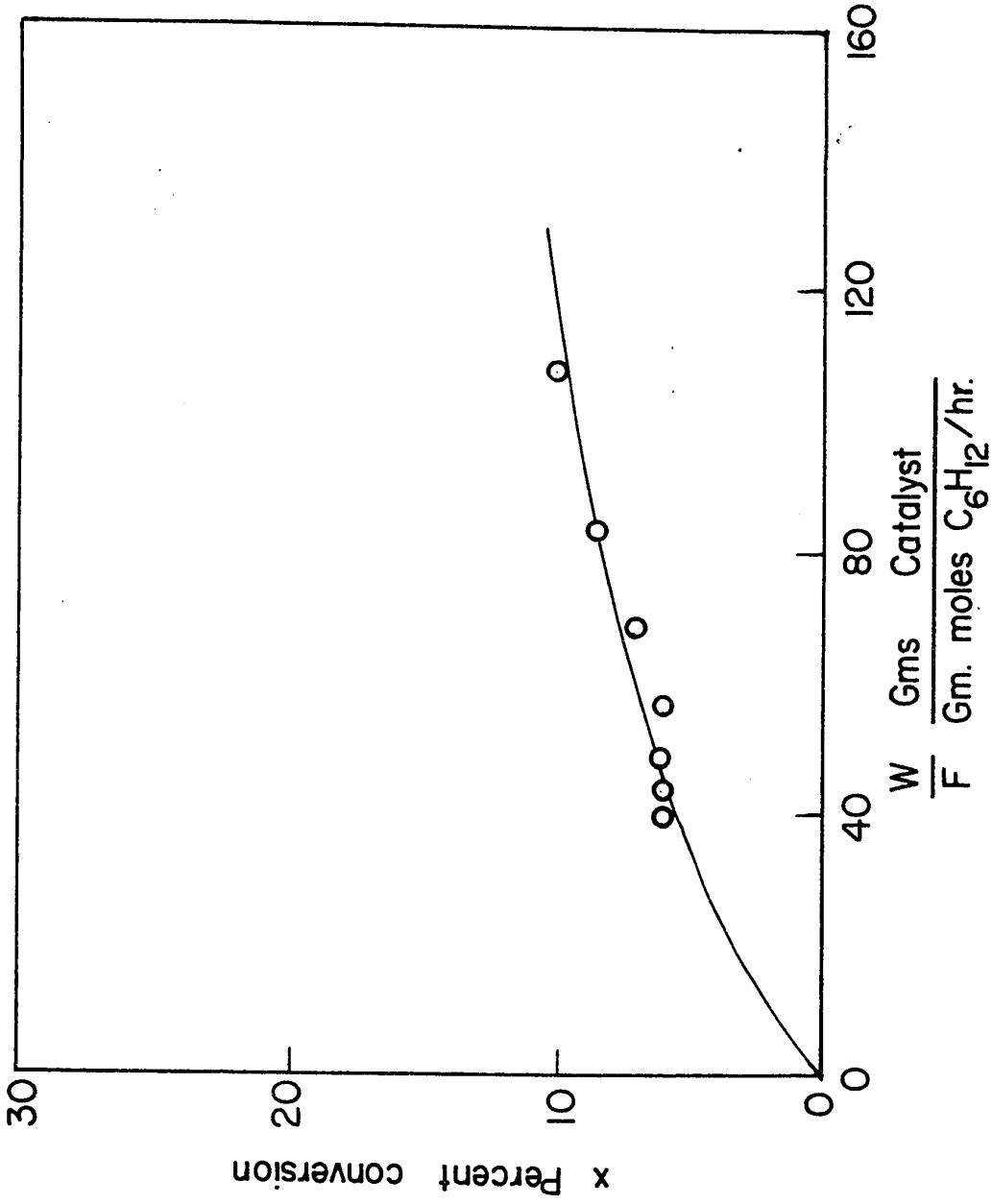

Figure 16 Conversion curve at 530°C.
Cobalt oxide on alumina.

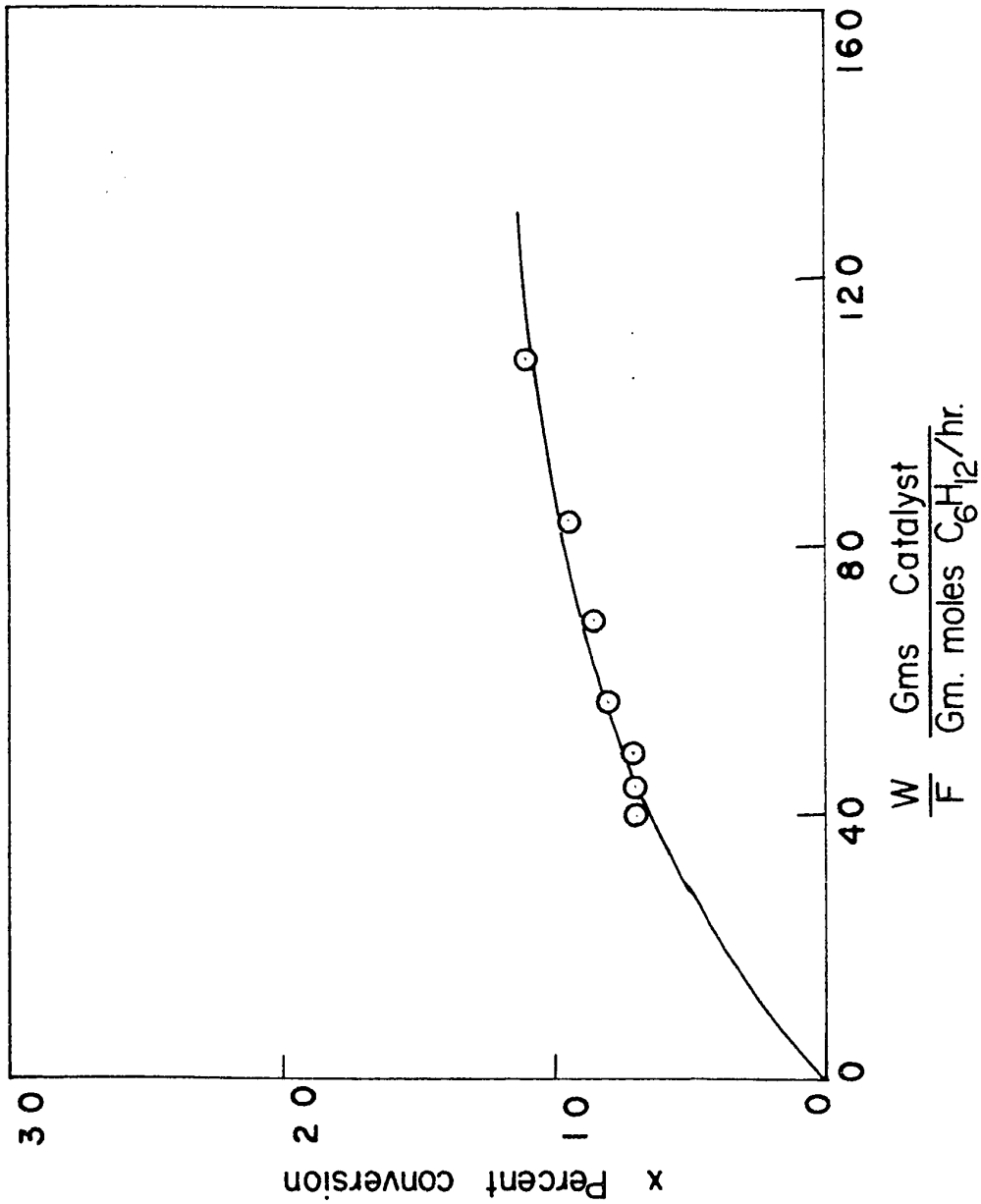

Figure 17 Conversion curve at 540°C.
Cobalt oxide on alumina.

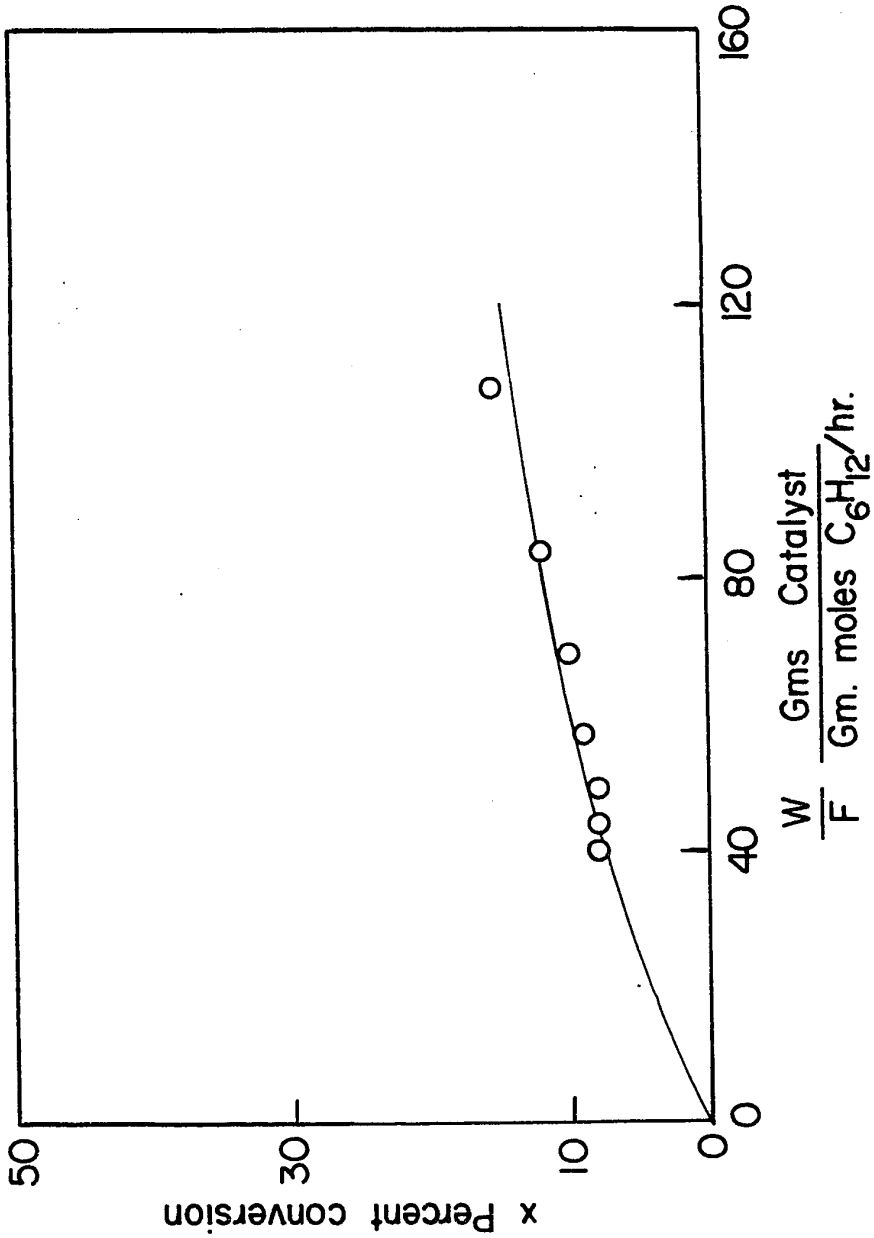

Figure 18 Conversion curve at 550°C.
Cobalt oxide on alumina.

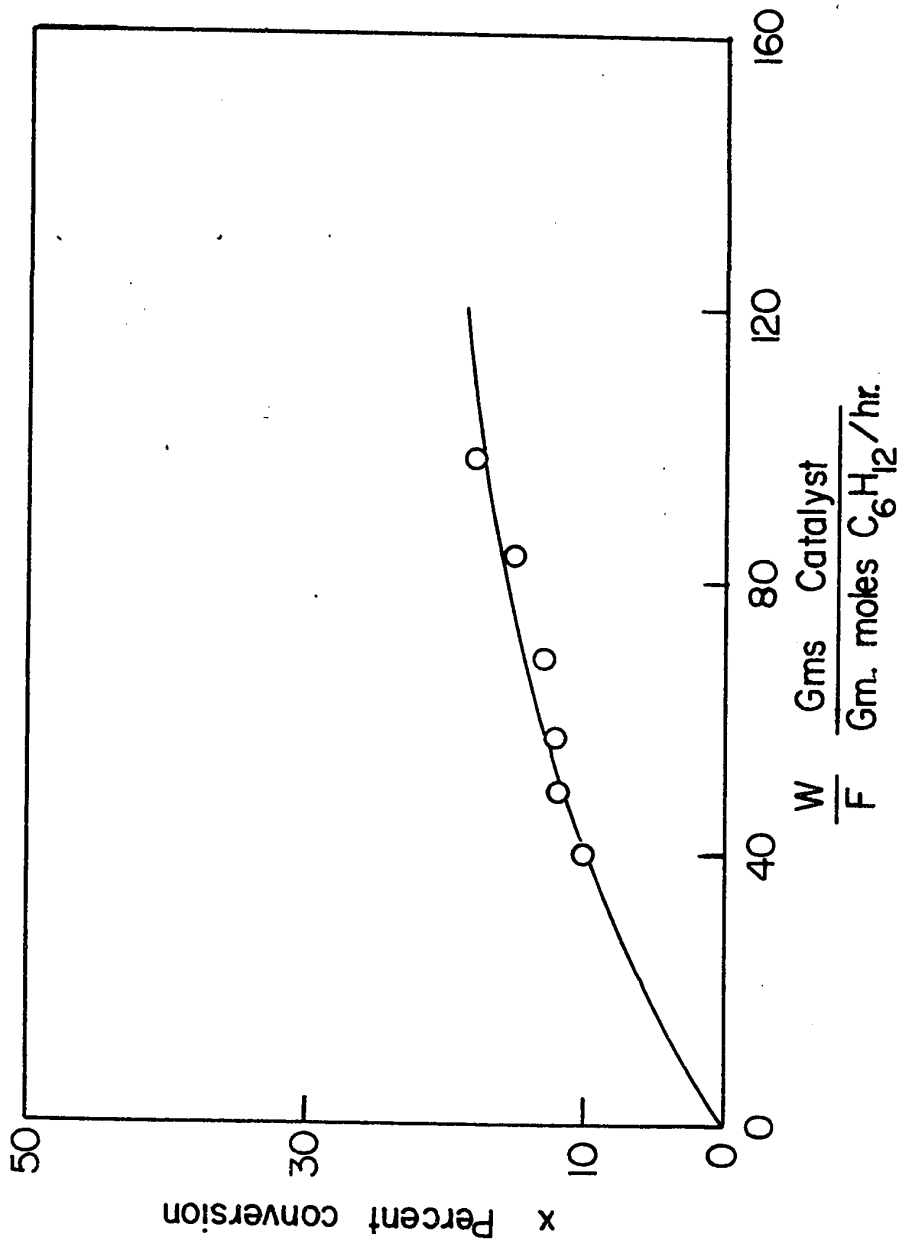

Figure 19 Conversion curve at 560°c.
Cobalt oxide on alumina.

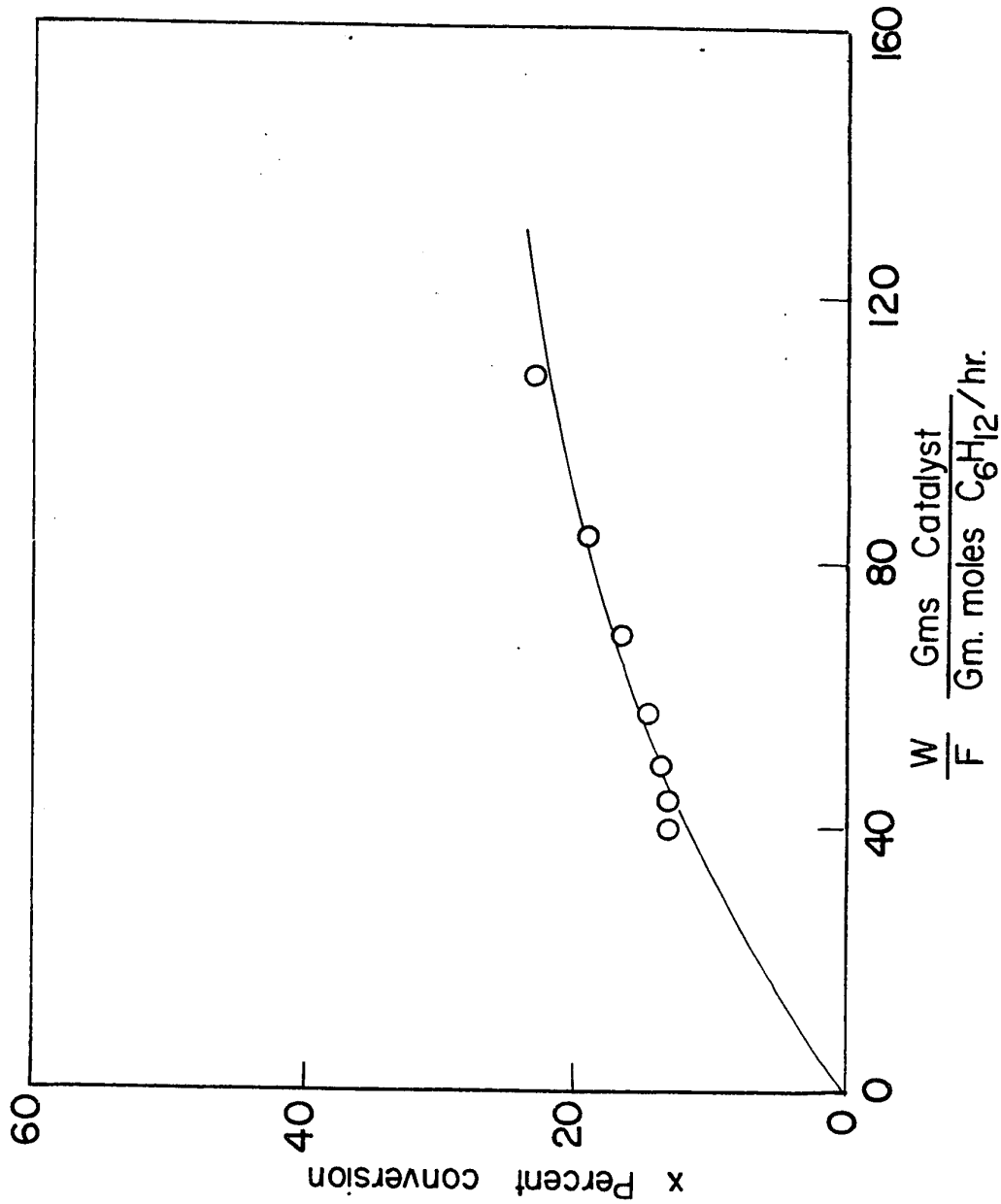

Figure 20 Conversion curve at 570°C.
Cobalt oxide on alumina.

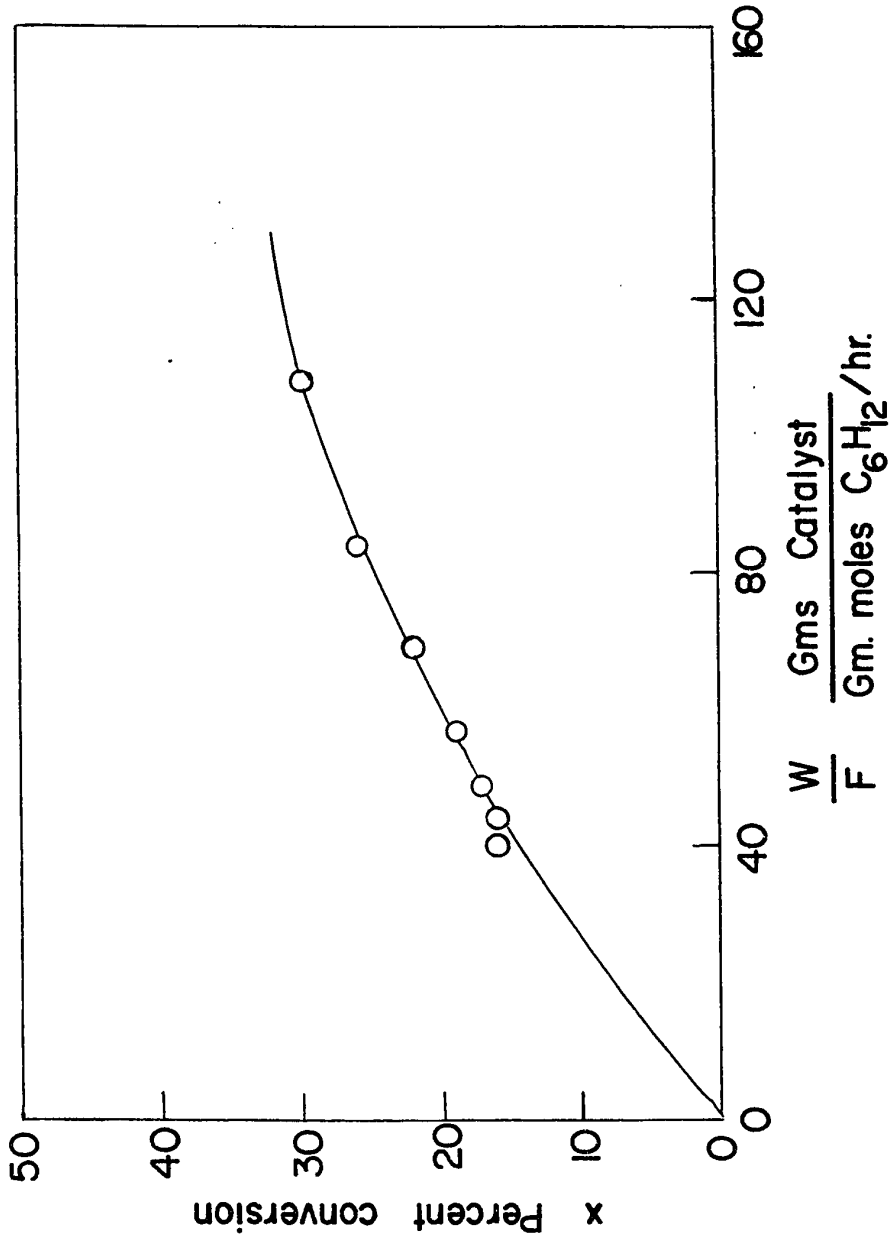

Figure 21 Conversion curve at 580°C - Cobalt ozide on alumina.

and the curves were extrapolated to $(W/F) = 0$. From the intercepts, the values of initial rates were obtained. These are given in table 11.

V. Test for film diffusion:

Tests for the effects of film diffusion in an experimental reactor are usually made by varying the feed rate and weight of catalyst at the same time (to give the same value of (W/F) at different velocities) and then noting the conversion.

The conversion is measured at a value of (W/F) at which the gas velocity is low. Then it is measured again at a high velocity, but with more catalyst to keep the ratio, (W/F), constant. The two values of conversion will coincide if the effect of diffusion is negligible. If the conversions are different, there is a diffusion effect.

There are two ways to test this effect. One is to make a series of runs at different velocities with the amount of catalyst adjusted to a constant (W/F) ratio. These data are then plotted as conversion vs. velocity. If difusion has no effect the plot will be a horizontal line parallel to the abscissa.

The other method is to make two series of runs at varying values of (W/F) but with a constant weight of catalyst in each series. The weight should be different by

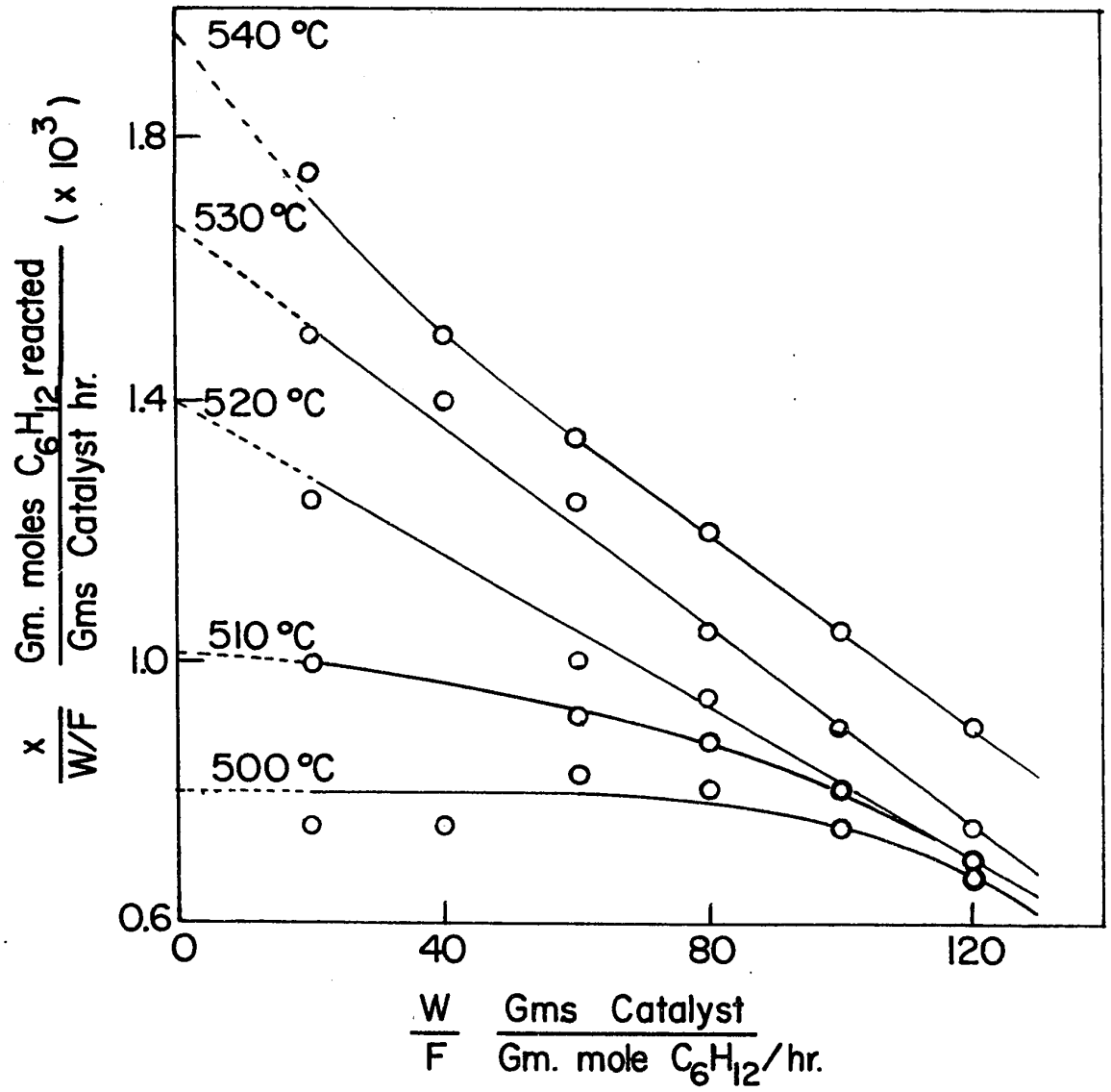

Figure 22 Determination of initial rates - Cobalt oxide on alumina.

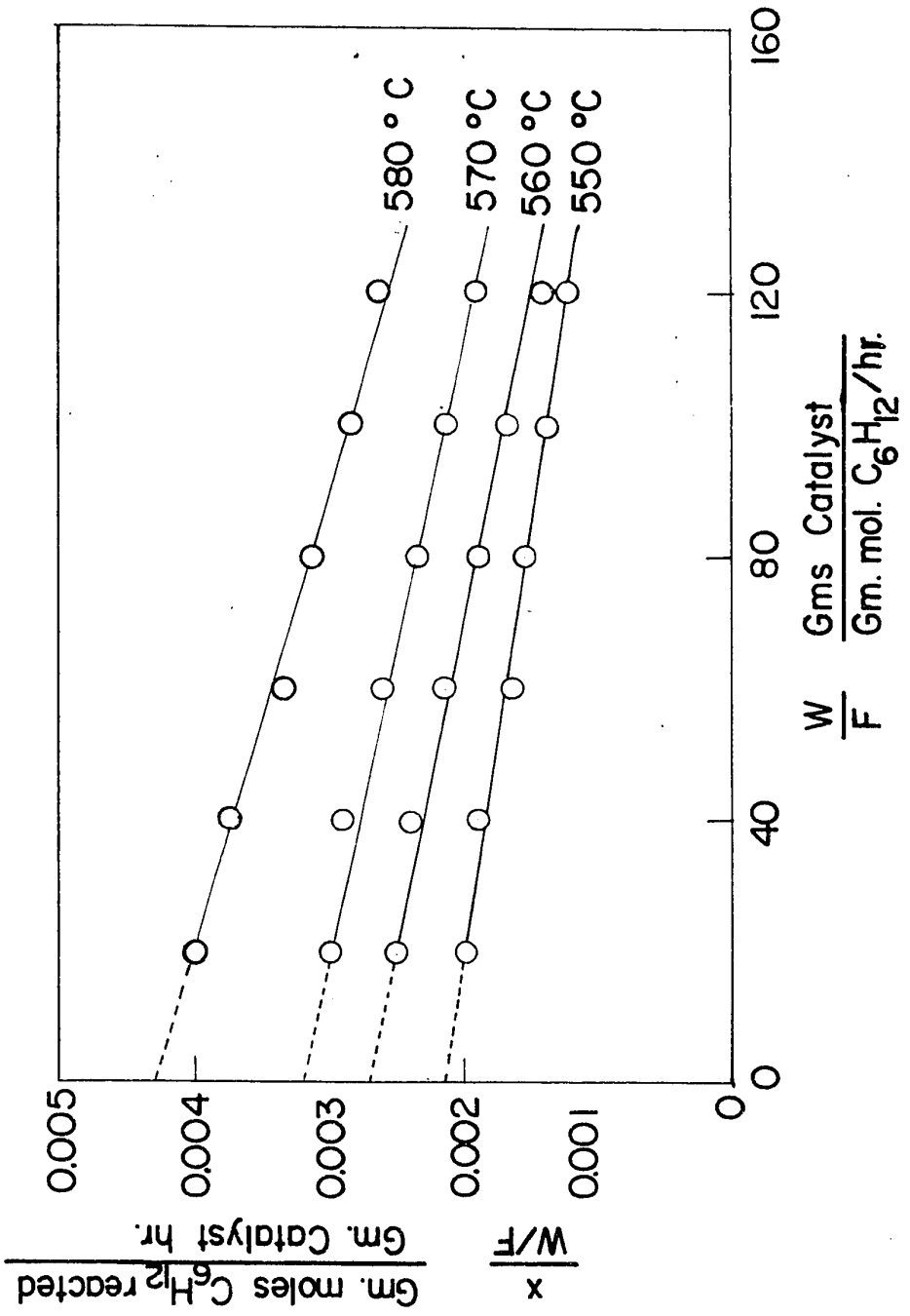

Figure 23 Determination of initial rates - Cobalt oxide on alumina.

a factor of two in each of the two series. A plot of x vs. (W/F) is made for each series. If the two curves coincide, there is no diffusion effect but if they are different there is an effect due to the diffusion of the gas from the main stream to the surface of the catalyst.

The importance of accurate chemical analysis must be emphasized. In cases of both the reactors, differential or integral, accurate chemical anlysis is essential.

In the first case the conversion is small and in the latter case any inaccuracy in a conversion value may greatly affect the shape of conversion vs. time factor curve.

Conversion vs. time factor curves that differ merely because of inaccurate chemical analysis may lead to the conclusion of an entirely different mechanism for the same reaction.

The first method of varying both W and F, but keeping a constant value of (W/F), was used. The results are shown in figures 24 to 26. The plots suggest that diffusion is not the controlling mechanism for this reaction.

VI. Test for Adsorption.

The effect of feed composition upon initial rates was studied by plotting feed composition (partial pressure of cyclohexane in feed) against initial rates. The results are

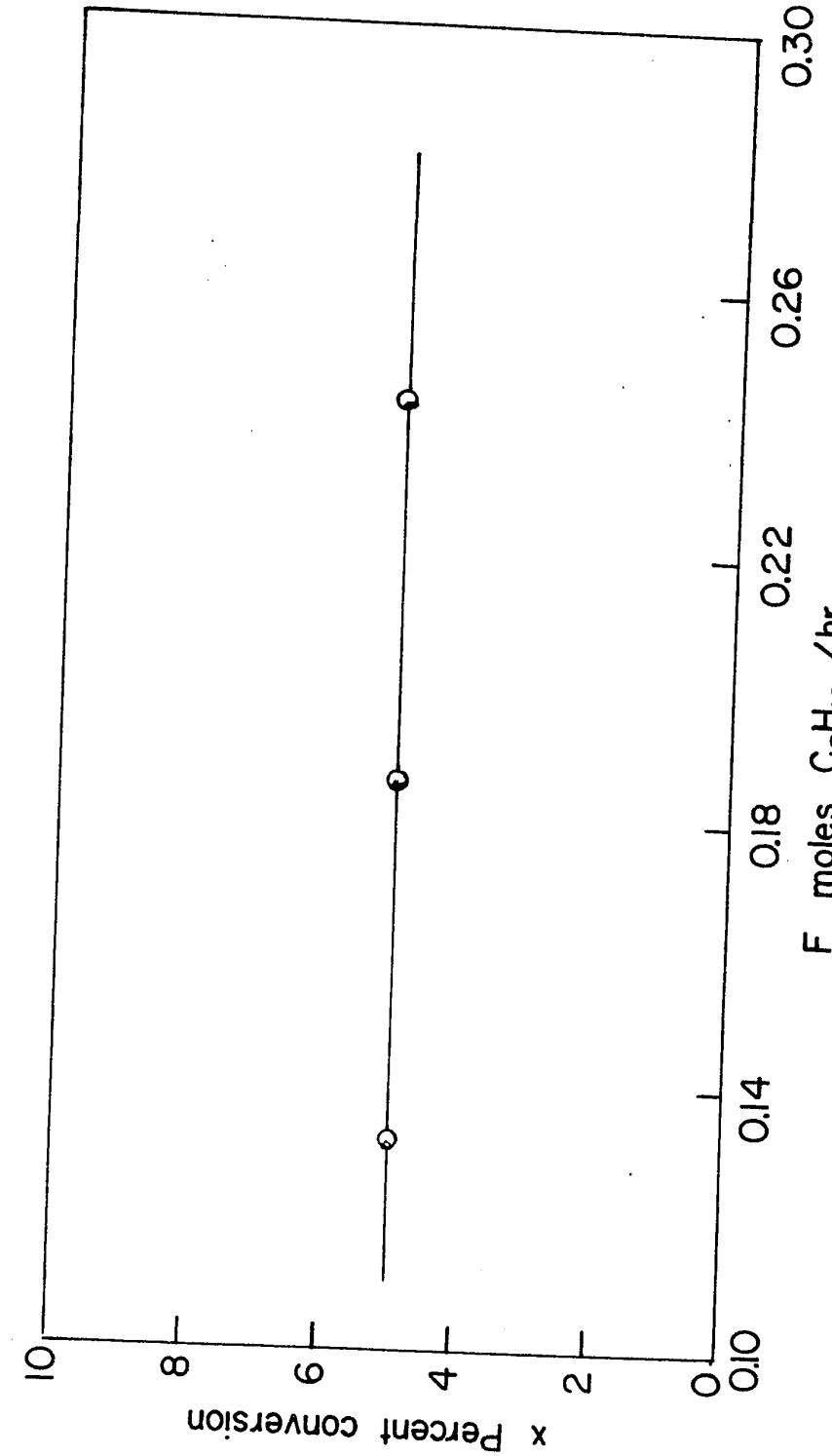

Figure 24 Test for film diffusion - Cobalt oxide on alumina.
T = 550°C; W/F = 37

Figure 25 Test for film diffusion - cobalt oxide on alumina.

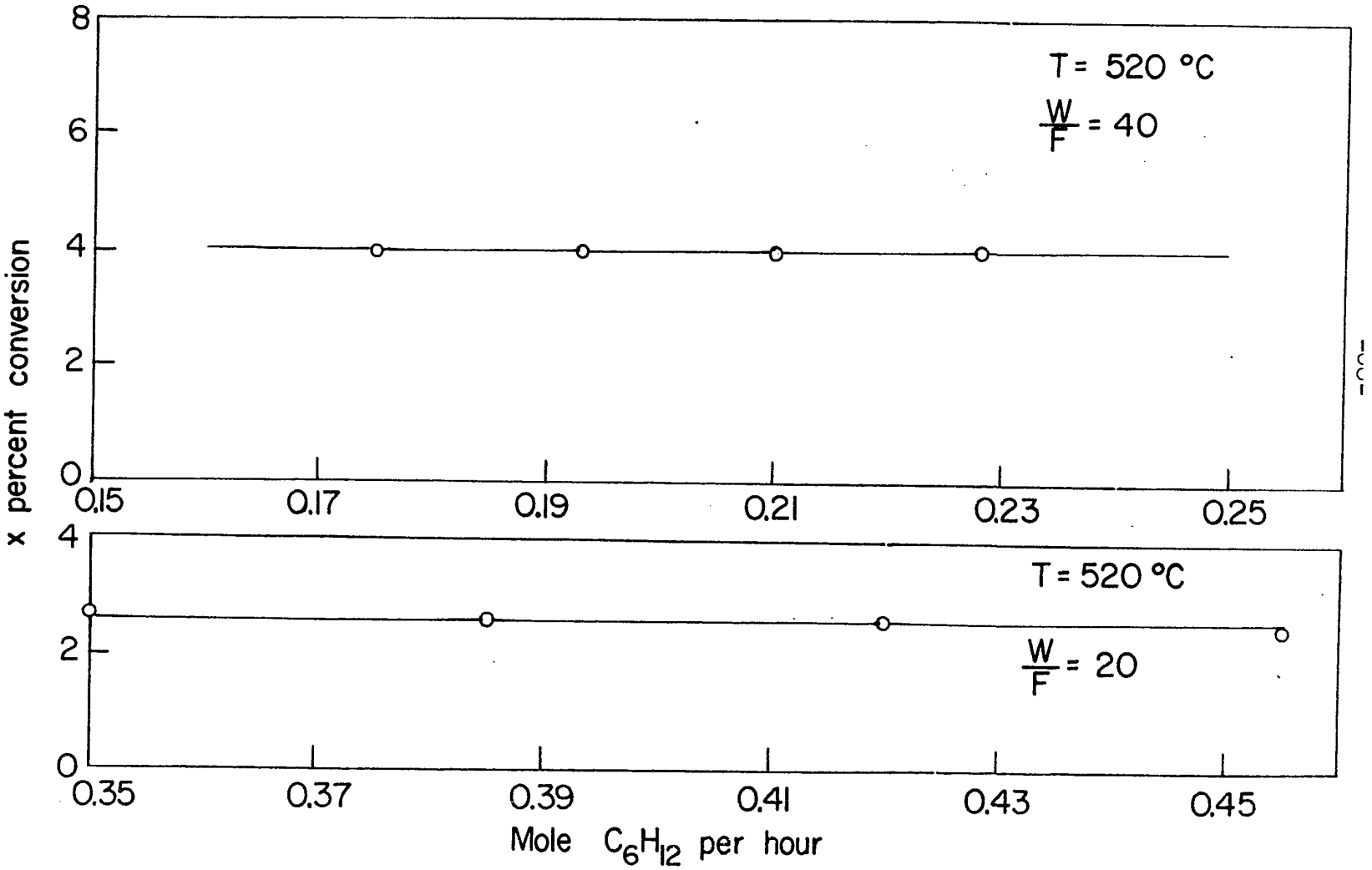

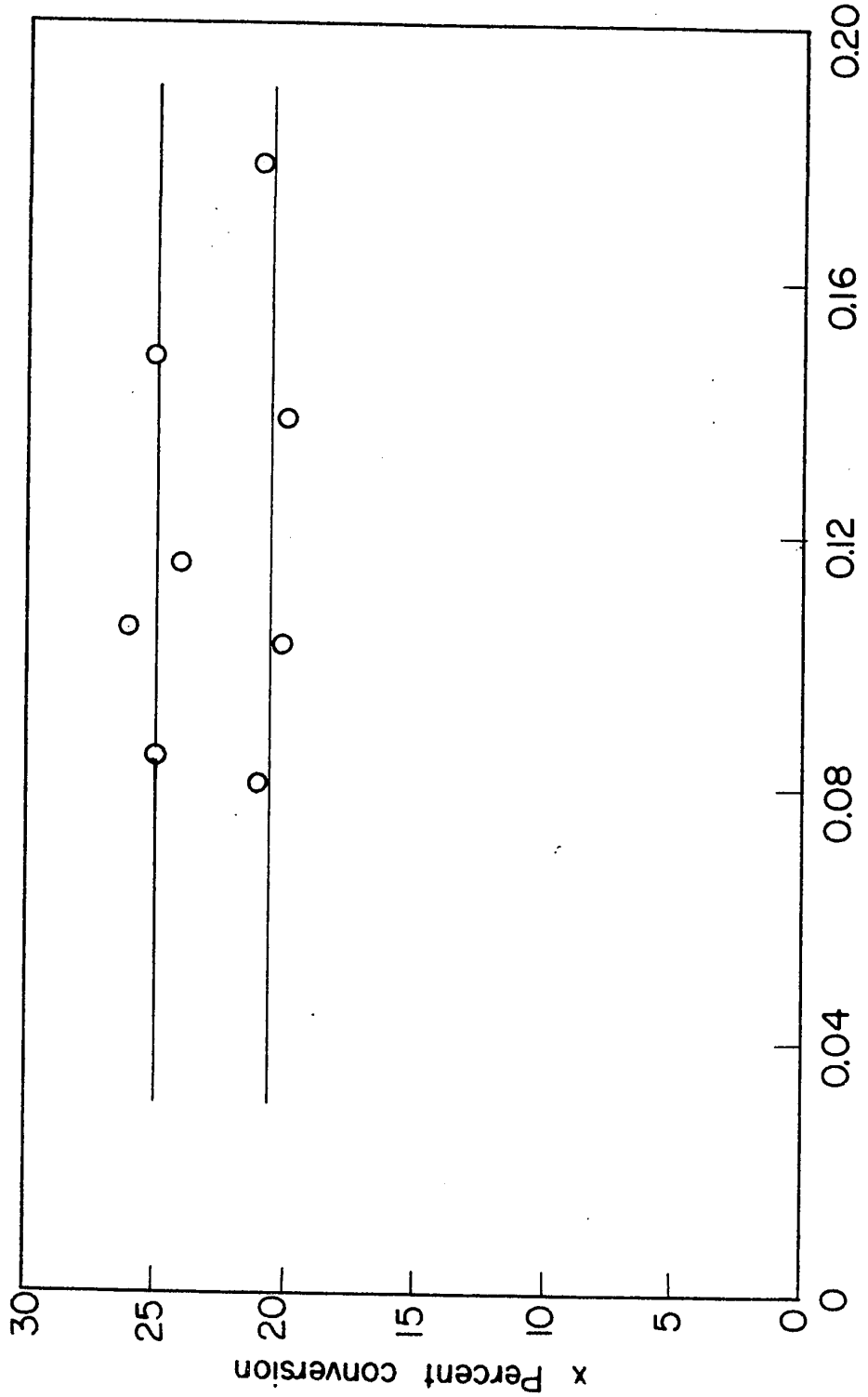

Figure 26 Test for film diffusion - nickel oxide on alumina.
T = 430°C; W/F = 60,50.

shown in figures 27 and 28. Yang and Hougen (18) have shown the various types of curves that can be obtained from a plot of this nature.

Yang and Hougen suggested that if the reaction rate was zero in the absence of either A or B and attained a maximum value near the middle of the composition range, then surface reaction was controlling. Examination of figures 27 and 28 show that the curves follow a similar pattern.

VII. The rate equation.

Rates are generally expressed by a combination of three terms, the kinetics term, the potential term and the adsorption term, arranged as follows:

$$r = \frac{(\text{kinetics term})\ (\text{potential term})}{(\text{adsorption term})^n}$$

In tables 1 and 2, Yang and Hougen (18) have given the expressions for the various terms and in table 4 the authors have suggested that if in the reaction, $A \rightleftharpoons R + S$, the rate of reaction is controlled by the surface reaction, then the exponent of the adsorption term would be 2. The rate equation can then be expressed as

$$r = \frac{k\left(p_A - \frac{p_R (p_S)^3}{k}\right)}{(1 + p_A K_A + p_R K_R + p_S K_S)^2} \qquad (1)$$

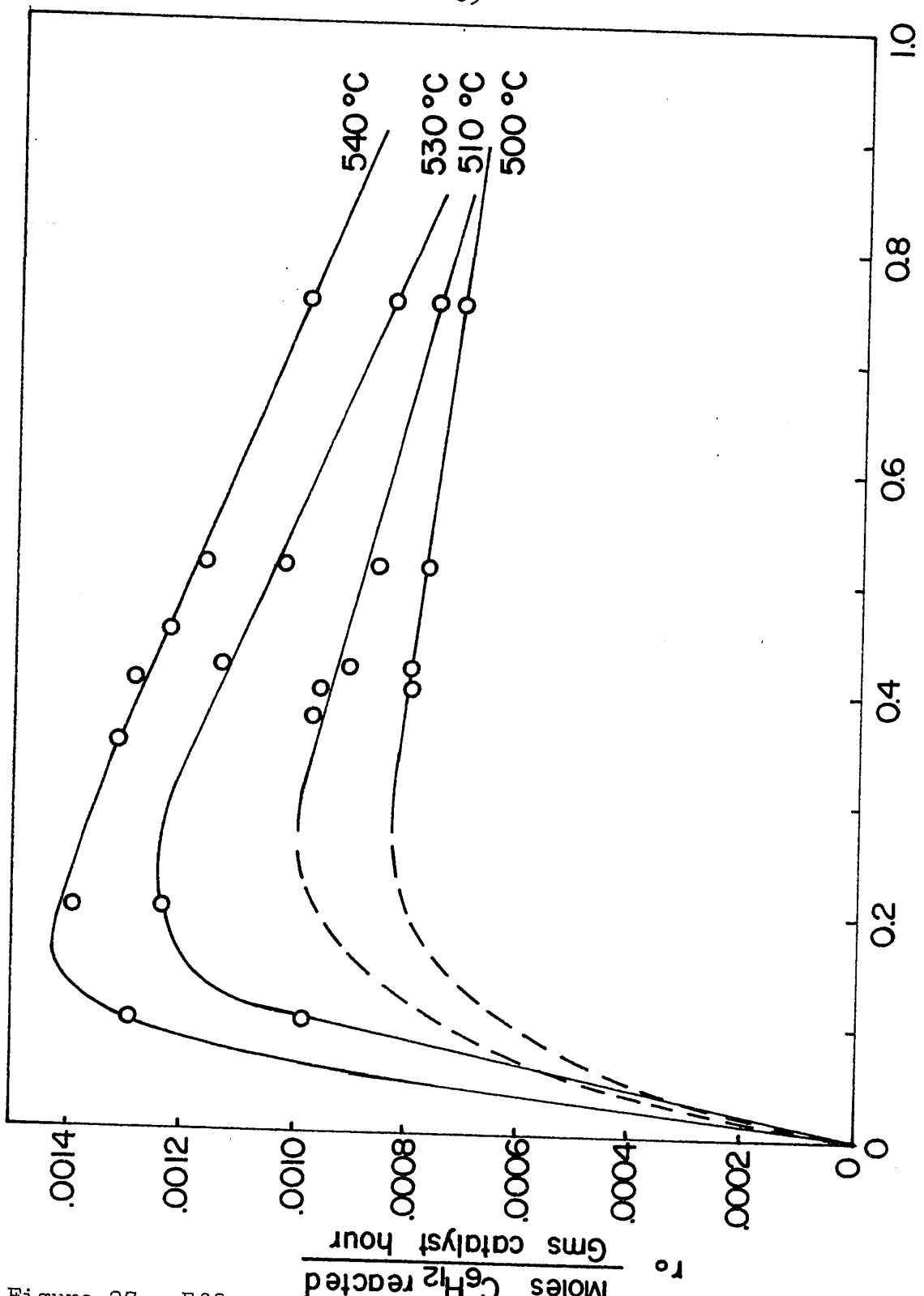

Figure 27 Effect of feed composition on initial rate - cobalt oxide on alumina.

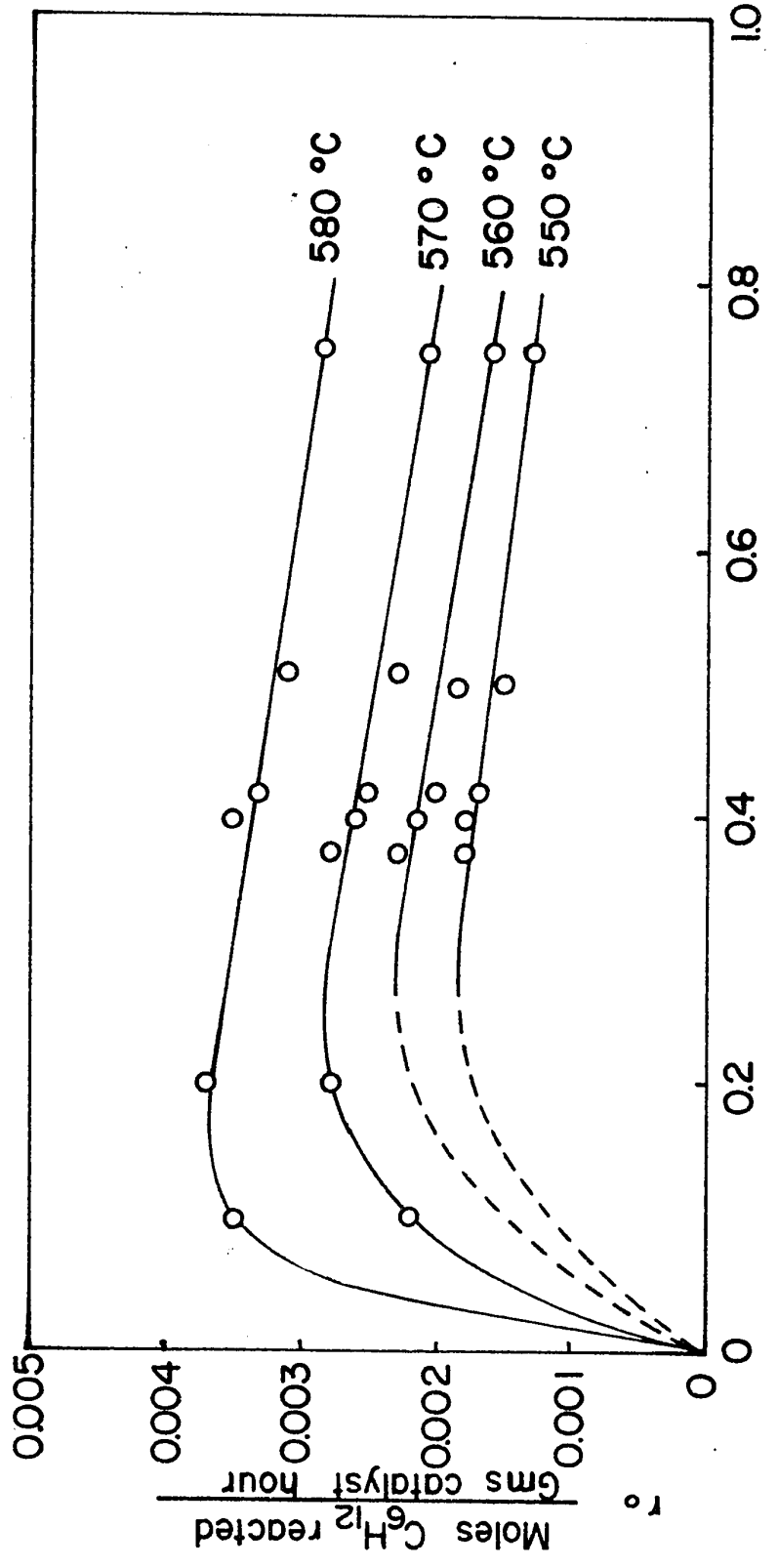

Figure 28 Effect of feed composition on initial reaction rate - cobalt oxide on alumina.

VIII. Calculation of the reaction velocity constant 'k'.

Initial rates for the pure reactants present in stoichiometric proportions and in the absence of products can readily be calculated from the rate equation. Or alternately, since the initial rates have already been calculated, the equation could be used to calculate the reaction velocity constant k.

For initial rate, i.e. when no products are present, the rate equation (1) reduces to the form,

$$r_o = \frac{k\, p_A}{(1 + p_A K_A)^2} \qquad (9)$$

Re-arranging the equation (9),

$$1 + p_A K_A = \left(\frac{p_A}{r_o} \cdot k\right) \qquad (10)$$

As an example, the calculation of k value at a temperature of 500°C (over cobalt oxide on alumina) is shown below.

Flow rate, ΔP = 10 mm, p_{A_1} = 0.75 atm.
Flow rate, ΔP = 20 mm, p_{A_2} = 0.42 "
At 500°C, r_o = 0.00088

$$1 + 0.75\, K_A = \left(\frac{0.75}{0.00088} \times k\right)^{\frac{1}{2}}$$

$$= \frac{0.865}{0.0296} \cdot (k)^{\frac{1}{2}}$$

$$= 29.22\, (k)^{\frac{1}{2}} \qquad (11)$$

$$1 + 0.42\ K_A = \left(\frac{0.42}{0.00088} \times k\right)^{\frac{1}{2}}$$

$$= \frac{0.646}{0.0296} (k)^{\frac{1}{2}}$$

$$= 21.82\ (k)^{\frac{1}{2}} \qquad (12)$$

The equations (11) and (12) were solved to give,

$$k = 0.00648$$

and $$K_A = 1.800$$

Similarly, the calculations were carried out for other temperatures. The results are given in Table 12.

IX. The Arrhenius Plot:

The theory of Arrhenius equation is based upon the variation of the equilibrium constant with temperature, i.e. the Van't Hoff equation,

$$\frac{d \ln k}{dT} = \frac{\Delta H}{RT^2} \qquad (13)$$

Since the equilibrium constant is equal to the ratio of k and k', the forward and reverse rate constants, equation (13) may be written as,

$$\frac{d \ln k}{dT} - \frac{d \ln k'}{dT} = \frac{\Delta H}{RT^2} \qquad (14)$$

The right-hand side of equation (14) could also be divided into two parts provided the overall heat of reaction

is broken up into an energy change for each direction as follows:

$$\Delta H = H - H' = E - E' \tag{15}$$

Equation (15) then takes the form,

$$\frac{d \ln k}{dT} - \frac{d \ln k'}{dT} = \frac{E}{RT^2} - \frac{E'}{RT^2} \tag{16}$$

The two separate expressions, one for the forward and one for the reverse reaction, having a difference in agreement with the equilibrium requirement are,

$$\frac{d \ln k}{dT} = \frac{E}{RT^2} \tag{17}$$

$$\frac{d \ln k'}{dT} = \frac{E'}{RT^2} \tag{18}$$

Integration of (17) yields the Arrhenius equation

$$k = A \cdot e^{-E/RT} \tag{19}$$

(or)
$$\text{Ln } k = \text{Ln } A - \frac{E}{RT} \tag{20}$$

According to this equation, a plot of Ln k vs. $\frac{1}{T}$ should give a straight line with a slope of $(-E/R)$ and an intercept of Ln A.

The activation energy E was interpreted by Arrhenius as the excess over the average energy that the reactants must possess in order for the reaction to occur. The only limitation on E is that the difference E - E' must be equal to the

overall heat of reaction, i.e. the average energy difference between the products and reactants. This suggested the existence of an intermediate state of activated reactants (complex). The overall reaction could then be looked upon as taking place by the following two-step process.

Reactants ⟶ activated reactants (complex) ⟶ products

The energy change for the formation of activated products is E and for the second part of the process, $(-E')$.

The Arrhenius theory can give no information about the numerical values of activation energies although it is clear that E must be greater than H for an endothermic reaction and E' greater than the absolute value of H for an exothermic reaction.

The apparent activation energies for the various catalysts were calculated by plotting log k against $1/T$ and are given in table 14.

Sample calculation:

Catalyst - Cobalt oxide on alumina.

The slope of the straight line in the temperature range 500 - 580°C was,

$$-\frac{66}{139} \cdot \frac{0.1}{0.01}$$

$$= -\frac{660}{139}$$

$$\text{Ln } k = \text{Ln } A - \frac{E}{RT} \qquad (20)$$

$$\text{Log } k = \text{Log } A - \frac{E}{2.303\ RT} \qquad (21)$$

$$= \text{Log } A - \frac{E}{4.576\ T} \qquad (22)$$

Equating the slopes,

$$-\frac{E}{4.576\ T} = -\frac{660}{139}$$

$$E = \frac{660}{139} \times 4.576$$

$$= 21.728 \text{ k cals/mole}$$

The intercept gives the value of Log A. But, since the plot has been made from a definite value on the x-axis and not from zero, A had to be obtained by calculation. This was done as follows:

Temperature : 500°C

$$\log k = \log A - \frac{E}{4.576\ T} \qquad (22)$$

(or)
$$\log A = \log k + \frac{E}{4.576\ T} \qquad (23)$$

$$= \bar{3}.8116 + \left(\frac{21728}{4.576 \times 773}\right)$$

$$= \bar{3}.8116 + 6.1423$$

$$= 3.9539$$

(or)
$$A = 8992$$

Similarly the value of A was calculated at various temperatures and the average value taken. This is shown in table 13.

Following an exactly similar procedure, the values of activation energies and frequency factors for all other catalysts were evaluated. These are shown in figures 29 to 35 and table 14.

X. The Compensation Effect:

Activity variations shown by a series of related catalysts, such as a series of different metals, or a given metal treated in a variety of ways, or an alloy series, may be the result of variations in the activation energy E, or in the pre-exponential factor A, or in both simultaneously. It is important to the attainment of the maximum information concerning a given system that these quantities be determined in addition to the activity. The activity is of course defined by the rate constant k, or less satisfactorily by the rate under constant conditions of partial pressures. Uncertainty arises if rates, rather than rate constants are employed, since any change in the orders of reaction with temperature will destroy the proportionality. It is unfortunate that while many studies have been made concerning variation in rates over a series of catalysts, few have given evidence on concomitant changes in reaction orders. If varying amounts of catalysts are used, it is well to establish the proportionality between the amount and the rate: there are subtle reasons why the proportionality may sometimes fail.

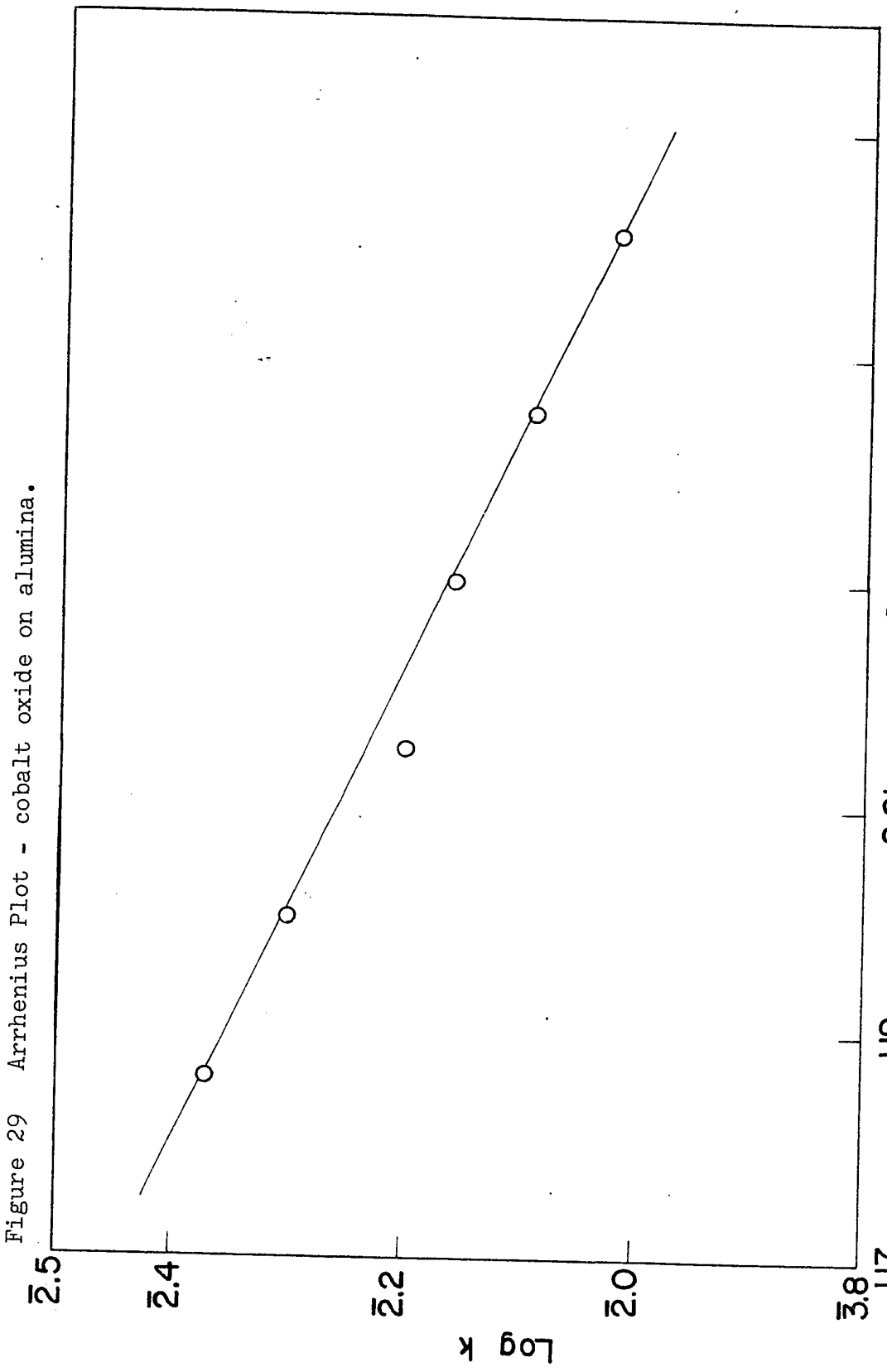

Figure 29 Arrhenius Plot - cobalt oxide on alumina.

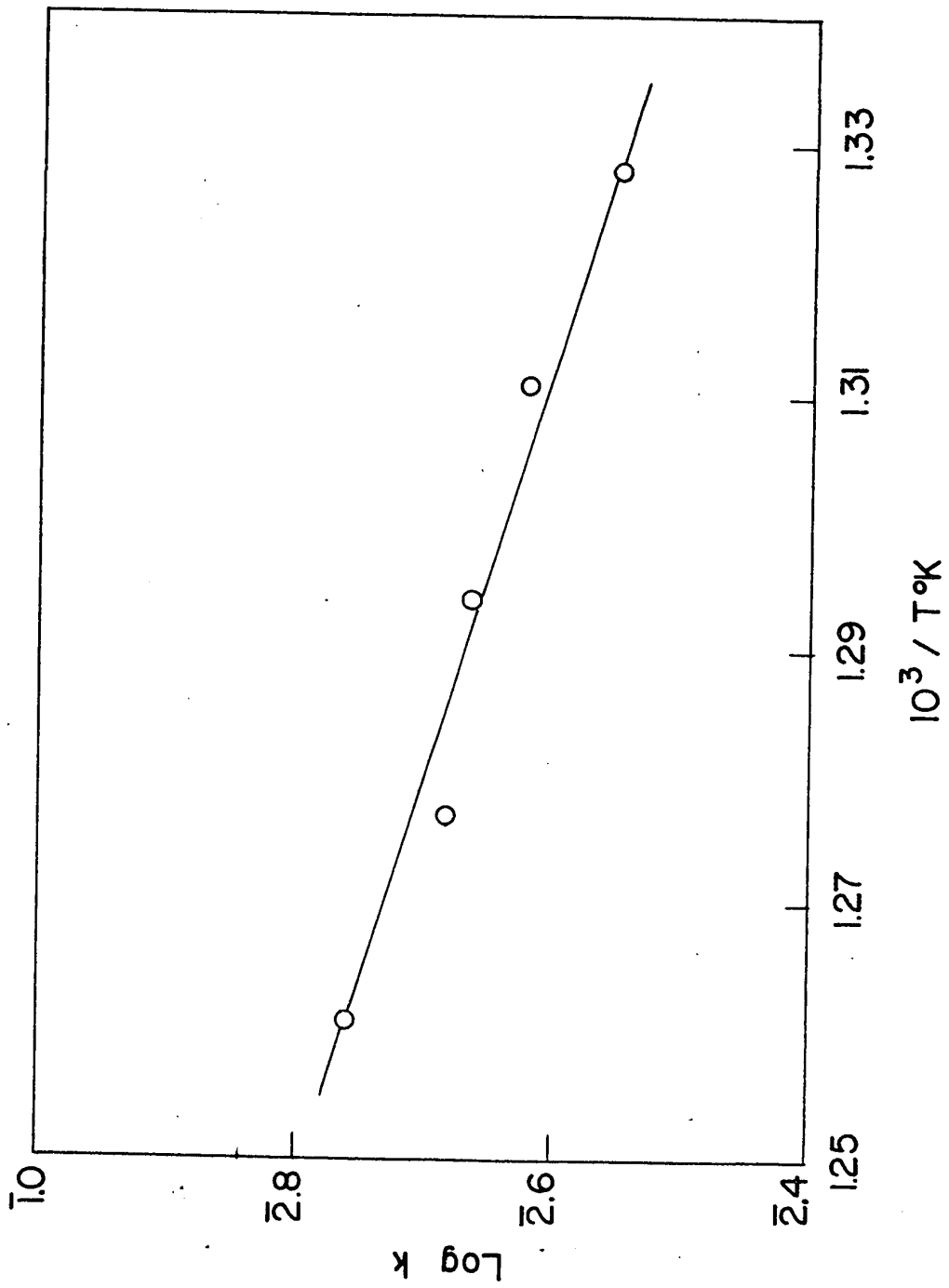

Figure 30 Arrhenius Plot - nickel oxide.

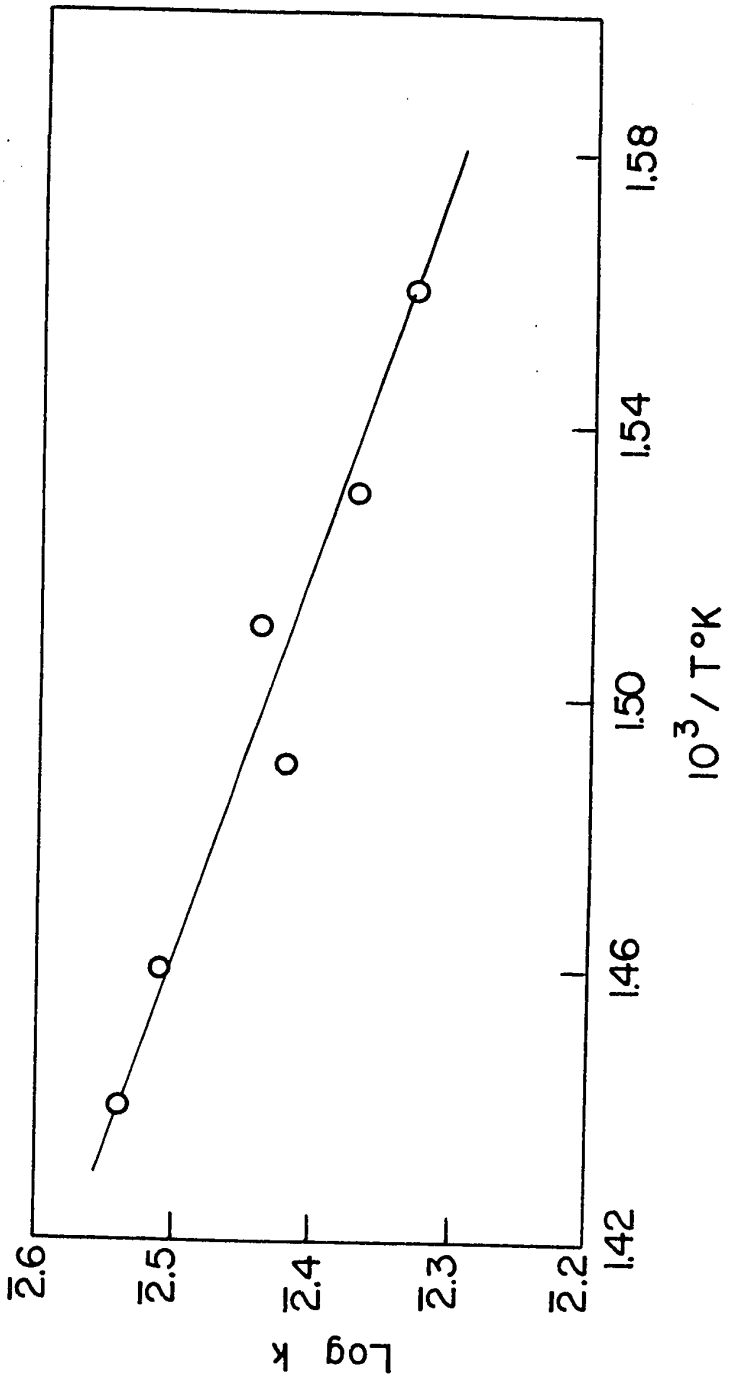

Figure 31 Arrhenius Plot - nickel oxide on pumice.

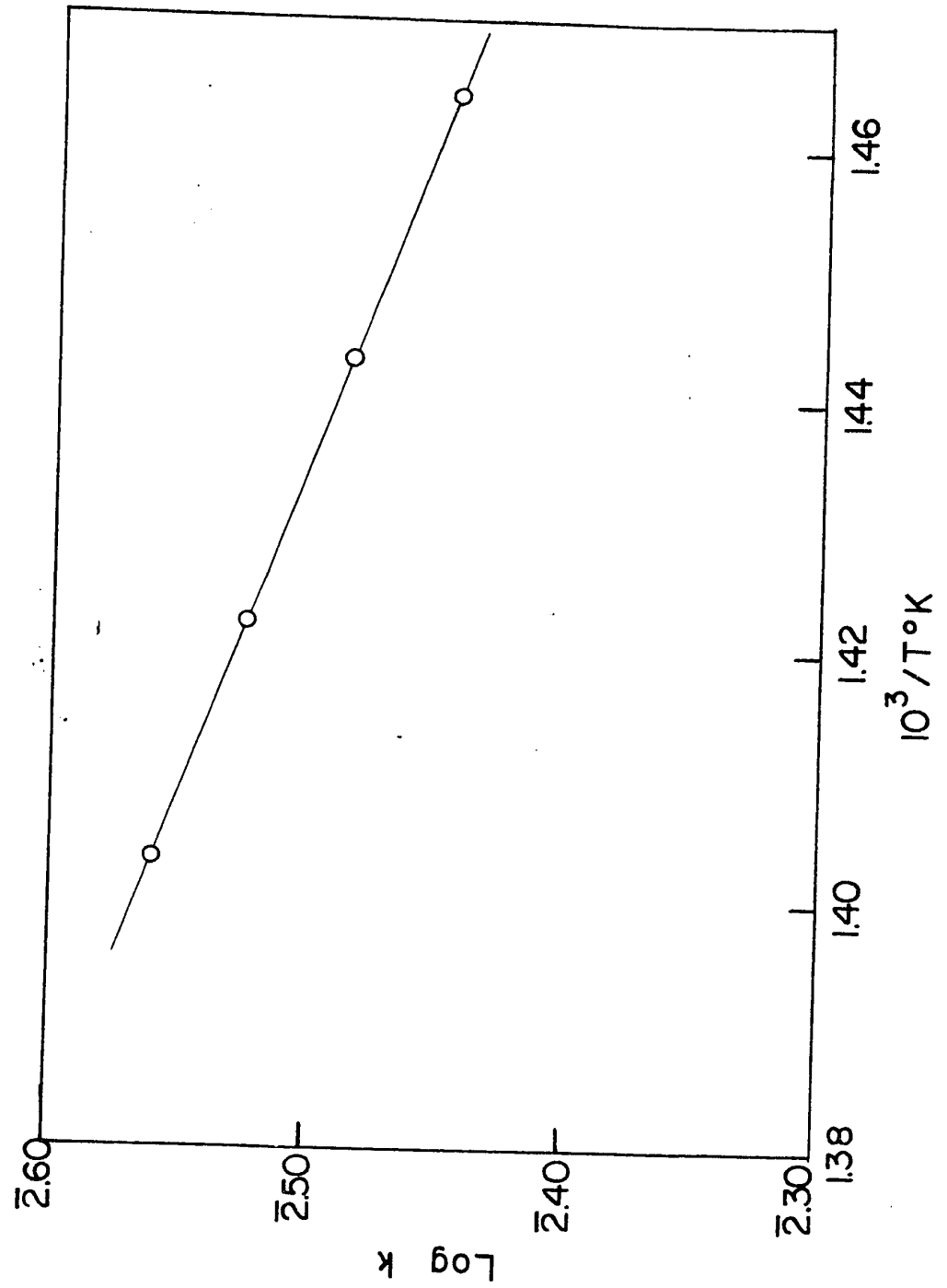

Figure 32 Arrhenius Plot - nickel oxide on alumina.

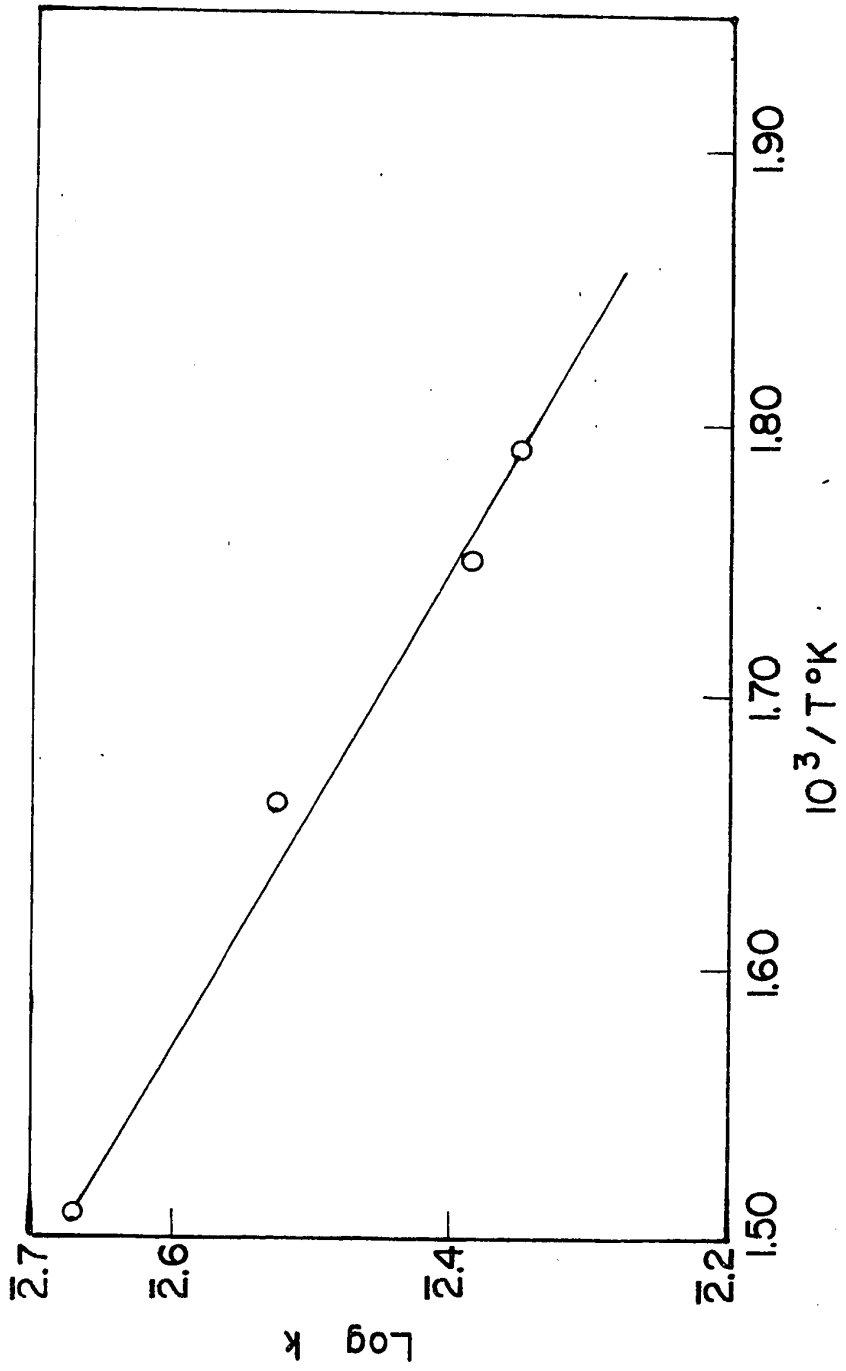

Figure 33 Arrhenius Plot - nickel oxide on kieselguhr.

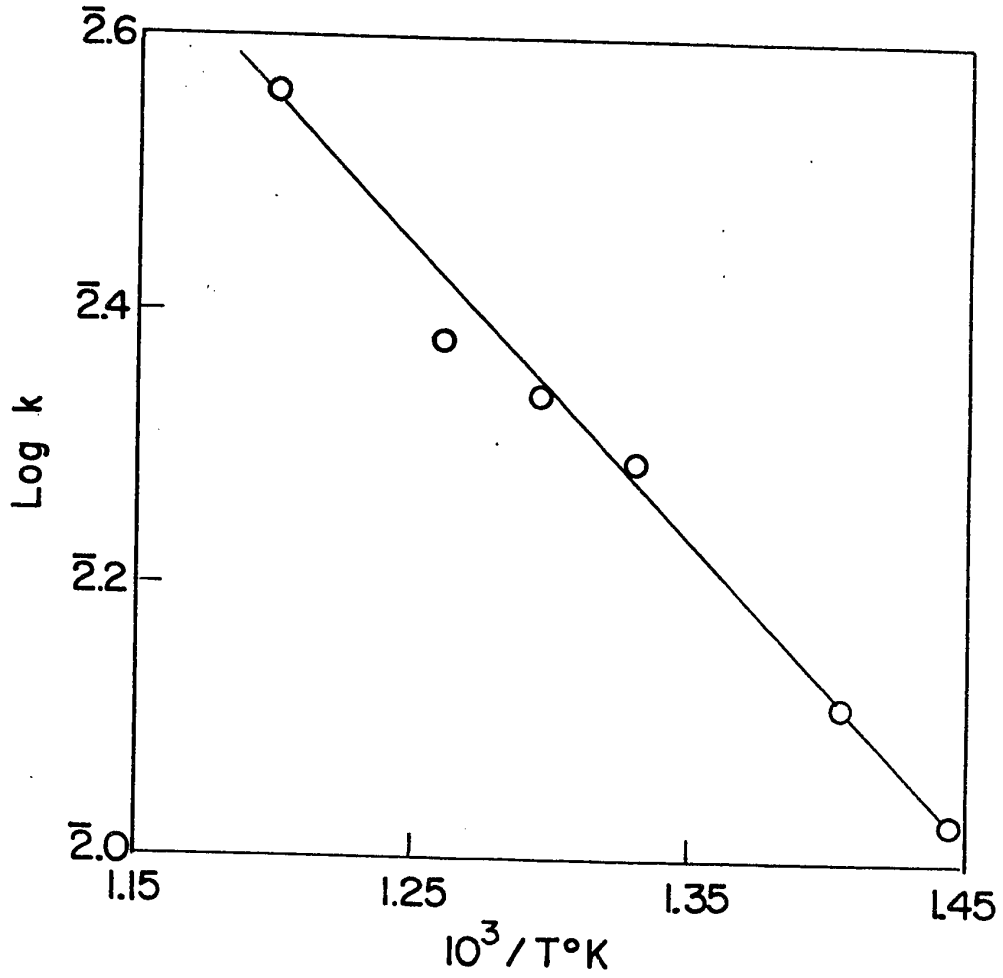

Figure 34 Arrhenius Plot - nickel oxide, chromium oxide.

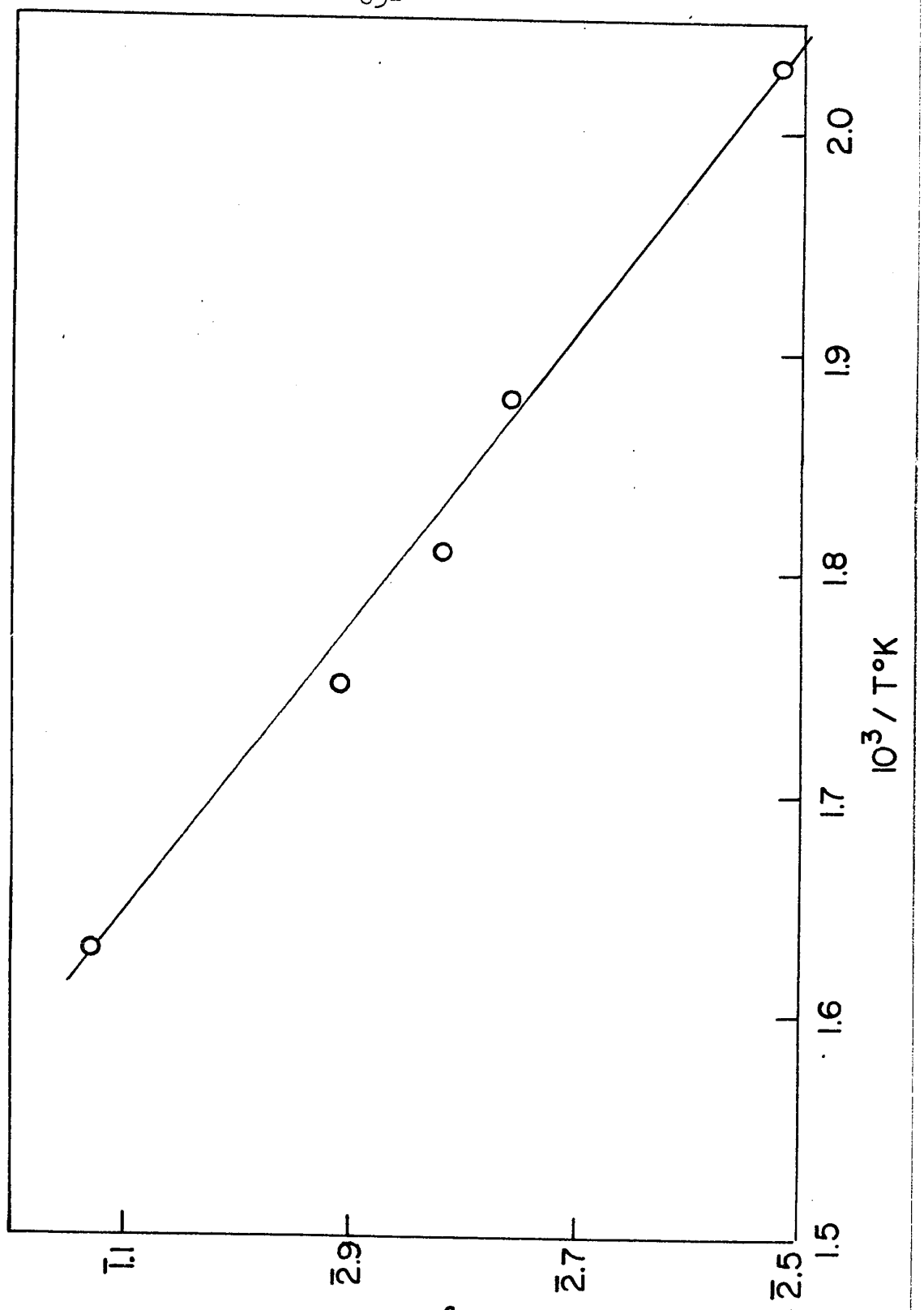

Figure 35 Arrhenius Plot - platinum on alumina.

Phenomenological Description of the Compensation Effect:

Of great significance is the frequently observed relationship between the activation energy E and the pre-exponential factor A for a given reaction over a series of related catalysts. It is usually of the form

$$\text{Log } A = m E + C$$

and is referred to as a compensation effect or the Theta rule. The former name is meaningful since an increase in log A at constant E implies a higher rate, while an increase in E at constant log A implies a lower rate: simultaneous increases or decreases in E and log A therefore tend to compensate from the standpoint of the rate when such a compensation operates. It is possible for striking variations in E and log A through a catalyst series to yield only relatively small changes in activity; alternatively when the effect does not operate (that is, when either E or log A alone changes) striking variations in activity result. Such cases, although rare, are of particular significance. It is clearly of importance to the proper understanding of the mechanism of catalytic action to know how the basic kinetic parameters, as well as the rate, respond to changes in catalyst structure.

The variation of activity through a catalyst series at a given temperature will be referred to as an activity pattern. The form of this pattern is clearly a function of temperature. The relative activities are usually described by one of two

ways: either,

(1) by comparing the temperatures required to effect a certain rate, or conversion,

(2) by comparing the rates at some representative temperatures.

The drawbacks of the first method are

(a) that the activity order is not unique but depends on the arbitrarily chosen rate, and

(b) it is only quantitative.

The statement that "catalyst 1 is 50^{o} more active than catalyst 2 at 10 percent conversion" may have some practical value, but is useless in a fundamental investigation. Where only this type of information is recorded in the literature and where further computation is impossible, it has been assumed that relative activities are proportional to the reciprocal of the absolute temperature required to effect the chosen conversion. Method 2 is therefore much to be preferred in that it places relative activities on a readily understandable and quantitative footing, and it enables the temperature-dependence of the activity order to be assessed.

Figure 36 shows the compensation effect for the catalysts used in this work. It can be seen that all catalysts of nickel follow the compensation effect fairly well. In addition, cobalt oxide on alumina also obeys the linear

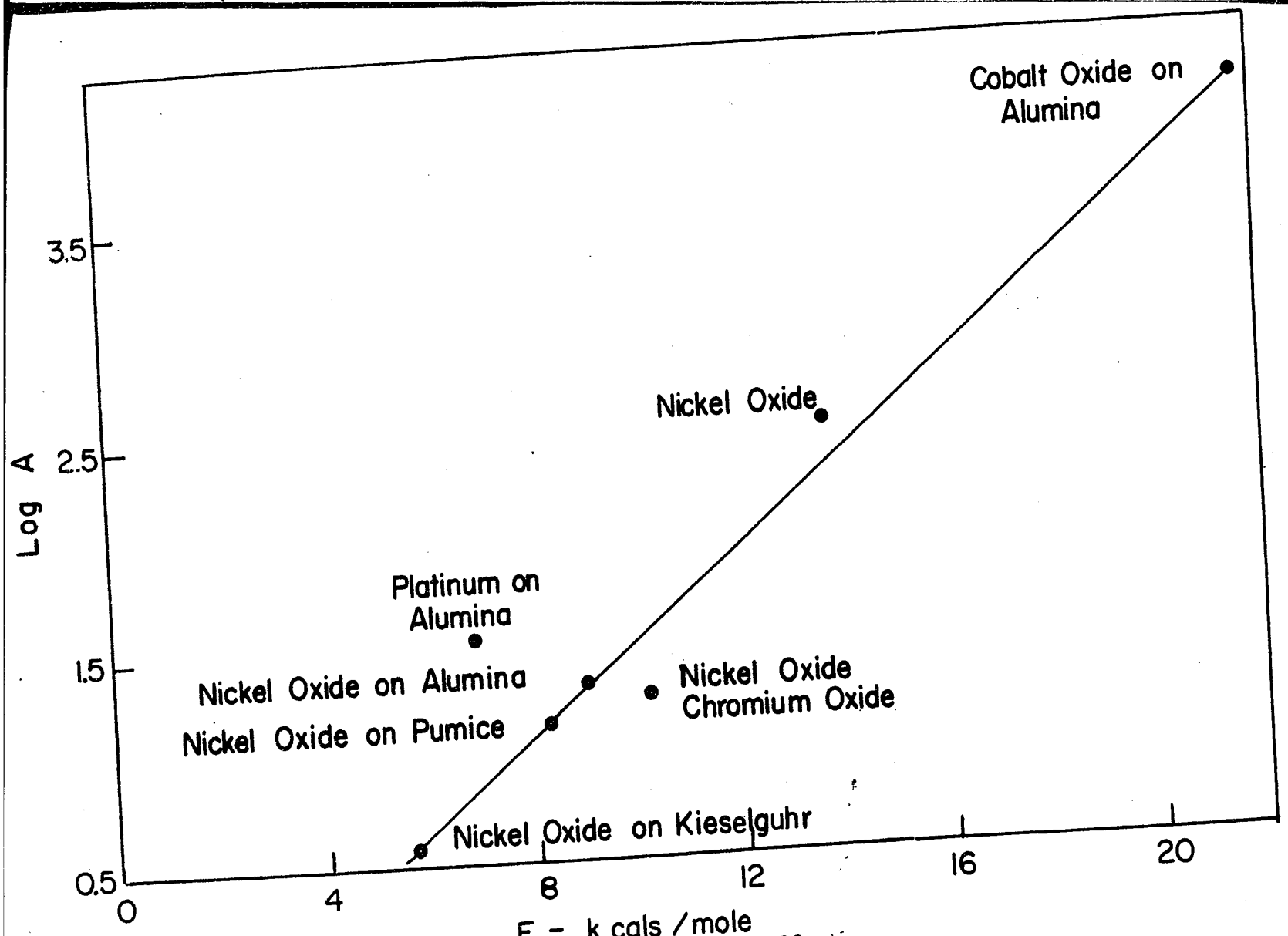

Figure 36 Compensation effect.

relationship. Even though this is different from nickel catalyst it could be attributed to the fact that cobalt oxide on alumina behaved very similar to nickel catalyst probably by virtue of cobalt being in the same group as nickel.

The only catalyst that did not follow the pattern is, as can be seen from the figure, platinum on alumina. This is to be expected because the reaction over platinum on alumina catalyst showed an extremely high catalytic activity. Also this catalyst is widely different from the other catalysts tried.

XI. Conversion dependence on flow rate.

Earlier it was mentioned that Hougen suggested that it is very difficult to calculate the time of contact with flow rate or to establish the relationship between them. However, flow rate is certainly a measure of contact time. It was suggested by earlier workers, that for low values of conversion, it was independent of flow rate. With almost all the catalysts tried this was found to be generally true, provided the conversion remained low. But in every case when the conversion was high, it was observed that there was a definite decrease in conversion with increasing flow rate. With increasing flow rate, obviously, the reactants contact the catalyst for a shorter time and this probably results in a decreased conversion.

A plot of ΔP (representing flow rate) with conversion is given in figure 37.

XII. Discussion of results.

(1) Cobalt Oxide on Alumina:

About seventy runs were carried out over this catalyst with three different amounts of catalyst. The activation energy was found to be 22 k.cals/mole and the frequency factor 8992. The maximum value of conversion obtained was around 30%. The catalyst was found to follow the compensation effect, even though it was farther away from the cluster of points obtained for nickel oxide catalysts. The purpose of trying cobalt oxide on alumina was to compare it with the other catalysts of nickel oxide.

(2) Platinum on alumina:

The behaviour of platinum on alumina was markedly different from the other catalysts. The conversion obtained was very high (92% cyclohexane was converted to benzene). Conversion could be obtained even with comparatively lesser amounts of catalyst and the compensation effect was not obeyed. A value of 6.9 k.cals/mole and 35.8 were obtained for the activation energy and frequency factor respectively.

(3) Palladium on alumina:

Palladium on alumina was found to be less active than

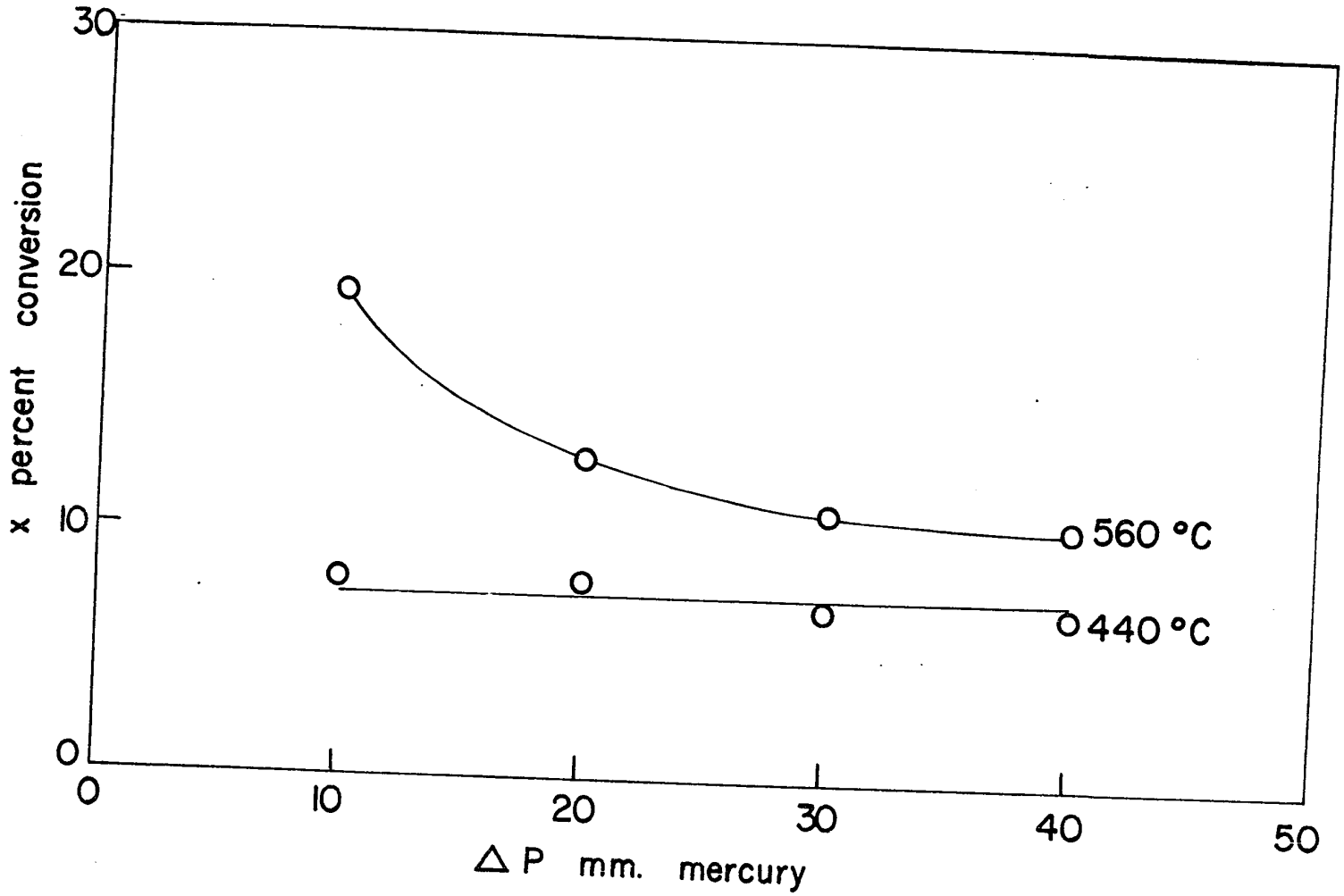

Figure 37 Conversion dependence on contact time.

platinum on alumina even though the conversion obtained was higher than for the other catalysts. It was very difficult to obtain consistent results with palladium. This could probably be attributed to the fact that the hydrogen atom formed in the primary phase of the reaction gets more firmly bound to the palladium surface rather than to the platinum surface resulting in its retarding action being more evident. This agrees with an earlier study by Magyar and Hodossy (13).

(4) Pure nickel oxide and nickel oxide on pumice:

These were the only catalysts in the form of powders, the others being pellets. Though no difficulty was experienced with pellets, powdered catalysts were difficult to work with. Runs were smooth and normal at the beginning but after some time and particularly at higher rates of flow of reactants, the particles had a tendency to clog and increase the resistance to gas flow resulting in an increased pressure drop. This, in turn, rendered the data inaccurate due to the fact that the flow rates were varying. The following values were obtained,

	E - k.cals/mole	A
Pure nickel oxide	13.7	327.9
Nickel oxide on pumice	8.3	14.6

Pure, unsupported, nickel oxide showed a conversion that was the least as compared to the other catalysts. Nickel oxide

on pumice also showed a lower conversion (though higher than that for pure nickel oxide), the maximum value being around 15%. Though three different percentages of nickel (in nickel oxide on pumice) between 10 and 30% Ni were tried as catalysts yet no appreciable difference in the values of conversion was noticeable. This could probably be because the data was not too dependable.

(5) Nickel oxide on alumina and nickel oxide on kieselguhr:

The behaviour of these two catalysts were very similar. They differed only in the magnitude of the kinetic parameters which were found to be as follows:

	E - k.cals/mole	A
Nickel oxide on alumina	9.0	50.9
Nickel oxide on kieselguhr	5.7	3.7

A maximum conversion of about 30% at about 430°C was observed with nickel oxide on alumina while nickel oxide on kiesulghur showed a slightly lower conversion at about 350°C. The latter was slightly more active than the former because of obtaining approximately the same conversion at a lower temperature. Both catalysts were found to obey the compensation effect.

(6) Nickel oxide, chromium oxide:

Nickel oxides in the form of pellets and powders over

various supports, a different element, (but in the same group as nickel) cobalt oxide on alumina and a completely different set of catalysts, platinum and palladium, have been considered. In order to make the comparison complete, a mixed catalyst of nickel and chromium oxides was also studied. The reaction over nickel-chromium oxide was found to behave very much similar to the rest of the nickel catalysts. A value of 10.2 k.cals/mole for the activation energy and 17.4 for the frequency factor was obtained. The value of the maximum conversion obtained was around 20% and it was found to follow the compensation effect close to the nickel catalysts.

XIII. Correlation of data:

The following procedure suggested by Johanson and Watson (19) was used to see how best the rate equation fitted the experimental data.

The values of k and K_A were first determined as mentioned earlier. Because of the similarity in their nature it was assumed that $K_R = K_A$. This was found to be a common procedure as revealed by a survey of the literature. Since k, K_A, K_R and r were known, K_S was easily evaluated.

(W/F) was evaluated as follows:

Catalyst: cobalt oxide on alumina

Weight of catalyst : 9.1 Gms.

P : 10 mm.

$F_{C_6H_{12}}$ - flow rate cyclohexane - 0.084 $\frac{gm\ mols}{hr}$

F_{N_2} - " " nitrogen - 0.028 "

(W/F) experimental : 108

Temperature : 580°C

Conversion : 30%

k : 0.03183

$K_A = K_R$: 1.813

K_S : 1.847

K value - taken from table 15.

Basis of calculation : one hour

Moles C_6H_{12} entering : 0.084

" N_2 " : 0.028

Conversion : 0.30

$$C_6H_{12} = C_6H_6 + 3H_2$$

For every mole of C_6H_{12} converted, one mole of C_6H_6 and three moles of H_2 are produced.

Moles C_6H_{12} leaving : 0.059

" N_2 " : 0.028

" C_6H_6 " : 0.025

" H_2 " : 0.075

" total " : 0.187

p_A - partial pressure C_6H_{12} : $\frac{0.059}{0.187}$ = 0.315 atm.

" " N_2 : $\frac{0.028}{0.187}$ = 0.150 "

p_R - " " C_6H_6 : $\frac{0.025}{0.187}$ = 0.134 "

p_s - " " H_2 : $\frac{0.075}{0.187}$ = 0.401 "

Total : 1.000 "

Substituting the values of k, p_A, p_R, p_s, K, K_A, K_R and K_S in the rate equation,

$$r = \frac{k\left(p_A - \frac{p_R (p_s)^3}{k}\right)}{(1 + pAK_A + p_RK_R + p_sK_s)^2} \qquad (1)$$

$$r = \frac{0.0106}{4.068} = 0.00261$$

Since $\frac{W}{F} = \int_0^x \frac{dx}{r} = \frac{x}{r}$, (6)

$$\frac{W}{F} = \frac{0.30}{0.00261} = 115$$

For T = 580°C, P = 10 mm, x = 0.30,

(W/F) experimental = 108

(W/F) calculated = 115

Similarly, for 580°C, the value of (W/F) was calculated for various flow rates and the procedure repeated for other temperatures.

Figure 38 shows the comparison curves for the catalyst cobalt oxide on alumina, and 39 and 40 for the catalyst nickel

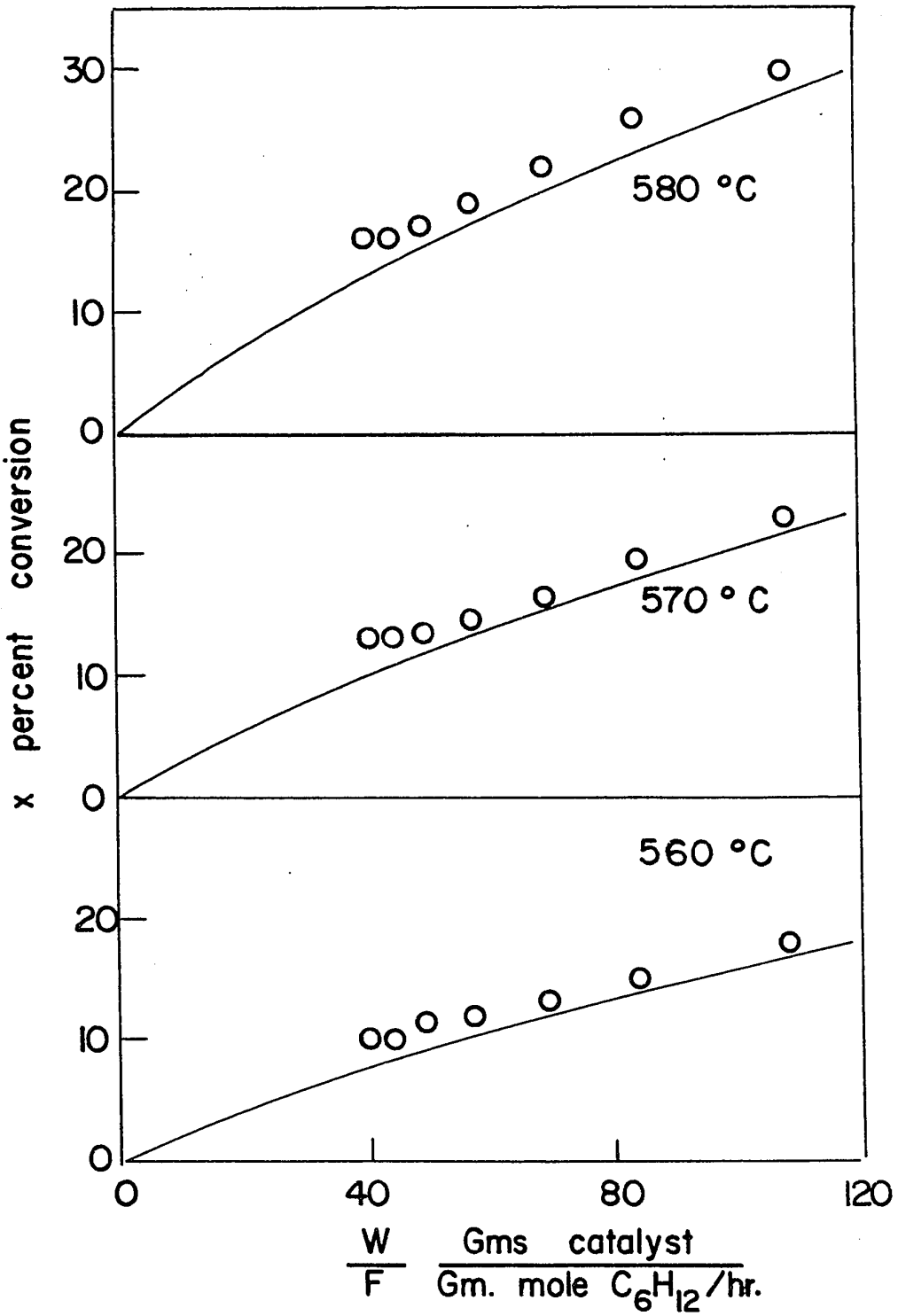

Figure 38 Comparison of experimental and calculated data - Cobalt oxide on alumina.

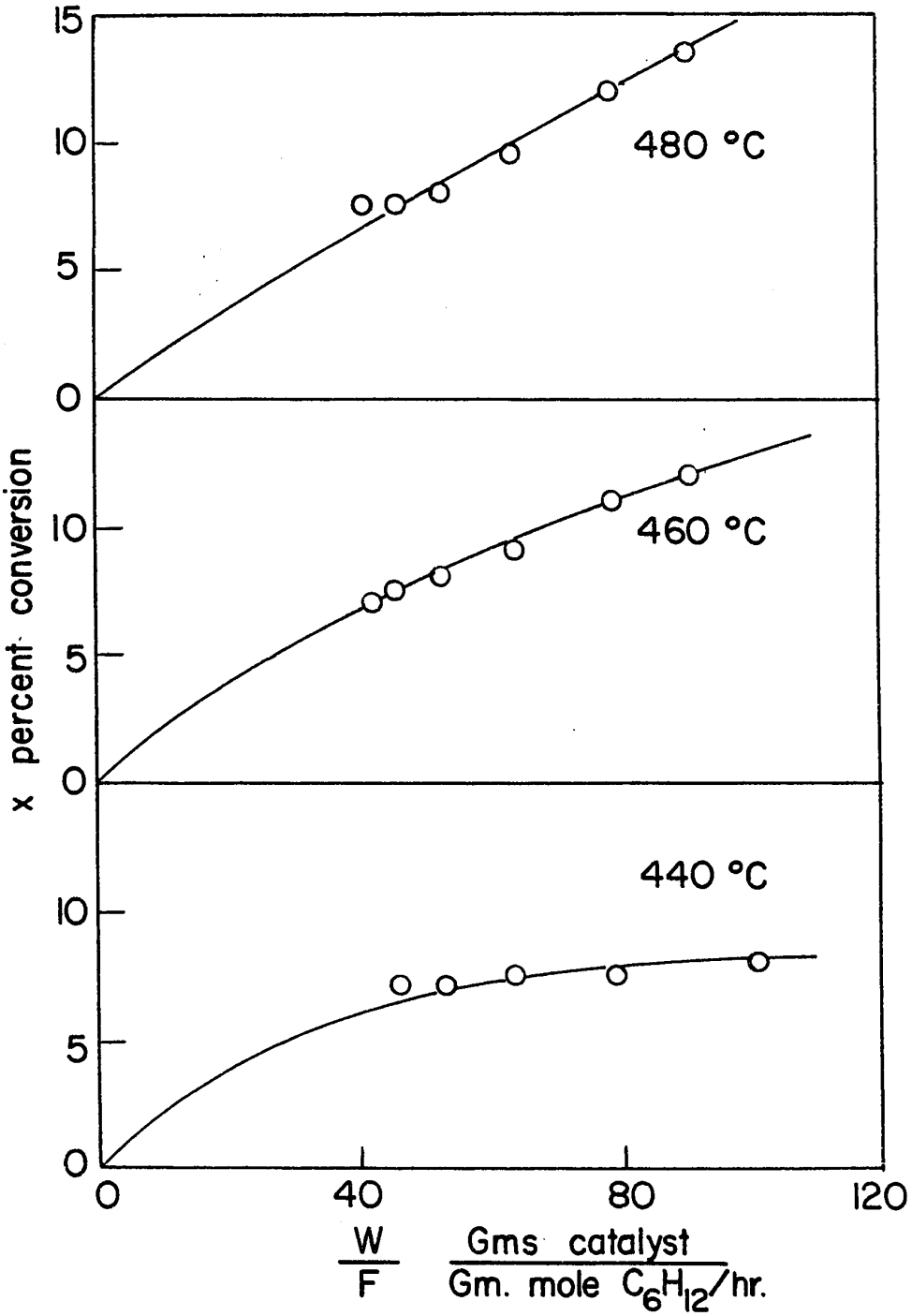

Figure 39 Comparison of experimental and calculated data - nickel oxide, chromium oxide.

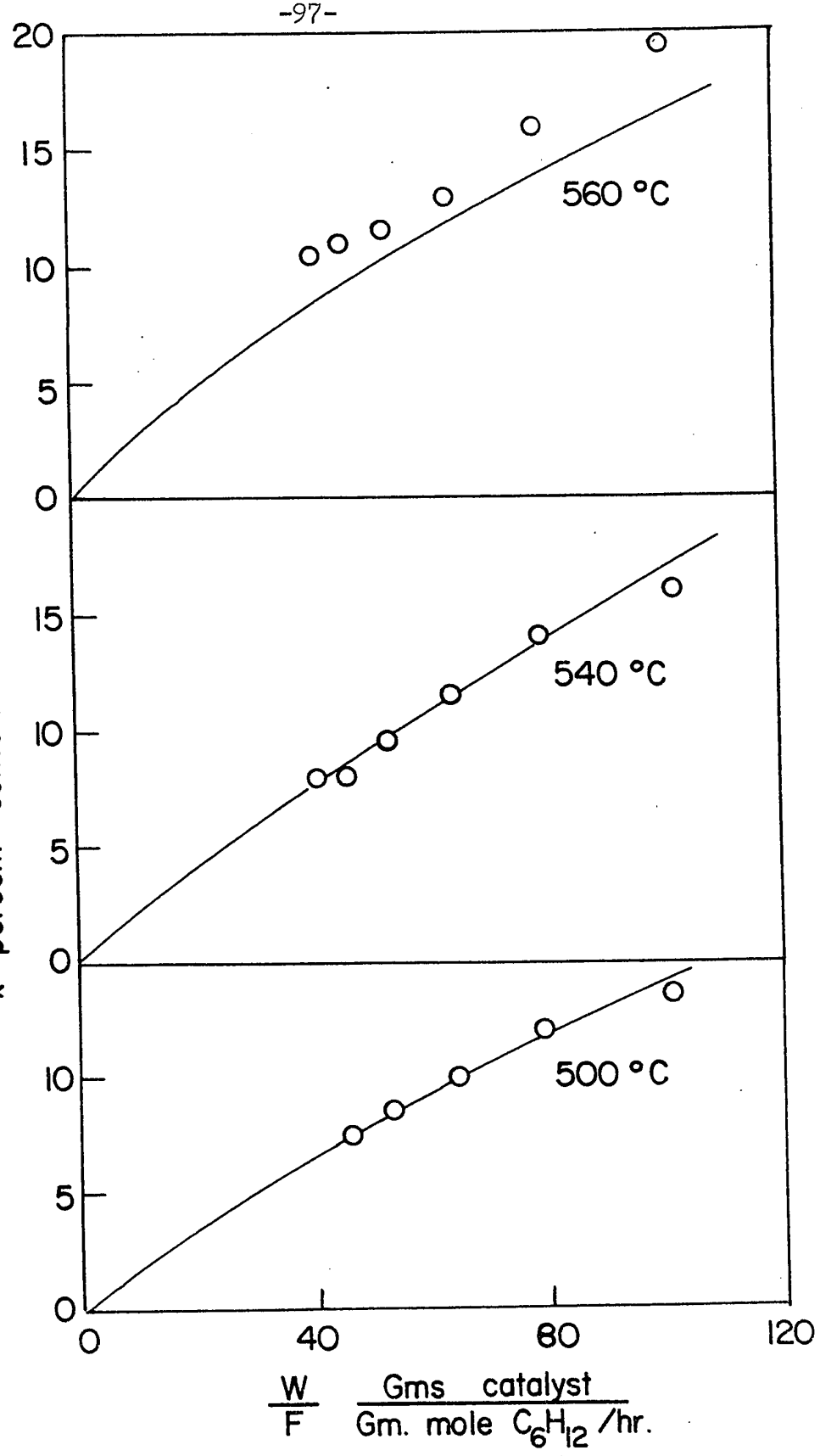

Figure 40 Comparison of experimental and calculated data - nickel oxide, chromium oxide.

oxide, chromium oxide. It is evident from the curves that the agreement is excellent for lower temperatures (lower conversions) but show a slight deviation at higher temperatures (higher conversions).

The solid line in figures 38 to 40 represent the curve for calculated values of (W/F) vs. x and the points, the experimental values of (W/F) vs. x. The maximum deviation was found to be 16.4 %.

Calculations were also carried out to find out the calculated value of (W/F), using the following equation:

$$r = \frac{k\left(p_A - \frac{p_R (p_s)^3}{k}\right)}{(1 + p_A K_A + p_R K_R + p_s K_s)} \qquad (25)$$

and the results are shown in figure 41. The dotted line represents the calculated curve using equation (25) and the solid line using equation (1). When compared with the experimental points it is obvious that equation (1) fits the experimental data much better than equation (25).

Figure 41 Comparison curves for nickel oxide over alumina at 430°C.

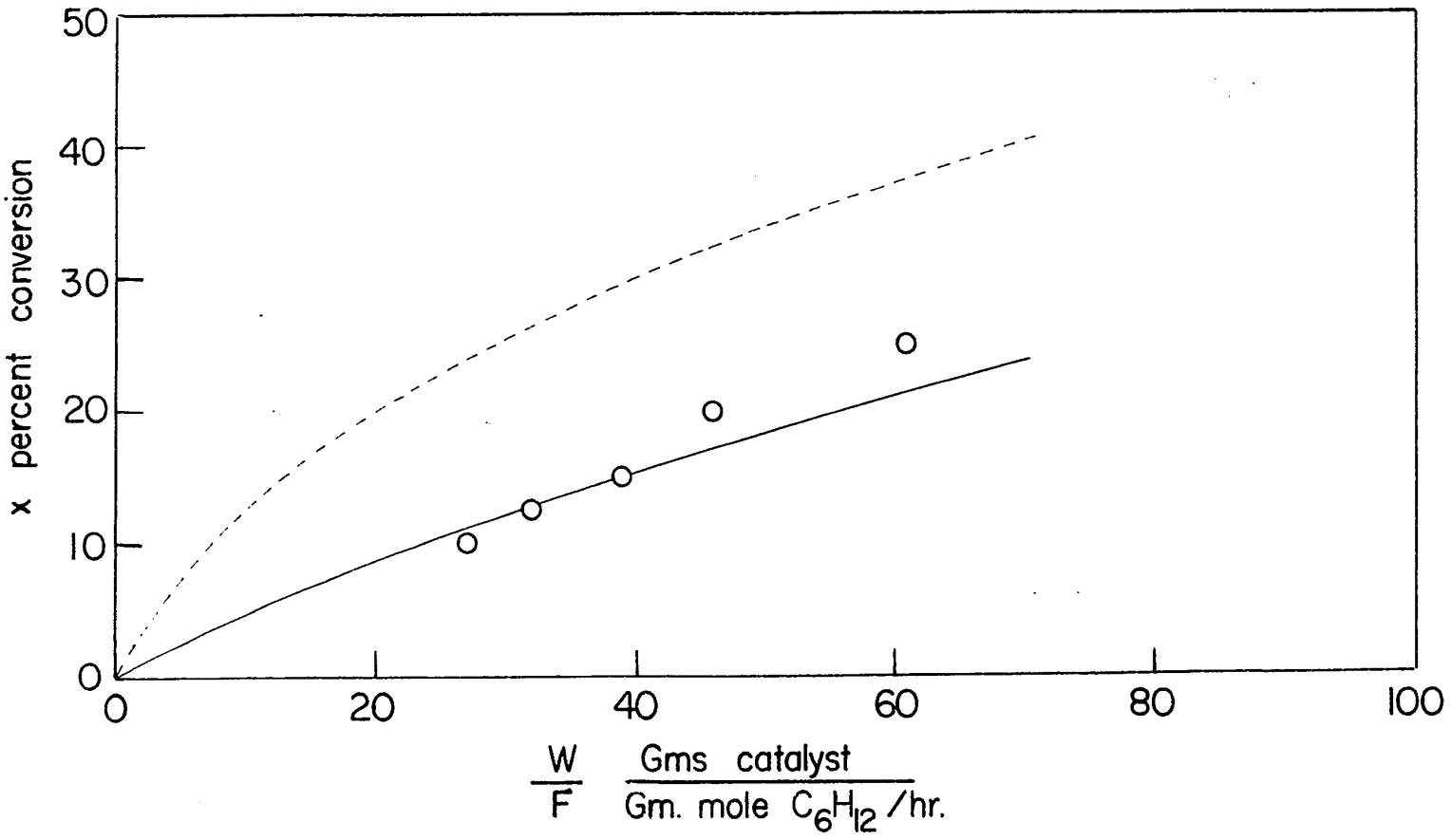

CHAPTER VI.

CONCLUSIONS AND RECOMMENDATIONS

VI. CONCLUSIONS AND RECOMMENDATIONS

The variation of conversion with temperature, as exhibited by platinum on alumina catalyst, was found to be in excellent agreement with the observations of Ross and Valentine. A maximum conversion of nearly hundred percent was attained by platinum on alumina as compared to about thirty percent or less with the other catalysts.

Another observation in keeping with earlier studies was that conversion was independent of flow rates for low values of conversions. However it was found that at higher conversions this was not the case and conversion did show a tendency to decrease with increasing flow rates.

The experimental data were reproducible except in the case of palladium.

It was established that diffusion was not the rate-controlling step. The shape of the curves in a plot of partial pressure of cyclohexane against initial rate suggests that surface reaction and not adsorption was controlling.

Study of the compensation effect revealed that all catalysts of nickel oxide and cobalt oxide followed this effect while platinum did not fit the pattern.

The equipment, being of glass, eliminated the possibilities

of studying the reaction at high temperatures and at pressures greater than one atmosphere.

The inert term has been omitted in the rate equation and this has to be considered.

Use of capillary flow meter to measure the flow involves certain errors which could only be minimised and never eliminated. The calibrations for liquid and gas flows are not very accurate. The range of flow rates were rather limited and so very low and very high flow rates could not be attained. This, in turn, resulted in the experimental points falling in a relatively limited area. Use of two flowmeters and two inlet streams, one for low and another for high flow rates would probably be a good approach to collect a wide range of data.

It is suggested that the difficulties encountered with catalysts, in the form of powders, could be overcome by passing the reactants from the bottom instead of from the top of the reactor.

The limitations involved in this work are fully realised and yet certain useful information has been deduced, thus providing the background for more advanced work.

CHAPTER VII

APPENDICES.

Appendix A

Nomenclature.

NOMENCLATURE

A	frequency factor
a, b	constants
C	concentration of reactants
C_o	concentration of reactants entering catalyst bed
C_1	concentration of reactants after contacting a certain mass of catalyst
C_f	concentration of reactants leaving catalyst bed
E	activation energy
F	flow rate
F_c	flow rate of cyclohexane
F_N	flow rate of nitrogen
H	enthalpy
ΔH^o	standard-state enthalpy change
k	reaction velocity constant
k	velocity constant of forward reaction adsorption
k'	velocity constant of reverse reaction or desorption
K	thermodynamic equilibrium constant
K_A	adsorption equilibrium constant for cyclohexane

K_R	adsorption equilibrium constant for benzene
K_S	adsorption equilibrium constant for hydrogen
m	constant
P	pressure
ΔP	difference in pressures
p_A	partial pressure of cyclohexane
p_{A_1}	partial pressure of cyclohexane entering
p_{A_2}	partial pressure of cyclohexane leaving
p_R	partial pressure of benzene
p_s	partial pressure of hydrogen
R	gas constant
r	reaction rate
r_o	initial reaction rate
S_1, S_2	surface area per unit reactor volume
t	time
T	temperature
T_1, T_2	reaction residence time
W	mass of catalyst
x	distance
X	conversion

Appendix B

Bibliography.

BIBLIOGRAPHY

1. Ross, R. A. and Valentine, J. H., J. Catalysis 2, 39-44 (1963).

2. Potapova, A. A., Zhur. Obshchei Khim. 29, 421-8 (1959)

3. Wright, W., and Waller, Sol W., J. Am. Chem. Soc. 76, 5305-8 (1954).

4. Tetenyi, P., Kislay, J. and Babernics, L., Acta Chim. Acad. Sci. 29, 35-45 (1961).

5. Agronomov, A. E., and Mardashev, Yu S., Zhur Fiz. Khim. 35, 2047-51 (1961).

6. Mcgough, C. B., University microfilms, Ann Arbor, Michigan, dissertation abstracts 22, 827-8 (1961).

7. Minachev, Kh. M., Markov, M. A., and Shukina, O. K., Neftekhimya 1, 489-93 (1961).

8. Magyar, M. and Hodossy, L., Magyar kem. Folyoirat 65, 373-8 (1959).

9. Mcgough, C. B., and Houghton, G., J. Phy. Chem. 65, 1887-91 (1961).

10. Tetenyi, P., Babernics, L., Guczi, L., and Sachter, K., Acta Chim. Hung. Tomus 40 (1964).

11. Magyar, V. M., and Neweth, K., ibid. 379-83.

12. Magyar, V. M., and Neweth, K., Veszpremi Vegyipari Egyetem Kozlemenyei 2, 35-40 (1958).

13. Magyar, V. M., and Hodossy, L., Veszpremi Vegyipari Egyetem Kozlemenyei 2, 27-33 (1958).

14. Rubinshtein, A. M., Freidlin, L. Kh., and Borunova, N. V., Isvest. Akad. Nauk S.S.S.R., Otdel. Khim. Nauk, 766-7 (1958).

15. Bridges, J. M., Rymer, G. T., and Macives, D. S., J. Phy. Chem. 66, 871-7 (1962).

16. Weisz, P. B., and Swegler, E. W., J. Phy. Chem. 59, 823-6 (1955).

17. Ross, R. A., and Walsh, B. G., J. App. Chem. 11, 469-74 (1961).

18. Yang, K. H., and Hougen, O. A., Chem. Eng. Prog. 46, 146-157 (1950).

19. Johanson, L. N., and Watson, K. M., Nat. Pet. News, Tech. Sec., Aug-Sept. (1946).

20. American Petroleum Institute, Project 44, "Selected values of physical and thermodynamic properties of hydrocarbons and related compounds" (1953).

21. Kirk, R. E., and Othmer, D. F., "Encyclopedia of Chemical technology", vol. 4, The Interscience Encyclopedia Inc., New York (1954).

22. Hougen, O.A., and Watson, K. M., "Chemical Process Principles", Part II, John Wiley & Sons, New York (1947).

23. Hougen, O. A., and Watson, K. M., "Chemical Process Principles", Part III, John Wiley & Sons, New York, (1947).

24. Smith, J. M., "Chemical Engineering Kinetics", McGraw-Hill, New York (1956).

25. Walas, S. M., "Reaction Kinetics for Chemical Engineers", McGraw-Hill, New York (1959).

26. Perkin-Elmer Corp., "Instructions for model 154-D Vapor Fractometer", Norwalk, Conn., (1963).

27. Perry, J. H., "Chemical Engineer's Hand-book", Third Edition, McGraw-Hill, New York (1950).

28. Emmett, P. H., "Catalysis", Vol. I, Reinhold Publishing Corp., New York (1955).

29. Frankenburg, W. G., Rideal, E. K., and Komarewsky, V. I., "Advances in Catalysis", A.P., New York (1954).

30. Laidler, K. J., "Chemical Kinetics", McGraw-Hill, New York (1965).

Appendix C

Tables

TABLE 1.

Calibration of Chromatograph.

S. No.	C_6H_{12} %	C_6H_6 %	Areas of Peaks	
			C_6H_{12}	C_6H_6
1	100	0	88	0
2	80	20	71	23
3	60	40	54	44
4	50	50	44	53
5	40	60	35	61
6	20	80	17	82
7	0	100	0	90

TABLE 2 (a): Experimental Data

Catalyst: Cobalt Oxide on Alumina. W_1 = 5.0 Gms

Serial No.	Catalyst Temp.		C_6H_{12} flow.mm	Analysis		% Conversion x
	m.volts	°C		C_6H_{12}	C_6H_6	
1	17.92	329	10	86	0	0
2	19.60	359	"	"	"	0
3	21.84	400	"	"	"	0
4	23.37	428	"	"	"	0
5	24.97	456	"	"	"	0
6	26.64	486	"	"	"	0
7	28.11	513	"	84	1	5
8	30.01	546	"	83	3	6
9	31.28	568	"	79	8	11
10	17.70	325	20	86	0	0
11	19.44	356	"	"	"	0
12	21.70	397	"	"	"	0
13	23.26	426	"	"	"	0
14	24.76	453	"	"	"	0

Table 2 (a) Continued

Catalyst: Cobalt Oxide on Alumina. W = 5.0 Gms.

Serial No.	Catalyst Temp. m.volts	Catalyst Temp. °C	C_6H_{12} flow.mm	Analysis C_6H_{12}	Analysis C_6H_6	% Conversion x
15	26.61	486	20	86	0	0
16	28.11	513	"	87	1	2
17	29.93	545	"	84	2	5
18	31.18	566	"	82	5	8
19	17.46	321	30	86	0	0
20	19.37	355	"	"	"	0
21	21.64	396	"	"	"	0
22	23.14	424	"	"	"	0
23	24.68	451	"	"	"	0
24	26.68	487	"	"	"	0
25	28.09	512	"	85	1	4
26	29.62	540	"	84	2	5
27	30.87	562	"	83	4	7

TABLE 2 (b): Experimental Data

Catalyst: Cobalt Oxide on Alumina. W_2 = 7.0 Gms.

Serial No.	Catalyst Temp. m.volts	Catalyst Temp. °C	C_6H_{12} Flow.mm	Analysis C_6H_{12}	Analysis C_6H_6	% Conversion x
28	17.10	314	10	86	0	0
29	18.21	334	"	"	"	0
30	20.64	378	"	"	"	0
31	22.65	414	"	"	"	0
32	24.53	448	"	"	"	0
33	27.51	502	"	87	3	3
34	30.20	550	"	85	6	8
35	17.17	315	20	86	0	0
36	18.06	332	"	"	"	0
37	20.24	371	"	"	"	0
38	22.39	410	"	"	"	0
39	24.17	442	"	"	"	0
40	27.42	500	"	86	4	5
41	30.13	548	"	87	5	3

Table 2 (b) Continued

Catalyst: Cobalt Oxide on Alumina. W_2 = 7.0 Gms.

Serial No.	Catalyst Temp. m. volts	Catalyst Temp. °C	C_6H_{12} flow.mm	Analysis C_6H_{12}	Analysis C_6H_6	% Conversion x
42	17.10	314	30	86	0	0
43	18.08	332	"	"	"	0
44	20.26	371	"	"	"	0
45	22.11	405	"	"	"	0
46	24.04	440	"	"	"	0
47	27.10	495	"	86	3	3
48	30.09	548	"	86	4	5
49	17.92	329	40	86	0	0
50	20.20	370	"	"	"	0
51	21.66	398	"	"	"	0
52	23.85	436	"	"	"	0
53	27.29	498	"	86	3	3
54	30.07	548	"	86	5	6

TABLE 2 (c): Experimental Data

Catalyst: Cobalt Oxide on Alumina. W_3 = 9.1 Gms.

Serial No.	Catalyst Temp.		C_6H_{12}	Analysis		% Conversion
	m.volts	°C	flow.mm	C_6H_{12}	C_6H_6	x
55	17.13	314	10	86	0	0
56	19.45	356	"	"	"	0
57	22.48	412	"	"	"	0
58	25.78	471	"	"	"	0
59	27.29	498	"	74	9	11
60	28.79	525	"	77	7	7
61	30.23	550	"	73	13	13
62	32.31	586	"	57	31	32
63	16.95	312	20	86	0	0
64	19.17	352	"	"	"	0
65	22.39	410	"	"	"	0
66	25.54	467	"	"	"	0
67	26.92	492	"	78	5	6

Table 2 (c) Continued

Catalyst: Cobalt Oxide on Alumina. W_3 = 9.1 Gms.

Serial No.	Catalyst Temp. m.volts	°C	C_6H_{12} flow.mm	Analysis C_6H_{12}	C_6H_6	% Conversion x
68	28.27	516	20	79	3	4
69	30.07	548	"	76	10	9
70	31.92	580	"	68	18	18
71	16.70	307	30	86	0	0
72	19.07	350	"	"	"	0
73	21.94	402	"	"	"	0
74	25.32	463	"	"	"	0
75	26.71	488	"	79	3	4
76	28.01	511	"	79	3	4
77	29.77	542	"	77	8	7
78	31.67	575	"	70	16	16
79	16.53	304	40	86	0	0
80	19.15	351	"	"	"	0

Table 2 (c) Continued

Catalyst: Cobalt Oxide on Alumina. W_3 = 9.1 Gms.

Serial No.	Catalyst Temp. m.volts	Catalyst Temp. °C	C_6H_{12} flow.mm	Analysis C_6H_{12}	Analysis C_6H_6	% Conversion x
81	21.88	400	40	86	0	0
82	25.03	458	"	"	"	0
83	26.45	484	"	81	1	2
84	27.60	504	"	80	2	3
85	29.34	534	"	78	7	6
86	31.23	568	"	73	12	12

TABLE 3 (a): Experimental Data

Catalyst: Nickel Oxide on Alumina. W_1 = 5.1 Gms.

Serial No.	Catalyst Temp. m.volts	Catalyst Temp. °C.	C_6H_{12} flow.mm	Analysis C_6H_{12}	Analysis C_6H_6	% Conversion x
87	13.95	257	10	86	0	0
88	16.30	300	"	"	"	"
89	18.54	340	"	"	"	"
90	19.65	360	"	"	"	"
91	20.58	377	"	"	"	"
92	21.89	400	10	79	8	7
93	23.26	426	"	67	21	21
94	24.18	442	"	67	22	22
95	21.89	400	20	76	8	10
96	23.19	424	"	75	9	12
97	24.43	447	"	79	11	7
98	26.32	481	"	79	10	7
99	21.80	399	30	79	4	4

Table 3 (a) Continued

Catalyst: Nickel Oxide on Alumina. W_1 = 5.1 Gms.

Serial No.	Catalyst Temp. m.volts	Catalyst Temp. °C.	C_6H_{12} flow.mm	Analysis C_6H_{12}	Analysis C_6H_6	% Conversion x
100	23.27	426	30	78	6	8
101	24.24	444	"	81	7	5
102	26.24	480	"	82	7	3

TABLE 3 (b): Experimental Data

Nickel Oxide on Alumina. W_2 = 6.9 Gms.

Serial No.	Catalyst Temp.		C_6H_{12}	Analysis		% conversion
	m.volts	°C.	flow.mm	C_6H_{12}	C_6H_6	x
103	21.02	385	10	86	0	0
104	21.12	387	"	"	"	"
105	21.95	402	"	"	"	"
106	23.35	427	"	60	20	27
107	23.92	438	"	67	13	19
108	25.04	458	"	67	14	20
109	26.46	484	"	64	16	23
110	21.04	385	20	86	0	0
111	22.07	404	"	"	"	"
112	23.19	424	"	72	10	15
113	24.04	440	"	72	9	14
114	25.04	458	"	70	10	16
115	26.22	479	"	71	9	15

Table 3 (b) Continued

Catalyst: Nickel Oxide on Alumina. W_2 = 6.9 Gms.

Serial No.	Catalyst Temp. m.volts	Catalyst Temp. °C.	C_6H_{12} flow.mm	Analysis C_6H_{12}	Analysis C_6H_6	% Conversion x
116	21.94	402	30	76	3	10
117	23.19	424	"	74	6	12
118	23.67	434	"	74	6	12
119	24.90	455	"	73	7	13
120	25.86	473	"	74	6	12

TABLE 3 (c): Experimental Data

Nickel Oxide on Alumina. W_3 = 8.9 Gms.

Serial No.	Catalyst Temp. m.volts	Catalyst Temp. °C.	C_6H_{12} flow.mm	Analysis C_6H_{12}	Analysis C_6H_6	% conversion x
121	21.75	398	10	86	0	0
122	22.54	413	"	66	16	20
123	24.10	441	"	56	24	31
124	24.96	456	"	58	23	29
125	26.56	485	"	58	24	29
126	21.69	397	20	86	0	0
127	22.57	413	"	69	13	17
128	23.97	439	"	63	16	23
129	24.76	453	"	66	15	20
130	26.38	482	"	63	16	23
131	21.62	396	30	82	1	2
132	22.46	411	"	70	12	16
133	23.94	438	"	66	14	20
134	24.64	451	"	68	11	17
135	26.23	479	"	68	12	17

TABLE 4 (a): Experimental Data.

Nickel Oxide on Kiesulghur. W_1 = 5.5 Gms.

Serial No.	Catalyst Temp. m.volts	Catalyst Temp. °C.	C_6H_{12} flow.mm	Analysis C_6H_{12}	Analysis C_6H_6	% conversion x
136	12.53	231	10	80	2	4
137	14.48	266	"	73	10	12
138	15.53	286	"	69	13	16
139	18.41	338	"	68	13	18
140	19.65	360	"	58	25	29
141	21.08	386	"	86	0	0
142	22.67	415	"	73	11	12
143	12.35	228	20	82	1	2
144	14.31	264	"	78	7	7
145	15.52	286	"	74	8	11
146	18.04	331	"	73	8	12
147	19.60	360	"	67	17	19
148	21.35	391	"	69	15	17
149	23.97	438	"	76	6	9

Table 4 (a) Continued.

Catalyst: Nickel Oxide on Kiesulghur. W_1 = 5.5 Gms.

Serial No.	Catalyst Temp. m.volts	Catalyst Temp. $^{o}C.$	C_6H_{12} flow.mm	Analysis C_6H_{12}	Analysis C_6H_6	% conversion x
150	12.17	225	30	86	0	0
151	14.21	262	"	80	2	4
152	15.36	283	"	78	3	7
153	17.90	329	"	74	7	11
154	19.27	353	"	70	12	16
155	24.08	440	"	76	7	9

TABLE 4 (b): Experimental Data

Catalyst: Nickel Oxide on Kiesulghur. W_2 = 7.1 Gms.

Serial No.	Catalyst Temp. m.volts	Catalyst Temp. °C.	C_6H_{12} flow.mm	Analysis C_6H_{12}	Analysis C_6H_6	% conversion x
156	10.29	191	10	86	0	0
157	13.54	250	"	"	"	"
158	16.27	299	"	"	"	"
159	18.25	335	"	"	"	"
160	20.09	368	"	"	"	"
161	21.37	392	"	76	6	9
162	23.07	422	"	77	4	7
163	10.47	194	20	86	0	0
164	13.51	249	"	"	"	"
165	16.22	298	"	"	"	"
166	18.30	336	"	"	"	"
167	19.84	364	"	"	"	"
168	21.32	390	"	78	3	6
169	22.74	416	"	76	6	9

Table 4 (b) Continued

Catalyst: Nickel Oxide on Kiesulghur. W_2 = 7.1 Gms.

Serial No.	Catalyst Temp.		C_6H_{12}	Analysis		% conversion x
	m.volts	°C.	flow.mm	C_6H_{12}	C_6H_6	
170	10.57	196	30	86	0	0
171	13.26	245	"	"	"	"
172	16.18	298	"	"	"	"
173	18.18	334	"	"	"	"
174	19.70	361	"	82	2	2
175	21.26	389	"	79	2	5
176	22.60	414	"	75	6	10

TABLE 4 (c): Experimental Data.

Catalyst: Nickel Oxide on Kiesulghur. W_3 = 9.4 Gms.

Serial No.	Catalyst Temp.		C_6H_{12}	Analysis		% conversion
	m.volts	°C.	flow.mm	C_6H_{12}	C_6H_6	x
177	14.99	276	10	86	0	0
178	18.35	337	"	88	"	"
179	20.27	371	"	77	8	8
180	22.05	404	"	80	5	4
181	14.63	270	20	89	0	0
182	18.08	332	"	87	0	0
183	20.05	368	"	78	7	7
184	21.62	396	"	74	12	12
185	14.49	267	30	89	0	0
186	17.97	330	"	87	"	"
187	19.82	363	"	79	6	6
188	21.29	390	"	71	16	15

TABLE 5 (a): Experimental Data.

Catalyst: Nickel Oxide, Chromium Oxide. W_1 = 5.6 Gms.

Serial No.	Catalyst Temp. m.volts	Catalyst Temp. °C.	C_6H_{12} flow.mm	Analysis C_6H_{12}	Analysis C_6H_6	% conversion x
189	15.82	291	10	86	0	0
190	18.70	343	"	"	"	"
191	21.22	388	"	84	0	0
192	23.80	436	"	81	1	2
193	26.25	480	"	78	6	6
194	28.84	526	"	72	11	13
195	30.62	557	"	69	14	17
196	22.85	418	20	86	0	0
197	25.00	459	"	"	"	0
198	26.77	489	"	79	2	4
199	28.63	522	"	78	4	6
200	30.65	558	"	77	5	7
201	23.09	422	30	86	0	0
202	24.55	449	"	"	"	"

Table 5 (a) Continued.

Catalyst: Nickel Oxide, Chromium Oxide. W_1 = 5.6 Gms.

Serial No.	Catalyst Temp. m.volts	Catalyst Temp. °C.	C_6H_{12} flow.mm	Analysis C_6H_{12}	Analysis C_6H_6	% conversion x
203	26.70	488	30	81	1	2
204	28.47	519	"	78	4	6
205	30.40	553	"	79	3	6
206	22.73	416	40	86	0	0
207	24.59	450	"	"	"	"
208	26.52	484	"	81	1	2
209	28.23	515	"	79	1	4
210	30.24	550	"	79	2	4

TABLE 5 (b): Experimental Data.

Catalyst: Nickel Oxide, Chromium Oxide. W_2 = 8.5 Gms.

Serial No.	Catalyst Temp. m.volts	Catalyst Temp. °C.	C_6H_{12} flow.mm	Analysis C_6H_{12}	Analysis C_6H_6	% conversion x
211	22.82	418	10	96	0	0
212	23.96	438	"	92	3	7.5
213	25.89	473	"	86	10	13.5
214	28.19	514	"	86	10	13.5
215	29.79	542	"	83	13	16.5
216	32.18	584	"	75	21	25.0
217	22.18	406	20	96	0	0
218	23.78	435	"	92	2	7.5
219	25.45	466	"	89	6	10.5
220	27.75	506	"	91	5	8.0
221	29.50	538	"	88	8	11.5
222	31.78	577	"	83	12	16.5
223	21.92	401	30	96	0	0
224	23.48	430	"	93	1	6.5

Table 5 (b) Continued.

Catalyst: Nickel Oxide, Chromium Oxide. W_2 = 8.5 Gms.

Serial No.	Catalyst Temp. m.volts	Catalyst Temp. °C.	C_6H_{12} flow.mm	Analysis C_6H_{12}	Analysis C_6H_6	% conversion x
225	25.09	458	30	92	3	7.5
226	27.49	502	"	93	3	6.5
227	29.11	530	"	92	4	7.5
228	31.47	572	"	85	7	14.0
229	21.72	398	40	96	0	0
230	23.29	426	"	93	1	6.5
231	24.88	455	"	93	3	6.5
232	27.26	498	"	94	2	5.0
233	28.94	528	"	92	3	7.5
234	31.16	566	"	88	7	11.5

TABLE 6 (a): Experimental Data.

Catalyst: Platinum on Alumina. W_1 = 6.2 Gms.

Serial No.	Catalyst Temp. m.volts	Catalyst Temp. °C.	C_6H_{12} flow.mm	Analysis C_6H_{12}	Analysis C_6H_6	% conversion x
235	8.97	168	10	83	0	0
236	13.43	248	"	68	15	22
237	14.58	268	"	72	15	20
238	17.68	324	"	49	38	44
239	20.02	367	"	85	0	0
240	23.68	434	"	"	"	"
241	26.75	488	"	"	"	"
242	14.49	267	20	78	6	12
243	12.45	230	"	83	1	6
244	10.64	198	"	84	0	0
245	15.97	294	"	72	15	20
246	18.02	331	"	59	28	34
247	10.51	195	30	84	0	0
248	12.54	232	"	80	3	10

Table 6 (a) Continued.

Catalyst: Platinum on Alumina. W_1 = 6.2 Gms.

Serial No.	Catalyst Temp. m.volts	Catalyst Temp. °C.	C_6H_{12} flow.mm	Analysis C_6H_{12}	Analysis C_6H_6	% conversion x
249	13.90	256	30	76	8	14
250	15.93	293	"	72	12	18
251	17.62	324	"	61	22	30

TABLE 6 (b): Experimental Data.

Catalyst: Platinum on Alumina. W_2 = 8.1 Gms.

Serial No.	Catalyst Temp. m.volts	Catalyst Temp. °C.	C_6H_{12} flow.mm	Analysis C_6H_{12}	Analysis C_6H_6	% conversion x
252	10.58	196	10	71	17	20
253	12.47	230	"	45	45	50
254	14.08	260	"	18	77	80
255	15.62	287	"	7	88	90
256	17.04	313	"	5	91	92
257	17.99	330	"	41	52	56
258	11.32	210	20	78	6	12
259	13.66	252	"	66	21	26
260	15.29	282	"	53	36	40
261	17.29	318	"	42	49	53
262	18.60	341	"	36	54	58
263	11.20	208	30	84	1	5

Table 6 (b) Continued.

Catalyst: Platinum on Alumina. W_2 = 8.1 Gms.

Serial No.	Catalyst Temp. m.volts	Catalyst Temp. °C.	C_6H_{12} flow.mm	Analysis C_6H_{12}	Analysis C_6H_6	% conversion x
264	12.93	238	30	82	5	9
265	14.75	272	"	77	10	14
266	17.13	314	"	66	22	26
267	18.72	343	"	51	39	43

TABLE 6 (c): Experimental Data.

Catalyst: Platinum on Alumina. W_3 = 4.3 Gms.

Serial No.	Catalyst Temp. m.volts	Catalyst Temp. °C.	C_6H_{12} flow.mm	Analysis C_6H_{12}	Analysis C_6H_6	% conversion x
268	10.98	204	10	74	7	16
269	13.05	240	"	64	20	27
270	14.93	274	"	48	37	44
271	17.02	312	"	36	51	56
272	18.71	343	"	30	58	63
273	10.77	200	20	82	2	8
274	12.89	238	"	76	8	14
275	14.88	274	"	67	18	24
276	17.62	324	"	52	35	40
277	19.01	348	"	48	39	45
278	10.36	192	30	87	0	0
279	12.56	232	"	86	0	0
280	14.42	266	"	84	1	5

Table 6 (c) Continued.

Catalyst: Platinum on Alumina. W_3 = 4.3 Gms.

Serial No.	Catalyst Temp. m.volts	Catalyst Temp. °C.	C_6H_{12} flow.mm	Analysis C_6H_{12}	Analysis C_6H_6	% conversion x
281	16.28	299	30	78	6	12
282	17.29	325	"	76	8	14

TABLE 6 (d): Experimental Data.

Catalyst: Platinum on Alumina. W_4 = 5.2 Gms.

Serial No.	Catalyst Temp. m.volts	Catalyst Temp. °C.	C_6H_{12} flow.mm	Analysis C_6H_{12}	Analysis C_6H_6	% conversion x
283	11.50	213	10	74	7	16
284	12.55	232	"	66	16	24
285	14.32	264	"	50	34	41
286	16.77	308	"	31	55	61
287	18.49	339	"	23	65	70
288	10.61	197	20	80	2	10
289	12.55	232	"	76	6	14
290	14.35	264	"	67	15	23
291	16.18	297	"	56	26	34
292	17.63	324	"	53	30	38
293	10.43	194	30	82	0	0
294	12.28	227	"	80	4	10
295	13.91	258	"	75	8	15

Table 6 (d) Continued.

Catalyst: Platinum on Alumina. W_4 = 5.2 Gms.

Serial No.	Catalyst Temp. m.volts	Catalyst Temp. °C.	C_6H_{12} flow.mm	Analysis C_6H_{12}	Analysis C_6H_6	% conversion x
296	15.70	289	30	68	15	22
297	17.57	322	"	57	27	34
298	11.16	206	40	81	1	7
299	12.88	238	"	77	7	13
300	14.50	268	"	71	13	20
301	16.47	302	"	64	20	27
302	18.33	336	"	58	29	35

TABLE 7: Experimental Data.

Catalyst: Pure Nickel Oxide. W_1 = 1.1 Gms.

Serial No.	Catalyst Temp. m.volts	Catalyst Temp. °C.	C_6H_{12} flow.mm	Analysis C_6H_{12}	Analysis C_6H_6	% conversion x
303	13.64	252	10	88	0	0
304	16.14	296	"	"	"	"
305	18.94	348	"	"	"	"
306	21.35	391	"	"	"	"
307	24.10	442	"	86	2	2.5
308	26.84	490	"	85	3	4.0
309	30.44	554	"	84	6	10.0
310	13.70	252	20	88	0	0
311	16.18	297	"	"	"	"
312	18.90	346	"	"	"	"
313	21.42	392	"	"	"	"
314	24.27	444	"	88	1	0
315	26.99	493	"	87	2	1.5

Table 7 Continued.

Catalyst: Pure Nickel Oxide. W_1 = 1.1 Gms.

Serial No.	Catalyst Temp. m. volts	Catalyst Temp. °C.	C_6H_{12} flow.mm	Analysis C_6H_{12}	Analysis C_6H_6	% conversion x
316	31.02	564	"	85	4	4.0
317	13.50	249	30	88	0	0
318	15.96	294	"	"	"	"
319	18.78	344	"	"	"	"
320	21.36	391	"	"	"	"
321	24.17	442	"	88	1	0
322	26.71	488	"	86	2	2.5
323	30.43	554	"	88	3	3.0
324	13.44	248	40	88	0	0
325	16.02	294	"	"	"	"
326	18.61	341	"	"	"	"
327	21.32	390	"	"	"	"

Table 7 Continued.

Catalyst: Pure Nickel Oxide. W_1 = 1.1 Gms.

Serial No.	Catalyst Temp. m.volts	Catalyst Temp. °C.	C_6H_{12} flow.mm	Analysis C_6H_{12}	Analysis C_6H_6	% conversion x
328	24.11	441	40	88	0	0
329	26.78	489	"	87	1	2.0
330	30.27	551	"	88	2	3.0

TABLE 8 (a): Experimental Data

Catalyst: Nickel Oxide on Pumice (10%). W_1 = 4.6 Gms.

Serial No.	Catalyst Temp. m.volts	Catalyst Temp. °C	C_6H_{12} flow.mm	Analysis C_6H_{12}	Analysis C_6H_6	% Conversion x
331	5.14	98	10	80	0	0
332	7.87	148	"	"	"	"
333	9.93	185	"	"	"	"
334	11.82	219	"	"	"	"
335	13.96	257	"	"	"	"
336	15.95	293	"	"	"	"
337	17.84	328	"	"	"	"
338	19.61	360	"	"	"	"
339	22.06	404	"	"	"	"
340	24.09	440	"	70	2	15

TABLE 8 (b): Experimental Data.

Catalyst: Nickel Oxide on Pumice (10%). W_2 = 7.2 Gms.

Serial No.	Catalyst Temp.		C_6H_{12}	Analysis		% conversion
	m.volts	°C.	flow.mm	C_6H_{12}	C_6H_6	x
341	6.54	123	10	84	0	0
342	9.73	181	"	"	"	"
343	12.29	227	"	"	"	"
344	14.30	263	"	"	"	"
345	17.12	314	"	"	"	"
346	19.00	348	"	77	1	7
347	19.75	362	"	77	2	8
348	20.54	376	"	74	2	10
349	21.35	391	"	72	4	12
350	22.20	406	"	70	6	14
351	23.06	422	"	70	7	15
352	23.90	438	"	69	7	16

TABLE 8 (c): Experimental Data.

Catalyst: Nickel Oxide on Pumice (10%). W_3 = 10.5 Gms.

Serial No.	Catalyst Temp. m.volts	Catalyst Temp. °C.	C_6H_{12} flow.mm	Analysis C_6H_{12}	Analysis C_6H_6	% conversion x
353	9.84	183	10	84	0	0
354	15.10	278	"	"	"	"
355	16.83	309	"	"	"	"
356	19.00	348	"	"	"	"
357	20.96	384	"	74	2	10
358	21.68	397	"	72	4	12
359	22.39	410	"	70	5	14
360	24.63	450	"	71	6	13

TABLE 8 (d): Experimental Data.

Catalyst: Nickel Oxide on Pumice (30%). W_1 = 5.2 Gms.

Serial No.	Catalyst Temp.		C_6H_{12}	Analysis		% conversion
	m.volts	°C.	flow.mm	C_6H_{12}	C_6H_6	x
361	6.98	132	6	84	0	0
362	8.57	160	"	"	"	"
363	10.41	194	"	"	"	"
364	12.49	231	"	"	"	"
365	13.90	256	"	"	"	"
366	16.05	295	"	"	"	"
367	17.70	325	"	"	"	"
368	19.46	357	"	"	"	"
369	21.09	386	"	81	1	2
370	23.11	423	"	76	1	9
371	24.03	440	"	73	1	12

TABLE 8 (e): Experimental Data.

Catalyst: Nickel Oxide on Pumice (30%). W_2 = 7.3 Gms.

Serial No.	Catalyst Temp.		C_6H_{12}	Analysis		% conversion
	m.volts	°C.	flow.mm	C_6H_{12}	C_6H_6	x
372	11.94	221	6	84	0	0
373	13.18	243	"	"	"	"
374	16.21	298	"	"	"	"
375	18.25	335	"	"	"	"
376	19.93	365	"	80	2	4
377	21.92	401	"	75	1	10
378	23.44	429	"	74	2	11

TABLE 8 (f): Experimental Data.

Catalyst: Nickel Oxide on Pumice (30%). W_3 = 8.2 Gms.

Serial No.	Catalyst Temp. m.volts	Catalyst Temp. °C.	C_6H_{12} flow.mm	Analysis C_6H_{12}	Analysis C_6H_6	% conversion x
379	11.94	221	6	84	0	0
380	14.79	272	"	"	"	"
381	17.45	320	"	"	"	"
382	19.32	354	"	"	"	"
383	20.78	380	"	82	1	3

TABLE 9: W/F vs X Cobalt Oxide on Alumina.

Serial No.	P mm	W/F	Conversion Percentages at different temperatures								
			500	510	520	530	540	550	560	570	580
1	10	108	9.0	9.0	9.0	10.0	11.0	13.0	18.0	23.0	30.0
2	15	84	7.0	7.0	7.5	8.0	9.5	11.0	15.0	19.0	24.0
3	20	69	5.0	5.5	6.0	6.5	8.0	9.0	12.0	15.0	18.0
4	25	57	4.5	5.0	5.5	6.5	7.5	9.0	12.0	14.5	18.0
5	30	49	4.0	4.5	5.0	6.0	7.0	9.0	11.5	14.5	18.5
6	35	44	3.5	4.0	5.0	6.0	7.0	8.5	10.5	13.5	17.0
7	40	40	3.0	4.0	5.0	6.0	7.0	8.0	10.0	13.0	16.0

TABLE 10: Determination of Initial Rate. Cobalt Oxide on Alumina.

Serial No.	T. (°C)		$\frac{W}{F}$: 20.	40	60	80	100	120
1	500	x	0.015	0.030	0.050	0.065	0.075	0.080
		$x/(\frac{W}{F})$	0.00075	0.00075	0.00083	0.00081	0.00075	0.00067
2	510	x	0.020	0.035	0.055	0.070	0.080	0.085
		$x/(\frac{W}{F})$	0.00100	0.00088	0.00092	0.00088	0.00080	0.00077
3	520	x	0.025	0.040	0.060	0.075	0.080	0.080
		$x/(\frac{W}{F})$	0.00125	0.00100	0.00100	0.00094	0.00080	0.00067
4	530	x	0.030	0.055	0.075	0.085	0.090	0.090
		$x/(\frac{W}{F})$	0.00150	0.00138	0.00125	0.00106	0.00090	0.00075
5	540	x	0.035	0.060	0.080	0.095	0.105	0.105
		$x/(\frac{W}{F})$	0.00175	0.00150	0.00133	0.00119	0.00105	0.00088
6	550	x	0.040	0.075	0.100	0.125	0.140	0.150
		$x/(\frac{W}{F})$	0.00200	0.00188	0.00167	0.00156	0.00140	0.00125

Table 10 Continued

Determination of Initial Rate. Cobalt Oxide on Alumina.

Serial No.	T. (°C)		$\frac{W}{F}$: 20	40	60	80	100	120
7	560	x	0.050	0.095	0.130	0.150	0.170	0.170
		$x/(\frac{W}{F})$	0.00250	0.00238	0.00217	0.00188	0.00170	0.00142
8	570	x	0.060	0.115	0.155	0.190	0.215	0.225
		$x/(\frac{W}{F})$	0.00300	0.00288	0.00258	0.00237	0.00215	0.00188
9	580	x	0.080	0.150	0.200	0.250	0.285	0.315
		$x/(\frac{W}{F})$	0.00400	0.00375	0.00333	0.00313	0.00285	0.00263

TABLE 11: Initial Rates

Catalyst: Cobalt Oxide on Alumina.

Serial No.	T. (°C)	r_o ($\frac{\text{gm moles}}{(\text{hr})(\text{gm catalyst})}$)
1	500	0.00088
2	510	0.00101
3	520	0.00141
4	530	0.00167
5	540	0.00197
6	550	0.00215
7	560	0.00270
8	570	0.00320
9	580	0.00430

TABLE 12: Arrhenius Plot

Catalyst: Cobalt Oxide on Alumina.

Serial No.	T^oC	T^oK	$\frac{10^3}{T^oK}$	k	log k
1	500	773	1.294	0.00648	$\bar{3}$.8116
2	510	783	1.277	0.00750	$\bar{3}$.8751
3	520	793	1.261	0.01044	$\bar{2}$.0187
4	530	803	1.245	0.01234	$\bar{2}$.0903
5	540	813	1.230	0.01462	$\bar{2}$.1649
6	550	823	1.215	0.01598	$\bar{2}$.2036
7	560	833	1.200	0.01988	$\bar{2}$.2984
8	570	843	1.186	0.02378	$\bar{2}$.3762
9.	580	853	1.172	0.03183	$\bar{2}$.5028

TABLE 13: Calculation of Arhennius Constant

Catalyst: Cobalt Oxide on Alumina.

Serial No.	Temp °C	Log A	A	$(A)_{avg}$	$(\text{Log } A)_{avg}$
1	500	3.9539	8992		
2	510	3.9390	8690		
3	520	4.0061	10140		
4	530	4.0031	10070		
5	540	4.0050	10120		
6	550	3.9727	9390	9623	3.9833
7	560	3.9983	9960		
8	570	4.0085	10200		
9	580	4.0890	12300		

TABLE 14: Compensation Effect.

Serial No.	T^oC	T^oK	$\frac{10^3}{T^oK}$	k	log k	Catalyst	E kcals/mol	A	log A
1	480	753	1.328	0.0352	$\bar{2}.5465$	PURE NICKEL OXIDE	13.728	327.9	2.5157
2	490	763	1.311	0.0420	$\bar{2}.6232$				
3	500	773	1.294	0.0465	$\bar{2}.6675$				
4	510	783	1.277	0.0484	$\bar{2}.6848$				
5	520	793	1.261	0.0556	$\bar{2}.7451$				
6	370	643	1.56	0.0214	$\bar{2}.3294$	NICKEL OXIDE ON PUMICE	8.300	14.55	1.1629
7	380	653	1.53	0.0228	$\bar{2}.3585$				
8	390	663	1.51	0.0276	$\bar{2}.4421$				
9.	400	673	1.49	0.0261	$\bar{2}.4173$				
10	410	683	1.46	0.0331	$\bar{2}.5202$				
11	423	693	1.44	0.0350	$\bar{2}.5437$				
12	285	558	1.79	0.0222	$\bar{2}.3464$	NICKEL OXIDE ON KIESULGHUR	5.693	3.716	0.5701
13	300	573	1.75	0.0243	$\bar{2}.3856$				

TABLE 14: Continued: Compensation Effect.

Serial No.	T°C	T°k	$\frac{10^3}{T^\circ k}$	k	log k	Catalyst	E kcals/mol	A	log A
14	330	603	1.66	0.0335	$\bar{2}.5250$	NICKEL OXIDE ON KIESULGHUR	5.693	3.716	0.5701
15	390	663	1.51	0.0484	$\bar{2}.6849$				
16	410	683	1.464	0.0278	$\bar{2}.4440$	NICKEL OXIDE ON ALUMINA	9.002	50.88	1.3227
17	420	693	1.443	0.0305	$\bar{2}.4843$				
18	430	703	1.422	0.0336	$\bar{2}.5263$				
19	440	713	1.403	0.0364	$\bar{2}.5611$				
20	420	693	1.443	0.0107	$\bar{2}.0294$	NICKEL OXIDE CHROMIUM OXIDE	10.22	17.38	1.2400
21	440	713	1.403	0.0130	$\bar{2}.1139$				
22	480	753	1.328	0.0197	$\bar{2}.2945$				
23	500	779	1.294	0.0221	$\bar{2}.3444$				
24	520	793	1.261	0.0242	$\bar{2}.3838$				
25	560	833	1.200	0.0364	$\bar{2}.5611$				

Table 14 Continued: Compensation Effect.

Serial No.	T°C	T°k	$\frac{10^3}{T^oK}$	k	log k	Catalyst	E kcals/mol	A	log A
26	220	493	2.03	0.0329	$\bar{2}.5172$	PLATINUM	6.864	35.77	1.5536
27	260	533	1.88	0.0572	$\bar{2}.7574$	ON			
28	280	553	1.81	0.0665	$\bar{2}.8228$	ALUMINA			
29	300	573	1.75	0.0809	$\bar{2}.9079$				
30	340	513	1.63	0.1345	$\bar{1}.1287$				

TABLE 15

$T^{o}k$	ΔF^{o} $-(^{Kcals}/_{mole})$			Log k $= -\frac{\Delta F^{o} \text{ reaction } (\frac{cal}{mol})}{4.576\ T\ (^{o}k)}$	k
	C_6H_6	C_6H_{12}	Reaction		
0	24.000	- 20.010	44.010	-	
298.16	30.989	+ 7.590	23.399	- 17.1500 18.8500	7.0795×10^{-18}
300	31.053	7.810	23.248	- 16.9347 17.0653	1.1627×10^{-17}
400	35.008	20.660	14.348	- 7.8387 8.1613	1.4498×10^{-8}
500	39.242	34.070	5.172	- 2.2605 3.7395	5.4891×10^{-3}
600	43.663	47.860	- 4.197	+ 1.5286	3.3775×10^{1}
700	48.211	61.850	- 13.639	+ 4.2579	1.8019×10^{4}
800	52.838	75.960	- 23.122	+ 6.3161	2.0706×10^{6}
900	57.537	90.130	- 32.593	+ 7.9140	8.2035×10^{7}
1000	62.270	104.300	- 42.030	+ 9.1849	1.5308×10^{9}
1100	67.020	118.420	- 51.400	+ 10.2114	1.6270×10^{10}
1200	71.790	132.580	- 60.790	+ 11.0704	1.1760×10^{11}

Table 15 Continued

T(°k)	ΔF^o – (Kcals/mole)			$= -\frac{\Delta F^o}{4.576\ T\ (^oK)}$	Log k reaction $(\frac{cal}{mol})$	k
	C_6H_6	C_6H_{12}	Reaction			
1300	76.570	146.690	– 70.120		+ 11.7873	6.1277×10^{11}
1400	81.340	160.730	– 79.390		+ 12.3923	2.4677×10^{12}
1500	86.110	174.720	– 88.610		+ 12.9094	8.1170×10^{12}

Values of equilibrium constant k.

(Ref: 20)